RISK–CONSTRAINED STOCHASTIC ECONOMIC DISPATCH AND DEMAND RESPONSE WITH MAXIMAL RENEWABLE PENETRATION UNDER RENEWABLE OBLIGATION

by

Thabo Gregory Hlalele

Submitted in partial fulfillment of the requirements for the degree
Philosophiae Doctor (Electrical Engineering)

in the

Department of Electrical, Electronic and Computer Engineering
Faculty of Engineering, Built Environment and Information Technology

UNIVERSITY OF PRETORIA

July 2020

SUMMARY

RISK–CONSTRAINED STOCHASTIC ECONOMIC DISPATCH AND DEMAND RESPONSE WITH MAXIMAL RENEWABLE PENETRATION UNDER RENEWABLE OBLIGATION

by

Thabo Gregory Hlalele

Promoter(s):	Prof. R. M. Naidoo
Co-Promotors:	Prof. R. C. Bansal & Prof. J. Zhang
Department:	Electrical, Electronic and Computer Engineering
University:	University of Pretoria
Degree:	Philosophiae Doctor (Electrical Engineering)
Keywords:	Battery energy storage, dynamic economic dispatch, incentive based demand response programme, multi-objective optimisation, Pareto optimal solution, renewable energy sources, stochastic optimisation, residential load management, spinning reserves, scenario generation, renewable obligation, Weibull probability density function.

In the recent years there has been a great deal of attention on the optimal demand and supply side strategy. The increase in renewable energy sources and the expansion in demand response programmes has shown the need for a robust power system. These changes in power system require the control of the uncertain generation and load at the same time. Therefore, it is important to provide an optimal scheduling strategy that can meet an adequate energy mix under demand response without affecting the system reliability and economic performance. This thesis addresses the following four aspects to these changes.

First, a renewable obligation model is proposed to maintain an adequate energy mix in the economic dispatch model while minimising the operational costs of the allocated spinning reserves. This method considers a minimum renewable penetration that must be achieved daily in the energy mix. If the

renewable quota is not achieved, the generation companies are penalised by the system operator. The uncertainty of renewable energy sources are modelled using the probability density functions and these functions are used for scheduling output power from these generators. The overall problem is formulated as a security constrained economic dispatch problem.

Second, a combined economic and demand response optimisation model under a renewable obligation is presented. Real data from a large-scale demand response programme are used in the model. The model finds an optimal power dispatch strategy which takes advantage of demand response to minimise generation cost and maximise renewable penetration. The optimisation model is applied to a South African large-scale demand response programme in which the system operator can directly control the participation of the electrical water heaters at a substation level. Actual load profile before and after demand reduction are used to assist the system operator in making optimal decisions on whether a substation should participate in the demand response programme. The application of these real demand response data avoids traditional approaches which assume arbitrary controllability of flexible loads.

Third, a stochastic multi-objective economic dispatch model is presented under a renewable obligation. This approach minimises the total operating costs of generators and spinning reserves under renewable obligation while maximising renewable penetration. The intermittency nature of the renewable energy sources is modelled using dynamic scenarios and the proposed model shows the effectiveness of the renewable obligation policy framework. Due to the computational complexity of all possible scenarios, a scenario reduction method is applied to reduce the number of scenarios and solve the model. A Pareto optimal solution is presented for a renewable obligation and further decision making is conducted to assess the trade-offs associated with the Pareto front.

Four, a combined risk constrained stochastic economic dispatch and demand response model is presented under renewable obligation. An incentive based optimal power dispatch strategy is implemented to minimise generation costs and maximise renewable penetration. In addition, a risk-constrained approach is used to control the financial risks of the generation company under demand response programme. The coordination strategy for the generation companies to dispatch power using thermal generators and renewable energy sources while maintaining an adequate spinning reserve is presented. The proposed model is robust and can achieve significant demand reduction while increasing renewable penetration and decreasing the financial risks for generation companies.

LIST OF ABBREVIATIONS

BESS	Battery energy storage system
CDF	Cumulative distribution function
CO_2	Carbon dioxide
DC	Direct current
DED	Dynamic economic dispatch
DEED	Dynamic economic emission dispatch
DLC	Direct load control
DR	Ramp down
DR	Demand reduction
DRP	Demand response programme
EDRP	Emergency demand response programme
ESS	Energy storage system
EU	European union
FIT	Feed-in tariff
GEP	Generation expansion planning
MIQP	mixed integer quadratic programming
MPPT	Maximum power point tracking
PDF	Probability density function
PV	Photovoltaic
REC	Renewable energy certificates
RES	Renewable energy sources
RLM	Residential load management
RPO	Renewable purchase obligation
SCED	Security constrained economic dispatch
SO	System operator
SR	Spinning reserve
SRR	Spinning reserve requirement
SSRR	System spinning reserve requirement

LIST OF SYMBOLS

b	Index of buses
g	Index of thermal generators
v	Index of photovoltaic generators
m	Index of wind generators
s	Index of battery energy storage system
ω	Index of scenarios
l	Index of transmission lines
t	Index of time period
r	Index of generator spinning reserves
T	Time interval period
N_Ω	Set of scenarios
N_G	Set of thermal generators
N_M	Set of wind generators
N_V	Set of photovoltaic generators
N_R	Set of generator spinning reserves
N_S	Set of battery energy storage systems
N_L	Set of transmission lines
N_B	Set of buses
C_g	Thermal generator g marginal cost
C_m	Wind generator m tariff cost
C_v	PV generator v tariff cost
C_s	BESS generator s tariff cost
C_r	Thermal generator spinning reserve r operating cost
γ	Renewable energy penalty cost in US dollars
α	Renewable energy obligation requirement
ρ	Spinning reserve cost coefficient of the gth thermal generator in \$/MWh
ζ	Wind generator cost in \$/MWh

LIST OF SYMBOLS (continued)

φ	PV generator cost in \$/MWh
τ	BESS energy cost in \$/MWh
π_ω	Probability of occurrence of each scenario
η_c, η_d	BESS charging and discharging efficiency
π	Wind speed in m/s
Ω	Solar irradiance in W/m^2
Ω_{std}	Solar irradiance in the standard environment
σ	Weibull distribution scale parameter in m/s
β	Weibull distribution form parameter
R_c	A certain radiation point
$f_\Omega(\Omega)$	Solar irradiance probability distribution function
$f_\pi(\pi)$	Wind speed probability distribution function
$f_m(P_m)$	Probability distribution of random variable P_m
$f_v(P_v)$	Probability distribution of random variable P_v
$P_{b,t}$	System demand at bus b, and time t in MW
$P_{g,min}$	Minimum output power from the gth thermal generator in MW
$P_{g,max}$	Maximum output power from the gth thermal generator in MW
$E_{s,min}$	Minimum stored energy from s BESS generator in MWh
$E_{s,max}$	Maximum stored energy from s BESS generator in MWh
$P_{l,t,\omega}$	Transmission line power flow at time t and scenario ω in MW
$P_{m,t,\omega}$	Output power from the mth wind farm at time t and scenario ω in MW
$P_{v,t,\omega}$	Output power from the vth PV plant at time t and scenario ω in MW
$P_{s,max}$	Maximum output power from the s BESS plant at time t and scenario ω in MW
$SRR_{r,max}$	Maximum spinning reserve requirement for the gth thermal generator in MW
$SSRR$	System spinning reserve requirement for operating all thermal generators in MW
UR_g, DR_g	Ramp up and down limit for the gth thermal generator in MW/h
$P_{g,t}$	Scheduled output power for thermal generator g at time t
$P_{r,t}$	Scheduled output power for thermal generator spinning reserve r at time t
$P_{m,t}$	Scheduled output power for wind farm m at time t
$P_{v,t}$	Scheduled output power for PV generator v at time t
$u_{b,t}$	RLM status at bus b and time t

LIST OF SYMBOLS (continued)

$E_{s,t,\omega}$ Stored energy in the BESS system s at time t in scenario ω

$P_{g,t,\omega}$ Scheduled output power for thermal generator g at time t in scenario ω

$P_{r,t,\omega}$ Scheduled output power for thermal generator spinning reserve r at time t in scenario ω

$P_{m,t,\omega}$ Scheduled output power for wind farm m at time t in scenario ω

$P_{v,t,\omega}$ Scheduled output power for PV generator v at time t in scenario ω

$P_{s,t,\omega}$ Scheduled output power for BESS generator s at time t in scenario ω

$P_{s,t,\omega}^{d}$ BESS generator s discharge mode at time t in scenario ω

$P_{s,t,\omega}^{c}$ BESS generator s charging mode at time t in scenario ω

$x_{s,t,\omega}$ Binary status of the BESS generator s discharging mode at time t in scenario ω

$y_{s,t,\omega}$ Binary status of the BESS generator s charging mode at time t in scenario ω

ACKNOWLEDGEMENTS

I would like to express my deepest gratitude to my supervisor, Prof. Raj Naidoo for his time and dedication, patience and supervision and above all for providing me with financial support during the duration of my studies.

I would also like to express my sincerest gratitude to my external supervisors, Prof R. C. Bansal and Prof. J. Zhang for their patience and technical support. The training and supervision that I received from you is very much appreciated.

Finally, I would like to express my appreciation and love to my friends and family, especially my wife Colile Hlalele for the ever-lasting support which made it possible to complete this work.

TABLE OF CONTENTS

LIST OF TABLES

LIST OF FIGURES

CHAPTER 1   INTRODUCTION

The need for clean and renewable energy sources (RES) has resulted in new mandates to augment and in some cases replace conventional fossil-based generation with RES. Renewable energy is derived from natural sources such as the sun, wind, hydro power, biomass, geothermal, ocean and fuel cells. The limiting of greenhouse gas emission, the avoidance of the construction of new transmission circuit and large generating units, diversification of energy sources to enhance energy security, quality and reliability, and support for competition policy are some important drivers in environmental, commercial and national/regulatory aspects behind the growth of renewable energy sources.

1.1   PROBLEM STATEMENT

The need for increasing RES penetration is very important in modern power system. In this thesis the problem of integrating large scale RES is investigated. More importantly, the need to quantify it using renewable obligation policy is analysed. In addition, the use of demand response (DR) is also investigated as a tool to increase RES in the power system operation. Firstly, the uncertainty related to RES penetration is modelled for the purposes of integrating it to the power system. Thereafter, the stochastic programming is used to adequately quantify the maximum RES that can be injected in a small and large power system.

1.2   BACKGROUND

The economic dispatch (ED) optimisation is a classical power system operational problem that has been a subject of intense research for many years. The objective of the ED problem is to minimise the total fuel cost function of the generation units by selecting the optimal output power per generator. The typical cost function is minimised subject to several constraints that include the load balance, upper and lower limits of the generating units as well as the ramp up and ramp down of each generating unit [1], [2]. The ED problem can be divided into two parts, namely static and dynamic. The static ED problem mainly focuses at the snapshot of the power system to determine the optimal generator output.

While the static ED problem has the advantage of providing steady state performance of the power system, it cannot provide a dynamic output which is more important to provide an optimal solution for real time power system operation. This has led to the second ED problem commonly known as dynamic economic dispatch (DED) problem. Contrary to the static ED problem, the DED problem is performed over a finite horizon to determine the optimal operation of the power system [3]. Moreover, during the period between two consecutive schedules, the generators participate in managing power imbalance based on the participation factors from previous economic dispatch. This approach also has an advantage of "looking ahead" which takes into consideration the forecasted load trends to allocate output power per generator over a time horizon that is determined by the system operator (SO).

As a promising renewable energy source, the solar power has been attracting a great deal of attention as an alternative clean source of energy. However, the integration of RES to the grid still remains a challenge due to the stochastic nature and variability of the RES [4], [5]. This integration introduces many challenges to the operation and planning strategy of the grid operator [6], [7]. Moreover, the variability and uncertainty in RES have led to an increase in ancillary services requirements. Solar power can be considered less uncertain as compared to wind which is more uncertain [8], [9]. The variability of a PV generator is quantified by a distribution of frequencies derived from irradiance data; while the uncertainty is quantified by a probability distribution which depends upon the information about the likelihood of what the single true value of uncertain quantity is [10]. This intermittency nature of RES affects the efficient operation of the power system and increases associated costs because of the wind and solar variability. The capacity factor is described as a parameter to measure the effectiveness of the RES [11]. It is defined as the ratio of actual energy output of the plant to the installed capacity of the plant which is normally expressed as a percentage. In South Africa the Integrated Resource Plan (IRP) assumes a capacity factor that is between 19.4% to 25% for PV and a capacity factor between 30% to 36% for wind [12].

Several methods have been proposed to limit the uncertainty and variability of the RES for the DED problem. These methods are divided into two main approaches which are the probabilistic and deterministic approach. In [13], a method based on probabilistic approach for short term forecasting is used. The probabilistic method is selected and trained as base predictors in order to obtain a sample of the predictive distribution with optimal characteristics of sharpness and reliability. The field of PV power forecasting, probabilistic ensembles based on deterministic predictors are obtained through machine learning techniques such as gradient boosting, or assuming a specific normal distribution

from single predictors. For wind power, several investigations have looked at the prediction of wind speed for uses in determining the available wind power. These investigations have been based on fuzzy logic, neutral networks and time series [14].

The traditional real time constraint ED solves energy dispatch and ancillary service for one target interval. The additional advantage of real time DED is the inclusion of demand forecast. This advantage must be taken into consideration when adding RES since their output power can change by as much as 70% in 10 minutes or less [9]. The conventional DED solves the problem over a 24-hour period. The inclusion of RES will certainly affect the generation pattern which brings the need for spinning reserves for conventional generators in order to compensate the short fall that may arise from RES not meeting their forecasted energy output [15].

In recent times wind and PV solar generation integration studies have been fixed to one-time resolution, thus this makes it difficult to analyse the effect of variability and uncertainty within a single time frame. In [16], a real time DED algorithm is designed to compute real time dispatch as well as real time pricing that is compliant to the Midwest Independent System Operator's energy and ancillary market business rules. In [17] a methodology for stochastic DED is presented that guarantees secure operation in real-time scenario. While in [18], a discussion on various methods that can be used to deal with variability and uncertainty are presented ranging from reserve rules, demand response, storage and flexible transmission. The dynamic reserves are integrated into two settlement market clearing mechanism, where energy and reserves are dispatched and priced simultaneously. In addition, a stochastic mixed integer linear programming scheduling model minimizing system operating costs and treating load and wind power production as stochastic input is presented in [19].

Other forms of DED have also been proposed that include emission dispatch [20], [21]. In [22], a load dispatch model that minimises the emission is proposed and the effects of wind power on emission control are investigated. A better approach is proposed in [23] where a probabilistic methodology to estimate demand curve for operating reserves and the curves represent the amount the SO is willing to pay for the services using the membership function for the total fuel cost. The demand curve is quantified by the cost of unserved energy and the expected loss of load which accounts for uncertainty from generator contingencies, load forecasting errors and wind power forecasting errors. Moreover, a short-term forward electricity market clearing problem with stochastic security capable of accounting for non-dispatchable and variable wind power generation is presented [24]. The authors show that

the benefit of their approach is that it allows greater wind power penetration without affecting the network security. Many authors have used evolutionary algorithms to solve DED problems such as hybrid swarm intelligence algorithm found in [25] and harmony search algorithm found in [26]. The approach that is used for solving the optimisation problem is based on evolutionary algorithm due to the complexity added by the ramp rate, valve point effects, spinning reserve requirements, load balance constraints, operating limits, and network losses. Genetic algorithm is a numerical optimisation approach that is easy to implement and significantly faster than other algorithms.

1.2.1 Research gap

There is a lack of focus on the incorporation of RES obligation requirement from the supply side. In particular, there is no research that incorporates a renewable obligation (RO) in the optimal scheduling of RES while incorporating incentive based DRP for large scale residential customers.

1.3 RESEARCH OBJECTIVE AND QUESTIONS

The primary goal of this thesis is to present a combined DR and economic dispatch model under renewable obligation considering the current state of the network which has a lot of fluctuations due to RES integration. Firstly, this thesis focuses on increasing the RES penetration in the network under the current operating conditions. The renewable obligation model is introduced as a quantity-based instrument to measure the impact of RES penetration in a small and large power system network. To deal with the uncertainty related to RES penetration, demand response is introduced to handle the deferrable loads and incorporate it to the RO model. A new joint DRP under RO is presented under deterministic and stochastic scenarios to ascertain the level of RES penetration that can be achieved without affecting the network reliability and economic benefit. As such, an incentive-based demand response is implemented for residential customers participating in this program. Overall, the financial risk associated with a joint operation of RES and DR is evaluated for the conventional generation companies. Therefore, the research question listed below are addressed:

- What is the maximum RES penetration that can be achieved?
- What is the impact of DR on RES penetration level and operating cost?
- What is the benefit of a joint DR and economic dispatch under renewable obligation?

1.4 RESEARCH CONTRIBUTION

The contributions of this work are listed below:

1. A renewable obligation framework is mathematically modelled and incorporated into a security constrained economic dispatch (SCED) to allow maximum RES penetration while penalising generation companies for not complying with the minimum RES quota. This model is aligned to the quantity-based instrument which measures the quantity of RES injected into the grid to achieve a cost-effective energy mix.

2. A multi-objective optimisation model is presented with two objective functions. The first objective functions are related to the minimisation of the total operating cost and spinning reserve cost of thermal generators. The RO model is included in the first objective function to ensure a minimum RES quota is achieved, and if it is not achieved a penalty will be imposed to thermal generators. The second objective function maximises the total RES energy generated from wind and PV power plants.

3. A multi-objective economic dispatch model is presented which integrates deferrable demand within a real DLC DRP intermittent renewable energy under renewable obligation.

4. The combined incentive DRP and DED with RES quota obligation model are applied to large scale residential customers.

5. The BESS system is included to reduce the thermal generator spinning reserve requirement by utilising BESS for ancillary services.

6. Real data from South African DRP are taken in the optimisation model so that the system operator can decide whether a substation needs to respond to the DR request.

7. A combined risk constrained RO and demand response model is presented under value-at-risk (VaR) to decrease financial risk of the generation companies.

1.5   HYPOTHESIS AND APPROACH

In order to address the problems identified in this thesis, the following hypothesis are given as follows:

1. The proposed renewable obligation model will provide an adequate energy mix between renewable energy and conventional thermal generators.

2. Incorporating demand response will increase the renewable energy penetration and reduce the total operating cost of thermal generators.

3. Renewable obligation will decrease the total operating cost of thermal generators.

1.6 RESEARCH OUTPUTS

The resulting contribution from this research have been published in peer reviewed journals. A publication list of articles that resulted from the research is provided as follows:

1. T. G. Hlalele, R. M. Naidoo, J. Zhang, and R. C. Bansal, "Dynamic economic dispatch with maximal renewable penetration under renewable obligation," *IEEE Access*, vol. 8, pp. 38794 - 38808, 2020.

2. T. G. Hlalele, R. M. Naidoo, R. C. Bansal, and J. Zhang, "Multi-objective stochastic economic dispatch with maximal renewable penetration under renewable obligation," *Applied Energy*, vol. 270, pp. 1 - 16, 2020.

3. T. G. Hlalele, J. Zhang, R. M. Naidoo, and R. C. Bansal, "Multi-objective economic dispatch with residential demand response under renewable obligation," *Energy*, submitted June 2020, under review.

4. T. G. Hlalele, J. Zhang, R. M. Naidoo, and R. C. Bansal, "Risk-constrained stochastic economic dispatch with demand response under renewable obligation," still to be submitted.

1.7 OVERVIEW OF STUDY

The thesis is organised as follows. In Chapter 1 the thesis is introduced, the background and motivation for the current work is presented. Lastly the contribution of the current work is presented. In Chapter 2 a detailed literature review on the different renewable integration policy framework which ultimately builds the current research framework. The chapter also presents a background on the current state-of-the-art in terms of power system operation problem related to economic operation and demand flexibility. Thereafter, a brief introduction of modelling renewable energy sources is presented. In Chapter 3 the basic renewable obligation model is presented and integrated to the security constraint economic dispatch problem. The chapter models two renewable energy sources, i.e., wind and PV using the probability density function. The RES generators are incorporated into the model for a joint energy and reserve dispatch model. In Chapter 4 a residential load management (RLM) demand response programme is integrated to a renewable obligation model. A joint demand response and economic dispatch is presented for residential customers participating in an incentive-based demand response programme. In Chapter 5 an extension of the renewable obligation model presented in Chapter 3 is used to incorporate the uncertainty related to renewable energy sources. In this Chapter, a stochastic version of the RO model is presented to ascertain the actual impact of incorporating RES in a SCED under RO. In addition, battery energy storage system (BESS) is added to minimise the

required spinning reserves which reduces the total operating cost. In Chapter 6 a unified model from the previous chapters is modelled under uncertainty and financial risk to the generation companies. The impact of demand response is modelled to show the ability of load flexibility to increase RES penetration while decreasing financial risk to the system operator that owns thermal generators. This model shows that both RES and conventional generators can operate in a mutually beneficially system under demand response where both can increase their profitability without affecting the customers. Chapter 7 summarises the work presented in this thesis and provides suggestions for future work.

CHAPTER 2   LITERATURE STUDY

In this chapter a detailed literature review related to the modelling of renewable energy sources is presented. Thereafter, different types of demand response programmes are also reviewed to provide a detailed background.

2.1   INTRODUCTION

This chapter provides a detailed literature review on a renewable obligation policy framework and the incentive-based demand response programme. The different policy framework available for encouraging the penetration of renewable energy in the grid are discussed in details and the framework for this research is explained. Moreover, different types of demand response programme available to residential customers are explained. Finally, the modelling techniques used for renewable energy sources are also explained and the stochastic programming method for scenario generation and reduction are presented.

2.2   RENEWABLE ENERGY POLICIES

Policy makers around the worlds are implementing measures to accelerate the connection of renewable energy sources (RES) in order to meet low carbon or sustainable objectives. As such, the number of countries that have some form of target setting for utilising renewable energy has reached 164 as of 2016 [27]. There are two main categories of regulatory generation focused on renewable energy support mechanism: tariff-based instrument and quantity-based instrument. The tariff-based instrument provides an economic incentive for generating electricity using renewable energy sources. The Feed-in-Tariff (FIT) is an example of a tariff-based instrument. On the other hand, quantity-based instruments work by setting a minimum target for renewable energy in the overall energy mix and hold certain parties in the energy supply chain responsible for these targets. An example of the quantity-based instrument is the renewable obligation (RO) which imposes a minimum quota or a share of renewable production on electricity suppliers. Figure 2.1 shows the policy framework for the renewable energy

support mechanisms.
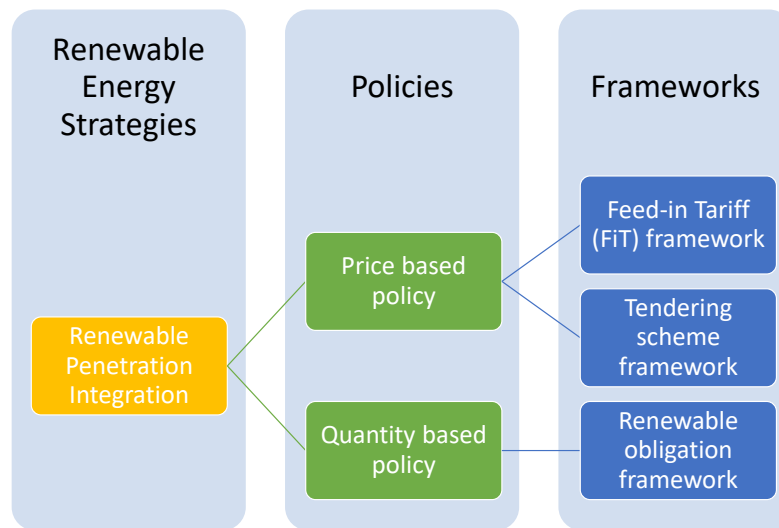
Figure 2.1. Global renewable energy support mechanisms.

2.2.1   Feed-in-Tariff

The FIT scheme guarantees energy price over long periods which may be more effective and may encourage RES investment. FIT schemes can improve rapid investment while reducing investment risks and improving energy cost transparency [28], [29]. Some of the advantages of FIT schemes shows that there is more controllability of electricity price rise and an improvement in energy security. However, some of the disadvantages of the FIT scheme shows that tariff can increase public costs and taxes, increase equipment costs and operation and maintenance fees while limiting RES investment returns. These limitations are the reason why the auction scheme was introduced to overcome this shortcoming.

2.2.2   Auctioning

An auction support mechanism is like FIT scheme, it is normally introduced in the market to support and complement the FIT scheme as it provides the same benefit to the FIT scheme. The only exception to the auction support mechanism comes from the tariff where the renewable energy supply companies contest for the most attractive tariff. This policy structure takes advantage of the FIT to complement its shortcomings by applying a policy mix instead of a single policy. For example, FIT guarantees the price of RES by setting fixed prices over the market price of electricity for a long period [30]. One of

the advantages of the auction scheme as opposed to FIT is the ability to mitigate the high price risk associated with RES technology energy cost since all competitors auction for the best energy tariff. The disadvantage of the auction is the high transaction costs for small RES power plants which is the reason why a renewable obligation scheme is introduced to overcome this challenge.

2.2.3 Renewable obligation

A renewable obligation policy mechanism obligates the thermal generators to acquire a percentage of their energy from renewable energy. This can be achieved in one of two ways, (i) by either supplying the RES from their own RES power plants or (ii) by purchasing renewable obligation certificates in the secondary spot market. The RO scheme is considered a market-oriented policy as the market competition among RES companies determines winners in RES market, unlike a guaranteed return under FIT [31]. As a result of this policy framework, the market participation encourages incentives for cost reduction. The main advantage of the RO policy is the sale of ROC in the secondary market which makes it an attractive option for a deregulated energy market.

2.3 RENEWABLE ENERGY MODELLING

The increase in renewable energy sources is very evident in today's power system operation. This increase in renewable energy penetration is largely attributed by the Paris Agreement which aimed to reduce the average global surface temperature below 2^oC [32] and thus minimise the greenhouse gas emission. As a result of this agreement there has been an upsurge in the integration of RES and distributed energy sources in the power system. These RES can be found in different capacity and sizes and different technologies ranging from wind, PV, CSP, geothermal and biomass. Although the benefit is clear from the reduction in greenhouse gas emission, there is still a challenge in their integration due to the corresponding variability and uncertainty, e.g., wind and PV. This is because most RES depends on the environmental condition for energy production. For example, wind energy production relies on the wind speed and PV energy production relies on the solar irradiance and temperature. All these environmental parameters make the integration of RES a challenge for power system operators since the dispatchability of generators depends on the knowledge of power production which is normally fixed.

To overcome this challenge, many researchers have studied the impact of RES penetration on the voltage, frequency, power quality environment, power system dynamics and power losses [33]. It is important to also consider the impact of RES penetration from weather-dependent sources to increase the accuracy of their production and to anticipate their variations on the power system operation.

The study of weather-dependent RES generation is broadly studied from two perspectives, that is, qualitative and quantitative methods.

In the following, various models for forecast and stochastic modelling in both dependent, independent, and the multi-dimensional state are shown in Figure 2.2
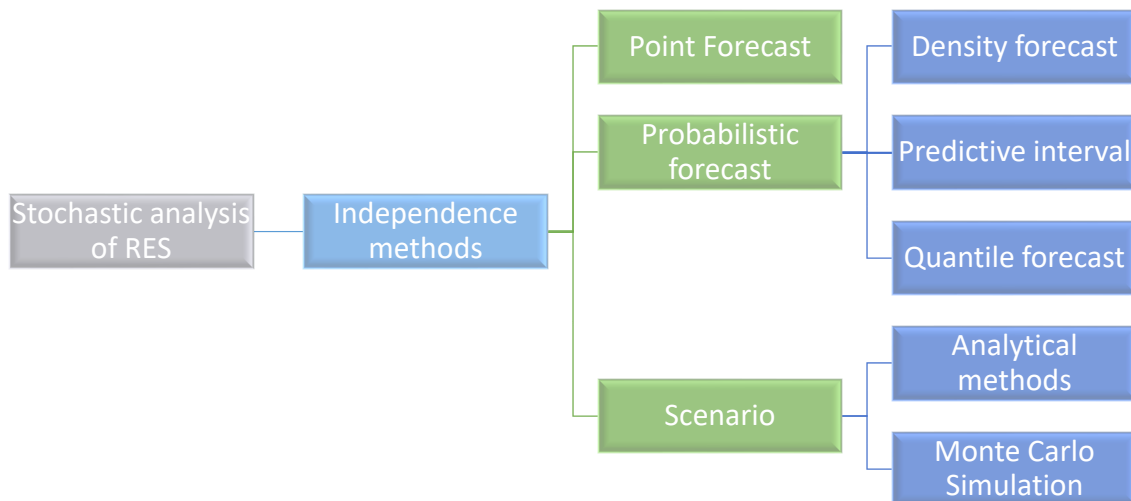
Figure 2.2. Various methods of stochastic analysis of renewable energy sources

2.3.1   Stochastic independency

Forecast and scenario are in fact extrapolation. In means that a model is built and fitted to a set of data. The correlation between different stochastic variables may not be considered, and the scenario generation or forecast is conducted, independently.

2.3.2   Point independency

Many scholars adopt advanced theories and methods to improve wind and solar power prediction accuracy. Most methods are deterministic prediction, that is, only a certain output value of wind and solar power at a certain moment in the future can be acquired. The point prediction results only provide single point forecast, and since this is the most basic method there are a lot of application in this regard [34]. Since both wind and PV are dependent on external environmental conditions, the deviation between forecasted and actual value is relatively large for this type of prediction method. This results in power system operation risks due to the large deviation of forecasted and actual value and poor

performance. Due to the limited nature of point forecast it is important to include the probabilistic forecast. The probabilistic forecast can provide more prediction information by including a prediction interval and probability density function [35].

The physical methods are based on numerical weather prediction model and are computationally extensive. The statistical methods provide prediction by using historical data [36]. This type of prediction assumes a linear relationship between historical and current data. The artificial intelligence methods use methods such as fuzzy logic, support vector machines and artificial neural network. A hybrid method combines the performance of AI methods with statistical method to provide better forecasting performance [37].

2.3.3   Probability forecast

Uncertainty of wind and solar power affects the power system operation and, therefore, it is important to model the uncertainty of wind and solar power using probability density functions. For the probabilistic forecast a range of all possible variations in wind and PV is generated within a predefined confidence interval which has the lower and upper bounds. This provides more flexibility as it has a wider range of possible outcomes of wind and PV output power. The probability density prediction provides more information by computing all the probability of all possible outcomes. The traditional approaches for probabilistic interval prediction include delta, Bayesian, mean-variance, bootstrap and quantile regression [37].

2.3.4   Forecast interval

Quantile forecast method does not deliver any information about forecast uncertainty level. To this end, the forecast interval is used in [38]. Forecast interval is usually proper for robust optimisation. Forecast interval has a nominal coverage rate and lower and upper bounds which define, for example, the probability that a wind farm generation is higher than a specific amount. Forecast interval can cover point forecast and quantile forecast through considering different nominal coverage rates. Therefore, full forecast distribution of stochastic variable like wind power can be obtained by this method [39].

2.3.4.1   Modelling of renewable energy sources

In this section the statistical modelling of Wind and PV generators is presented using the Weibull PDF.

2.3.4.2   Wind energy system

The intermittent output power of a wind turbine can be characterised as a random variable which is related to the wind speed at the hub of the turbine. The actual intermittent power can be represented as a function of wind speed (2.1), [6]. Moreover, the wind output power can be transformed from wind speed using a statistical transformation given in [40], [41].

$$P_{m,t,gen}(v_{m,t}) = \begin{cases} 0 & \text{if } \pi_{m,t} < \pi_m, \pi_{m,t} > \pi_o, \\ P_{m,r}\Gamma(t) & \text{if } \pi_m \le \pi_{m,t} \le \pi_r, \\ P_{m,r} & \text{if } \pi_r \le \pi_{m,t} \le \pi_o. \end{cases} \tag{2.1}$$

The wind speed $\pi_{m,t}$ is a random variable that varies over time; where π_m, π_r and π_o, are the wind turbine cut in speed, rated speed and cut out speed all in m/s. This means that the corresponding wind power is also a random variable and $\Gamma(t)$ is shown in (2.2).

$$\Gamma(t) = \left(\frac{\pi_{m,t} - \pi_m}{\pi_r - \pi_m} \right) \tag{2.2}$$

2.3.5   Weibull distribution function

The Weibull distribution function has been used by many authors [42], to model the percentage of time that the wind spends at a given speed on an annual basis. The Weibull distribution function is characterised by two parameters, namely the shape parameter κ and the scaling velocity σ as shown in (2.3).

$$f_\pi(\pi) = (\frac{\kappa}{\sigma})(\frac{\pi}{\sigma})^{\kappa-1} e^{(-1(\pi/\sigma)^\kappa)} \tag{2.3}$$

The cumulative distribution function (CDF) of the wind speed is given in (2.4).

$$F_\pi(\pi) = 1 - exp\left[-\frac{\pi^\kappa}{\sigma} \right] \tag{2.4}$$

The PDF of the wind power is a random variable, and when the wind speed is between cut-in and rated wind speed $P_{m,t}$ in the m-th period is given in (2.1). The Weibull PDF for the wind speed is transformed to the corresponding wind power distribution using linear transformation [43], [44]. More details can be found in [41], for the derivation of the wind power PDF. It follows from (2.4), that the CDF of the wind power is similar as shown in (2.5).

$$F_m(P_{m,t}) = \begin{cases} 0 & \text{if } P_{m,t} < 0, \\ 1 - e^{-(\frac{1+\frac{\delta p}{P_{m,r}}\pi_m}{e})^\kappa} & \text{if } 0 \le P_{m,t} \le P_{m,r}, \\ 1 & \text{if } P_{m,t} \ge P_{m,r}. \end{cases} \tag{2.5}$$

Therefore, the maximum forecast wind power is calculated using (2.6).

$$P_{m,t,gen} = P_m(\pi_{m,t})F_{\pi,m}(P_{m,t}(\pi_{m,t})) \tag{2.6}$$

2.3.6 Solar Energy System

For a PV energy system, a relationship among radiation resource, temperature and output power can be found in [23], which is also given by the function (2.7);

$$P_v(\Omega) = \begin{cases} P_{vr}(\Omega_t^2/\Omega_{std}R_c) & \text{if } 0 < \Omega_t < R_c, \\ P_{vr}(\Omega_t/G_{std}) & \text{if } \Omega_t > Rc, \\ 0 & \text{if } G_t = 0. \end{cases} \tag{2.7}$$

where PV cell temperature is neglected, and the solar active power generation can be controlled by maximum power point tracking (MPPT) algorithm or be charged into batteries. This means that the maximum penetration of the PV generator is limited by the available maximum active power generation which is subject to solar irradiation and temperature [4], [5].

2.3.7 Bimodal Weibull distribution function

The output power of a PV plant depends on irradiance and temperature. The distribution of irradiance at a location usually follows a bimodal distribution function. The distribution function is a linear combination of two unimodal functions. These unimodal functions can be modelled by Weibull, Log-normal and Beta PDF [16]. In this chapter a Weibull distribution as given in (2.8) is considered.

$$f_\Omega(\Omega_t) = \beta(\kappa_1/e_1)(\Omega_t/\sigma_1)^{\kappa_1-1}e^{((-\Omega_t/\sigma_1)^{\kappa_1})} + (1-\beta)(\kappa_2/\sigma_2)(\Omega_t/\sigma_2)^{\kappa_2-1}e^{((-\Omega_t/\sigma_2)^{\kappa_2})} \tag{2.8}$$

The Weibull PDF of solar PV output random variable is given in [5]. The maximum forecasted PV power is calculated by (2.9).

$$P_{v,t,gen} = P_v(\Omega_{v,t})F_{\Omega,v}(P_{v,t}(\Omega_{v,t})). \tag{2.9}$$

2.4 DEMAND RESPONSE FLEXIBILITY AND RES INTEGRATION

Demand response is a tool used to shift or reduce system load by taking advantage of high demand and low demand periods electricity prices. This tool can also be used to increase the level of RES penetration in the network by curbing the uncertainty of RES generators. This is achieved by using demand flexibility as reserves instead of the conventional spinning reserves from thermal generators. Therefore, any changes related to the uncertainty of RES production is managed by the demand flexibility. The core assumption of demand response is that consumer consumption is elastic and response to higher prices by demand reduction. Therefore, one of the main advantages of DR is its ability to balance these RES fluctuations and thereby increasing RES penetration.

There are some challenges with the implementation of DR, namely, (i) insufficient experience which leads to poor assumption in modelling and evaluations; and (ii) the need for a full automated smart

grid that will allow constant bi-direction communication between supplier and consumer of electricity. It has been shown that by addressing the two shortcomings, an effective demand response programme can yield positive economic results for both the consumer and the supplier [45]. Therefore, if a DR programme is successfully implemented, then an overall electricity price reduction can be achieved for both the consumers and supplier.

Another advantage of DR that is especially important is the coordination of this programme with RES penetration. One such example is the implementation of direct load control (DLC) for residential customers to provide load flexibility to reduce the impact of RES fluctuations. Another way that can increase RES penetration is the use of time of use tariff that changes electricity usage based on high demand and low demand prices which ultimately pushes customers to consume less energy during peak period due to the high cost of electricity. This shows that there is a clear price-base elasticity consumption pattern [46].

2.4.1   Demand response modelling techniques

In order to show the effectiveness of a joint demand response with RES penetration there are several DR models that can be used to increase RES penetration. Demand response is defined as the changes in electricity usage by end-use customers from their normal consumption patterns in response to changes in the price of electricity over time, or to incentive payments designed to induce lower electricity usage at times of high wholesale market prices or when system reliability is jeopardized [47]. In this section different DR frameworks are briefed.

2.4.2   Demand response programmes

Demand response programmes are classified into two main categories, i.e., price based and incentive-based programmes. In other literature this is classified as dispatchable and non-dispatchable with first being non-dispatchable and the last being dispatchable [33], [48]. The naming conversion largely depends on the scholars. The two categories and their sub-categories are shown in Figure 2.3. In first category, the customers are incentivized for changing their demand patterns as per instructions from the supply side. For the second category, the consumers are charged by different rates for different consumption periods which are related to demand patterns.

1. Direct load control programmes – in these programmes the customers participate in the program by allowing the utility to automatically switch on and off their appliances when it is required especially during peak demand periods [49]. In [50] residential customers participate in a DLC
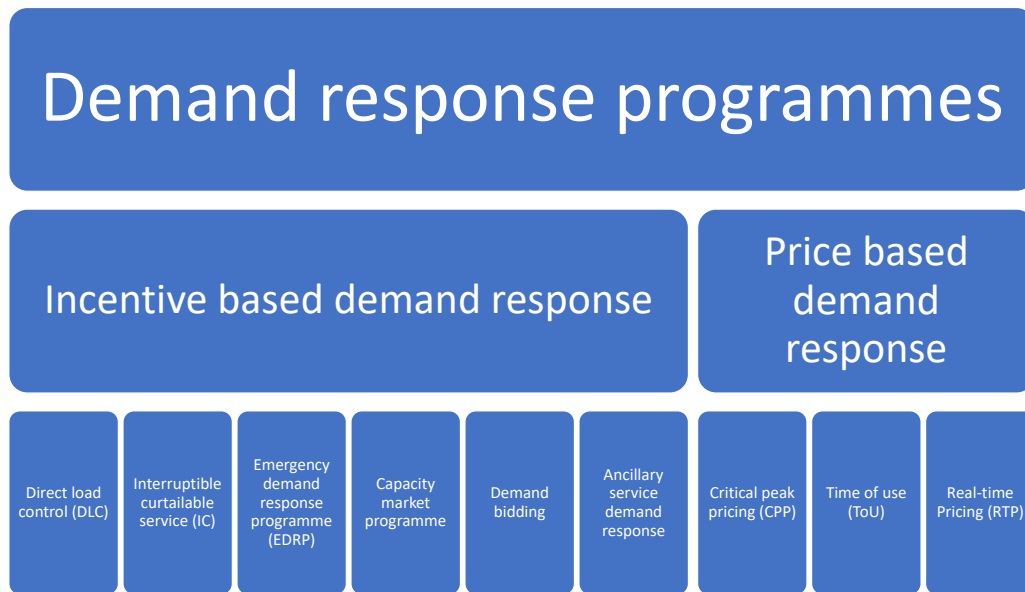
Figure 2.3. Demand response programme categories

program on a voluntarily basis by allowing the utility to switch on/off the air conditioning system while in [51] an incentive is paid to participating customers. This means that the participation of this program can be both incentivized and voluntarily.

2. Load curtailment program – in this type of program the utility pays customers to curtail their consumption and if they participating customer does not curtail then they pay a penalty to the utility for failing to meet their curtailment obligation. A typical example of such a program is implemented in [52] where industrial customers are participating in load curtailment to support utility generation flexibility.

3. Demand bidding programs – this is generally offered to large-scale consumers where consumption is anywhere over 1 MW [53]. Similar to load curtailment, the demand bid programs offer relief to a constrained network where the demand is very high, and generation is very expensive. The consumers can bid to curtail their consumption. Normally they participate in this program using the demand aggregator.

4. Emergency demand reduction – this is implemented during critical constraint on the power system and an instruction is sent out to reduce the demand in order to improve power system reliability [54].

Price-based DR programs: For the price-based demand response programmes, the consumers are charged with different rates for different consumption periods. This means that when consumption is very high a high price is also charged to consumers to encourage demand reduction. Therefore, by increasing the electricity price during peak demand period it is expected that consumers will reduce their demand.

1. Time of use (TOU) pricing – electricity price is normally divided into standard, peak and off-peak tariff. The consumers are charged based on their consumption and normally pay a high price during peak tariff which corresponds to high demand.

2. Critical peak price – this is like TOU with the exception that for the time when the power system is under critical conditions then the normal peak price is replaced by high tariff price.

3. Real-time pricing – The price of electricity is dependent on real time market supply-demand patterns and generally changes every hour which reflects the relationship between supply and demand. A day-ahead price is released to all consumers to allow customers to plan their energy consumption activities related to the market prices and decide whether demand bidding can be implemented [47].

2.4.3 Demand response conditions

For the implementation of DR programs, due to lack of enough experience, some assumptions should be considered in modelling approaches. Therefore, advantage of DR model highly depends on this assumption and it needs to be evaluated. Some models and assumptions are necessary as presented in the next section.

2.4.4 Demand aggregator and demand bidder

The framework for the demand bidding involves the demand aggregator. Demand aggregators are there to help customers quantify and participate in the demand bidding process by providing and analysing demand forecasts for participating customers. In the market structure framework, the demand aggregator is an independent entity such as a distribution company, load servicing entity or a financial entity. The demand entities are put in place to interface with the customers and the system operator or independent system operator to provide a smooth transition of demand response. They are responsible for aggregating customers bids and sending such bids to the system operator. A typical relationship between the system operator, customers and demand response aggregator is shown in Figure 2.4.

The main purpose of the DR aggregators is to evaluate the customers potential to dedicate the special
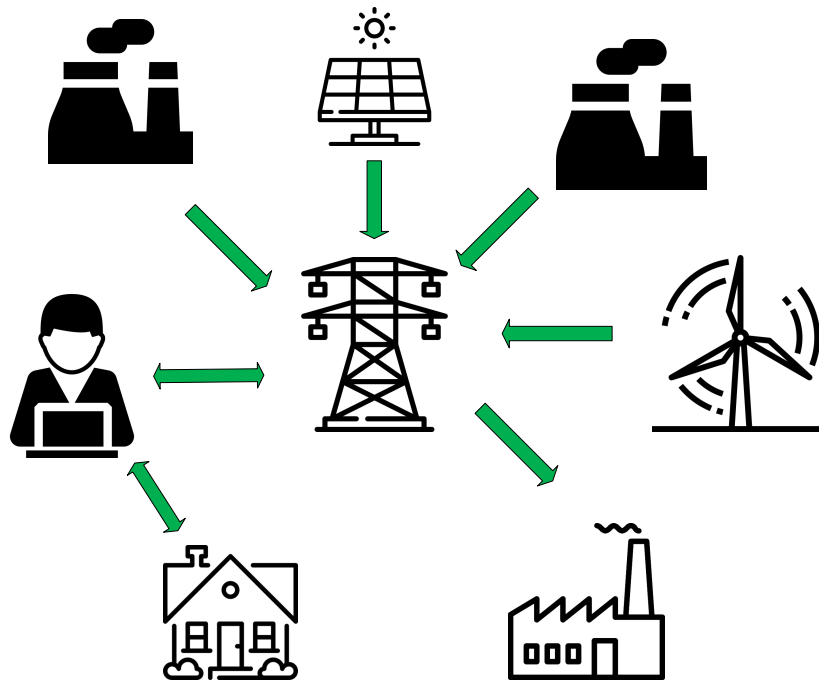
Figure 2.4. Demand bidder and demand aggregator

DR quantity and price based on physical and operational constraints. The DR aggregators provide demand bids to the SO and clear the market to maximise social welfare. Social welfare is defined as the sum of the surpluses of the producer and consumer.

2.5 SUMMARY

In this chapter a detailed background on the renewable energy policies is presented coupled with the types of demand response programmes available. As shown in the literature review, renewable obligation (RO) policy offers more advantage than the FIT and auction approach and direct load control (DLC) offers the simplest approach to DR. The next chapters will develop models for RO and DLC that can be integrated to the economic dispatch model to increase RES penetration and maximise profit for generation companies.

CHAPTER 3   MAXIMAL RENEWABLE PENETRATION UNDER RENEWABLE OBLIGATION

In this chapter, a renewable obligation model is presented for generation companies in order to attain an adequate energy mix in the daily power dispatch.

3.1   INTRODUCTION

In the past decade there has been an acceleration in the integration of variable renewable energy sources (RES) in the power grid as part of the transition towards decarbonisation of the electricity sector. The decarbonisation was motivated by the need to reduce greenhouse gas emission caused by thermal generators which threatens global climate change. Although greenhouse gas emission can be attributed to many other sectors such as residential, transport, industrial, and commercial, the largest contribution comes from the industrial sector, from electricity generation [55]. The EU has set a binding target for all its member states to reduce greenhouse gas emissions by 20% by 2020, whilst in South Africa a target has been set to reduce the total energy supply from conventional thermal generators to less than 30% by 2030 and a further 10% by 2050 [56].

There are generally two policy frameworks used to encourage the penetration of RES for a complete energy mix. The two frameworks are divided into quantity based and tariff-based instruments. Tariff and quantity-based instruments are the key funding frameworks used by regulators to encourage investment in renewable energy. A tariff-based instrument, such as the Feed-in Tariff (FIT), provides an economic incentive for generating electricity using RES. This type of instrument guarantees grid access, long term contracts for the electricity producer and purchase prices that are based on RES generation costs [57], [58]. In contrast, a quantity-based instrument is utilised to keep role-players within the energy value chain accountable for meeting the minimum renewable energy targets. A

renewable obligation (RO) is a quantity-based tariff instrument that requires electricity suppliers to adhere to the minimum renewable energy production quota. The failure to meet the obligation quota is penalised, and this approach encourages the generation companies to comply with their RES obligation. The renewable obligation certificates (ROC) are also awarded to companies that comply with their RES obligation which can further be traded in the market and typically one ROC certificate is equivalent to 1 MWh of renewable energy production. This quota mechanism has been adopted by countries such as Great Britain, Italy, Chile, Belgium and other parts of the US [59], [60].

A generation expansion planning (GEP) model is presented in [59], where the approach is to design an effective and efficient incentive policy that increases the level of RES injection in the grid. The approach adopted in [59], focuses on the inception level instead of the operational level. The design approach concept is based on stimulating an investment policy that increases the level of RES injection by specifically focusing on improving the cost competitiveness of RES in the short term by using a bi-level optimisation approach. The bi-level optimisation finds a minimum trade-off between economic benefit and environmental impact and the most efficient incentive policy that can achieve maximum RES penetration. In [60], a GEP problem is presented that evaluates different RES incentive schemes such as quantity based and tariff-based instruments. The work presented in [60] shows the impact of RES incentives and CO_2 mitigation policies in the GEP framework from the generation companies' point of view. The inclusion of RES in the grid has mostly been considered from the GEP perspective, with less focus on the operation point of view. A review of the different RES supporting schemes is presented in [61], for increasing the RES level in the grid; and the impact of feed-in tariff is analysed from the priority dispatch rule, negative prices and economic compensation.

In [62], a dynamic FIT is introduced for a wind farm that is integrated with thermal generators to encourage the maximum export of wind power generation without adversely affecting the conventional generators. The concept of dynamic cost coefficient is introduced in order to account for the variable wind speed and fluctuating power demand which increases the wind penetration in the overall energy mix. The economic dispatch model is presented to account for the hourly dispatch of thermal and wind generators using fuzzy logic to provide the best dynamic cost coefficient of the wind generators. In [63], a unit commitment model is used to quantify the operational impacts of incentivising RES generation when the energy prices are negative. The negative prices affect the flexibility of system operation and increase the thermal generator cycling costs. Therefore, it is important to consider the increase in RES penetration from an operational point of view such as economic dispatch within the

renewable energy obligation framework. Fundamentally, the classical economic dispatch problem optimises the schedule power of each generator in order to minimise the fuel costs while meeting the demand and machine ramp rates [1], [2].

The impact of increasing the RES in the network has resulted in a high requirement for spinning reserves which is used to balance the deviations emanating from variable RES generation. This increased level of RES penetration has resulted in a high cycling rate for thermal generators and has subsequently increased the maintenance costs of thermal generators and the overall operating expenses. Reference [64] presents, a security constrained economic dispatch (SCED) which focuses on the level of uncertainty caused by the increased level of RES penetration while considering the operational reserves. The approach proposed in [64] studies the impact of wind reserve margins from the market implication perspective by considering reserves policies that can mitigate the uncertainty associated with wind power generation. A probabilistic spinning reserve approach is presented in [65], which increases the integration of wind power generation using an algorithm that integrates the stochastic wind forecast of a day ahead security constrained unit commitment approach. In [66], a two stage SCED with robust optimisation is presented for reserve requirement and energy scheduling model where the operational risk is presented using a Wasserstein ball-based method. The model presented minimises the projected operating costs of producing energy while providing spinning reserves and satisfying the operational constraints.

A classical economic dispatch that incorporates the wind energy and system spinning reserves for optimal energy scheduling is presented in [67]. The model includes the under and over estimation of the available wind energy in the optimal scheduling of different generators. A similar approach is presented in [19] and [68] where a day ahead model is presented in a SCED model that minimises the spinning reserve requirements and ancillary services for high RES penetration in a FIT environment. The importance of spinning reserve requirements is further illustrated in [69], where a hybrid method is used for allocating SR in a risk based deregulated electricity market for the operation of a reliable system which includes high wind penetration. A new approach is presented in [70], where energy storage system (ESS) is used to complement high level of wind penetration in order to minimise transmission infrastructure expansion and increase the RES penetration in a FIT environment. The energy storage improves the accommodation of renewable generation by mitigating the emergency overflow under the post contingency state. In [71], a stochastic security constrained unit commitment with wind energy considering coordinated operation of price-based demand response and energy storage

is presented. The price-based demand response is formulated as a price response dynamic demand bidding mechanism. A multi-objective stochastic economic dispatch is presented in [72], which is based on two objective functions. One objective function minimises the expected power purchase costs and the second objective function minimises the pollution of gas emission from conventional thermal generators. A Pareto based algorithm is used to solve the multi-objective optimisation problem using the normal boundary intersection method. Moreover, the stochastic dispatch method is approached from scenario-based decomposition.

None of the referenced studies have investigated the RES penetration from an obligation point of view. Instead, they have focused on the underestimation and over-estimation of RES on the cost function to compensate for under performance and over performance of the RES [8], [73]. In this study, a novel multi-objective function that includes the RES quota is presented in order to minimise the operating costs of thermal generators, spinning reserve, and maximise the RES penetration. The basis for this approach emanates from the need to achieve a moderate energy mix in the network that includes RES and thermal generators. The model sets a target obligation that the SO imposes on the network. If the generators do not achieve a minimum obligation set out, then a penalty is imposed to the thermal generators. Moreover, it is important to note that in most practical systems, the RES contributes all its generated energy into the grid if it does not exceed the contractually agreed achieved capacity. This means there is no need for penalising the RES for over supply since a curtailment is already implemented in the operation of the RES generators. Hence, the only penalty that is imposed is the failure to meet the minimum quota set out by the SO. The contributions of this work are listed below:

1. A renewable obligation policy framework is mathematically modelled and incorporated into a SCED to allow maximum RES penetration while penalizing generation companies for not complying with the minimum RES quota. This model is aligned to the quantity-based instrument which measures the quantity of RES injected into the grid to achieve a cost-effective energy mix.

2. A multi-objective optimisation model is presented with two objective functions. The first objective function is related to the minimisation of the total operating cost and spinning reserve cost of the thermal generators. The RO model is included in the first objective function to ensure a minimum RES quota is achieved and if it is not achieved a penalty is imposed to thermal generators. The second objective function maximises the total RES energy generated from wind and photovoltaic (PV) power plants.

3.2   PROBLEM FORMULATION

The approach considered in this chapter assumes that wind and PV power generators are non-dispatchable. The following assumptions are made for the formulation of the DED problem with RES obligation;

1. All the RES (wind and PV) must be consumed first and the thermal generators must reduce their generation capacity to give preference to RES generators.

2. An hourly dispatch period is considered in all the case studies.

3. All RES is non-dispatchable and cannot be used as part of spinning reserves unless they have storage.

4. The SO is responsible for dispatching all the generators including RES generators.

5. Only thermal generators can be used for spinning reserve.

6. All the RES generators are owned by independent power producers (IPP).

7. We simplify the RO model by ignoring the secondary trading market of ROC.

3.2.1   Objective function

The objective function is made up of two objective functions, i.e. the fuel cost minimisation with renewable energy obligation requirement, and the RES energy maximisation function. The objective functions are as follows:

$$\min J_1 = C_T \tag{3.1}$$

$$\max J_2 = E_{RES} \tag{3.2}$$

3.2.1.1   Minimisation of the total operating cost C_T

The operating cost in (3.3), is made up of two parts. The first part of (3.3), is related to the operating cost for all generators. It includes the fuel cost for operating thermal generators, the spinning reserve cost to guarantee continuity of supply and the energy cost incurred by the SO to pay the IPPs for the RES generators. The second part of (3.3), is related to the policy requirement from the quantity-based instrument which is known as RO [74], [75]. This ensures that a total quantity of energy exported to customers includes a certain percentage of RES generation per day. The level of obligation is normally provided on an annual basis to the electricity suppliers and all the renewable energy suppliers provide their generated capacity on a monthly basis. The conventional electricity suppliers or generation companies are responsible for ensuring that a portion of their electricity supply comes from RES generators. If the generation companies do not meet their renewable obligation, a penalty is imposed.

In the second expression of (3.3), Υ represents the RO cost which is further calculated in (3.8).

$$C_T = \sum_{t=1}^{T} \left(\sum_{g=1}^{N_G} C_g(P_{g,t}) + \sum_{r=1}^{N_R} C_r(P_{r,t}) + \sum_{m=1}^{N_M} C_m(P_{m,t}) + \sum_{v=1}^{N_V} C_v(P_{v,t}) \right) + \Upsilon \qquad (3.3)$$

$C_g(P_{g,t})$ is the generator cost function which is a quadratic equation as shown in (3.4), where the units for the cost coefficients are $\$/MWh^2$, $\$/MWh$, and $\$/h$ and the generator spinning reserve cost is a linear function as shown in (3.5). In this chapter, the wind and PV plants are owned by the IPPs, therefore the SO must pay a price proportional to their scheduled power. The cost function for RES is given in (3.6) and (3.7).

$$C_g(P_{g,t}) = \sum_{g=1}^{N_G} \left(a_g P_{g,t}^2 + b_g P_{g,t} + c_g \right) \qquad (3.4)$$

$$C_r(P_{r,t}) = \rho_r P_{r,t} \Delta t \qquad (3.5)$$

$$C_m(P_{m,t}) = \zeta_m P_{m,t} \Delta t. \qquad (3.6)$$

$$C_v(P_{v,t}) = \varphi_v P_{v,t} \Delta t. \qquad (3.7)$$

The RO mathematical model is shown in (3.8).

$$\Upsilon = \gamma \left(\alpha \sum_{t=1}^{T} \left(\sum_{g=1}^{N_G} P_{g,t} + \sum_{m=1}^{N_M} P_{m,t} + \sum_{v=1}^{N_V} P_{v,t} \right) - \sum_{t=1}^{T} \left(\sum_{m=1}^{N_M} P_{m,t} + \sum_{v=1}^{N_W} P_{v,t} \right) \right)^+ \qquad (3.8)$$

The α value in (3.8), is the required RO which means that a portion of the total scheduled output power must come from RES, or else a penalty cost is imposed for the undelivered renewable generation. The notation $\Upsilon(\cdot)^+$ is the sigmoid function which is equal to γ if the RES obligation is unattained and 0 otherwise. The γ value in (3.8), is the penalty value that must be paid by generation companies if they do not meet the annual RES obligation. The obligation is set daily [74], [76] and the thermal generation companies are required to produce a percentage of their energy from RES. The generation companies' can also buy ROC from the eligible renewable electricity companies to complement their RES energy production shortfall. These ROCs are presented to the independent regulator to demonstrate compliance to the RO. If the thermal generation companies do not have enough ROC or renewable energy production to meet their obligation, then a penalty is paid to the SO.

3.2.1.2   Maximisation of the renewable energy penetration

The second objective function aims to maximise the injection of renewable energy into the grid. It is worth noting that the second objective on the maximum renewable energy is not completely covered by the minimisation of RO penalty cost in the first objective function. This is because although the renewable energy obligation can be achieved in the first objective function the amount of renewable energy scheduled to the grid may not be maximal. With the second objective function, the amount of dispatched renewable energy must be maximised to overcome the limitation of merely meeting the obligation without maximising the RES energy penetration. The second objective function is shown in

(3.9).

$$E_{RES} = \sum_{t=1}^{T} \left(\sum_{m=1}^{N_M} P_{m,i,t}\Delta t + \sum_{v=1}^{N_V} P_{v,t}\Delta t \right) \tag{3.9}$$

3.2.2   Constraints

The DED problem under investigation has five constraints which are considered as hard or soft constraints. These constraints are:

1. Real power balance which represents the sum of all generating units i.e. the thermal generators, wind power generators and PV plant generators that should meet the forecast demand as given in (3.10).

$$\sum_{g=1}^{N_G} P_{g,t} + \sum_{m=1}^{N_M} P_{m,t} + \sum_{v=1}^{N_V} P_{v,t} = \sum_{b=1}^{N_B} P_{b,t} \; \forall t \tag{3.10}$$

2. Generator ramp rate limits: This is only applicable to thermal generators. The ramp up (UR) and ramp down (DR) units are in MW/h as given in (3.11).

$$P_{g,t} - P_{g,t-1} \le UR_g \; \forall t \tag{3.11a}$$

$$P_{g,t-1} - P_{g,t} \le DR_g \; \forall t \tag{3.11b}$$

3. Generator limits: The generator limits are applicable to both thermal generators and RES generators. Equations (3.12) to (3.13) show the thermal generator limits. Since $P_{m,r}$ and $P_{v,r}$ are the dispatched wind and solar power into the power system, they are represented by (3.14) and (3.15), where the top limit is the forecast wind power generation and solar power generation at time t respectively, which include both the amount of power dispatched to the network and the remaining amount which is either consumed locally or curtailed due to line capacity limit.

$$\bar{P}_{g,t} \le min(P_{g,max}, P_{g,t-1} + UR_g) \; \forall t \tag{3.12}$$

$$\underline{P}_{g,t} \ge max(P_{g,min}, P_{g,t-1} - DR_g) \; \forall t \tag{3.13}$$

$$P_{m,t} \le P_{m,t,gen} \; \forall t \tag{3.14}$$

$$P_{v,t} \le P_{v,t,gen} \; \forall t \tag{3.15}$$

4. Spinning reserve constraints:

$$P_{g,t} + P_{r,t} \le P_{g,max} \; \forall g,t \tag{3.16}$$

$$0 \le P_{r,t} \le SRR_{r,max} \; \forall g,t \tag{3.17}$$

$$\sum_{r=1}^{N_R} P_{r,t} \ge SSRR \; \forall t \tag{3.18}$$

$$\sum_{g=1}^{N_G} P_{g,t} + \sum_{r=1}^{N_R} P_{r,t} \ge \sum_{b=1}^{N_B} P_{b,t} \; \forall t \tag{3.19}$$

where $P_{r,t}$ is the reserve contribution of unit g during time interval t. Constraint (3.16), shows that the sum of the thermal generator and spinning reserves is limited by the maximum thermal generator limit. Constraint (3.17), represents the maximum reserve contribution for each generator where $SRR_{r,max}$ is the maximum contribution of unit g to the reserve capacity. Constraint (3.18), requires that the total system spinning reserves be provided during period t and (3.19), simply means that the total generation and spinning reserve must be able to support the demand without the use of RES generators.

5. Network transmission constraints: For the economic dispatch problem, only the active power of the transmission line under RES forecast is considered, as shown in (3.20).

$$-P_{l,max} \leq P_{l,t} \leq P_{l,max} \ \forall l,t \tag{3.20}$$

The transmission line power of line l at time interval t, which is calculated by DC power flow and disregards system losses for large size power systems as shown in (3.21), [77] and [78]. A SCED approach is used in order to ensure that the power delivered matches the demand while ensuring that the transmission limits are respected.

$$P_{l,t} = \sum_{g=1}^{N_G} G_{l,g}P_{g,t} + \sum_{m=1}^{N_M} F_{l,m}P_{m,t} + \sum_{v=1}^{N_V} H_{l,v}P_{v,t} - \sum_{b=1}^{N_B} D_{l,b}P_{b,t} \tag{3.21}$$

where $G_{l,g}$, $F_{l,m}$, $H_{l,v}$ and $D_{l,b}$ denote the active power transfer coefficient factor between line l and thermal generator, wind farms, solar plant and loads; $P_{b,t}$ is the demand at bus b at time t.

In summary, the optimisation problem is formulated incorporating two objective functions; (3.1) and (3.2), which are subject to constraints, (3.10) - (3.21).

3.3   FORMULATION OF MULTI-OBJECTIVE OPTIMISATION MODEL

The proposed multi-objective optimisation model presented in the previous section is presented in its compact form as follows:

$$\min J(x) = \{J_1(x), J_2(x), \cdots, J_k(x)\} \ \forall k \in K \tag{3.22}$$

$$\text{s.t } h_i(x) = 0; \forall i \in N_I \tag{3.23}$$

$$g_j(x) \leq 0; \forall j \in N_J \tag{3.24}$$

where $J_1(x)$ to $J_k(x)$ represent multiple objective functions in (3.1) and (3.2) where the value of K is 2 and x is the output vector which consists of an optimal dispatch solution for thermal and RES generators. The equality constraint in (3.10) is indicated by (3.23) and the inequality constraints from (5.14) to (3.21) are denoted by (3.24).
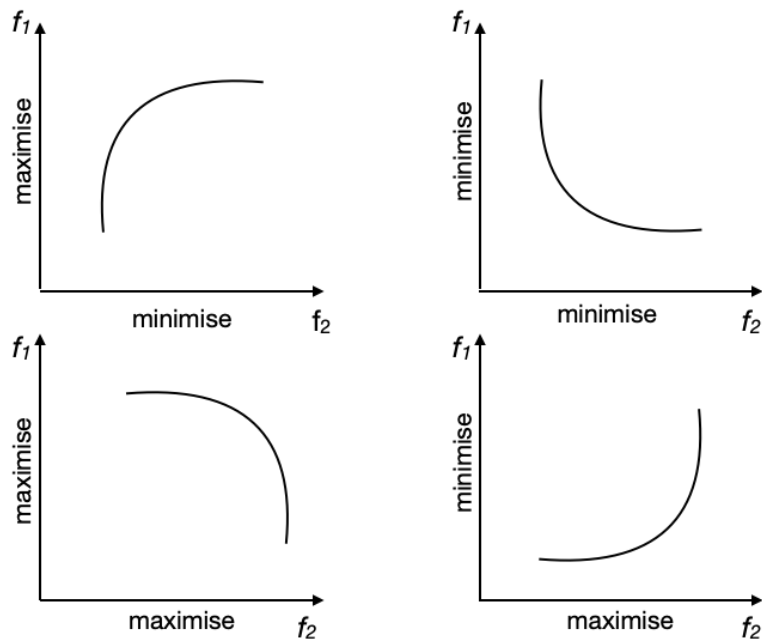
Figure 3.1. Pareto fronts for a bi-objective optimisation problem.

3.3.1   Pareto optimal solution

The multi-objective optimisation problem in (3.22) to (3.24), can be solved using the Pareto optimality principle. The optimal solution x^* in the feasible design space S is the Pareto optimal solution if and only if there exists no other point x in the set S such that $J(x) \leq J(x^*)$ with at least one $J_k(x) < J_k(x^*)$. The set of all Pareto optimal points refers to an optimal solution that is a compromise between the two objective functions. It also follows that an efficient solution exists if a point x^* in the feasible design space S is efficient and there is no other point in x in the set S such that $J(x) \leq J(x^*)$ with at least one $J_k(x) < J_k(x^*)$. Otherwise, x^* is inefficient. Therefore, the set of all efficient points is called the efficient frontier. The Pareto optimal set is on the boundary of the feasible criterion space which also has a unique point called the Utopia point. A point J^0 in the criterion space is called the utopia point if $J_k^0 = min\{J_k(x)\}$ for all x in the set S [79], [80]. This point is obtained by minimising each objective function without consideration of the other objective functions. Figure 3.1, shows the Pareto fronts for bi-objective minimisation and maximisation problems.

It also shows that the direction of the Pareto front depends on whether the bi-objective function is maximisation or minimisation as illustrated by objective functions f_1 and f_2. The Pareto optimal solutions show that there is no single dominant solution in the Pareto frontier and thus there is a set of

solutions that can gives an optimal Pareto solution. Moreover, it is clear from the Pareto frontier that there is a trade-off associated with each Pareto point.

3.3.2   Normalising objective functions

Since there are two objective functions that have different meanings and order of magnitudes, it is important to normalise the objective functions in order to reduce the difficulty in comparison. It is usually necessary to transform the objective functions so that they all have similar orders of magnitude. The objective functions are normalised in (3.25), as follows:

$$J_k^{norm} = \frac{J_k(x) - J_k^0}{J_k^{max} - J_k^0}, \ \forall k \in K \tag{3.25}$$

where J_k^0 is the best point also known as the Utopia point of the objective functions and J_k^{max} is the worst point of the objective functions. The overall objective function J_k^{norm} will give values within the range of 0 and 1.

3.3.3   Weighted sum objective function

The Pareto frontier is generated using the weighted sum approach where each point of the weighted sum gives a Pareto point. This is achieved by uniformly changing the weights from 0 to 1, which provides a series of Pareto points on the Pareto frontier. The two objective functions in (3.1) and (3.2) are presented in (3.26).

$$J^{norm}(x) = \lambda_1 J_1^{norm}(x) - \lambda_2 J_2^{norm}(x) \tag{3.26}$$

The weights are varied between 0 and 1 such that their sum is equal to 1. In order to generate the equidistant points for the weights on the Utopia line, the weight is selected as follows in (3.27) and (3.28):

$$\lambda_1 = q/w = 0, 0.02, 0.04, \cdots, 1. \tag{3.27}$$

$$\lambda_2 = 1 - q/w = 1, 0.98, 0.96, \cdots, 0. \tag{3.28}$$

where q and w are the anchor points of the two single objective optimisation functions. The q value is set as 1 and the w value is set as 50, which means there are 50 Pareto points that form the Pareto frontier. Therefore, a total of 51 equidistant Utopia points are created from the q and w.

3.4   NUMERICAL SIMULATIONS

In this section, two case studies are proposed for demonstrating the effectiveness of the proposed model. The proposed model is demonstrated on a modified IEEE Reliability Test System and IEEE 118-bus system [65], [42]. In the first test system, there are 32 thermal generators and 38 transmission lines, and all the hydro units have been replaced with thermal generators. The ramp rates and quadratic cost coefficients are taken from [65]. Four RES generators are added to buses 3, 5, 17, and 19 respectively,

that is, two wind farms and two PV plants. The data for the four RES generators can be obtained from [81], [82]. The second test system consists of 54 thermal generators and 186 transmission lines. Ten additional RES generators are added onto the system at buses 1, 33, 38, 52, 68, 75, 96, 102, and 117. In the second test system, a combination of five wind farms and five PV plants is used. The details of the quadratic cost coefficients, transmission limits and generator ramp rates can be found in [83]. Moreover, the fixed demand at each bus is a portion of the total capacity at each sampling period. The transmission flow limit is simulated by using DC power flow. A sampling interval of one hour is considered for generation dispatch and the optimisation problem is solved over a 24-hour period. In cases where RES penetration level is unattained, a penalty of $100,000$ per day is imposed on generation companies by the SO. In all case studies, a 10% RES penetration level is used as a base scenario for comparison. In addition, the system spinning reserve requirement is based on 10% of the maximum thermal generator capacity and the spinning reserve requirement of each generator is equivalent to the maximum generator capacity. The wind turbine characteristics in terms of the cut-in speed, rated speed and cut-off speed is 3 m/s, 13 m/s, and 25 m/s respectively. The optimisation problem presented in Section II is a quadratic programming problem; the model has been implemented using MATPOWER for power system analysis [84] in order to find the power transfer distribution factors used in the DC power flow; and the MATLAB FMINCON optimisation algorithm is used as a solver on a notebook with an Intel Core i5 at 2.70 GHz and 8 GB RAM. The optimisation problem is solved in approximately 5 to 10 minutes depending on the number of buses involved. The IEEE 24-bus RTS bus system is used to demonstrate the effectiveness of the modelling considering the following cases:

1. A comparison of the traditional DED model with the proposed model in terms of the maximum RES penetration that can be achieved, the operating cost, and the spinning reserve requirements;

2. A Pareto frontier optimal solution for the multi-objective optimisation problem; and

3. The impact of RO requirement on the model sensitivity.

Thereafter, IEEE 118-bus test system is also used to test the model on a large-scale network to quantify the effectiveness of the proposed model.

3.4.1   IEEE 24-bus RTS System

In this section, the proposed model benefits are demonstrated by comparing them to the classical economic dispatch approach. The maximum renewable energy penetration, the total operating cost,

and the power flow achieved for the proposed and classical economic dispatch model are used for comparison. The sizes of the two PV plants are 75 MW and 140 MW and the sizes of the two wind farms are 300 MW and 500 MW respectively. A total installed capacity of RES generators is 1015 MW. The IPP cost of energy for PV is 35 $/MWh and 39 $/MWh, while the cost of energy for wind is 34 $/MWh and 30 $/MWh respectively. Figure 3.2, shows the forecasted RES generation.
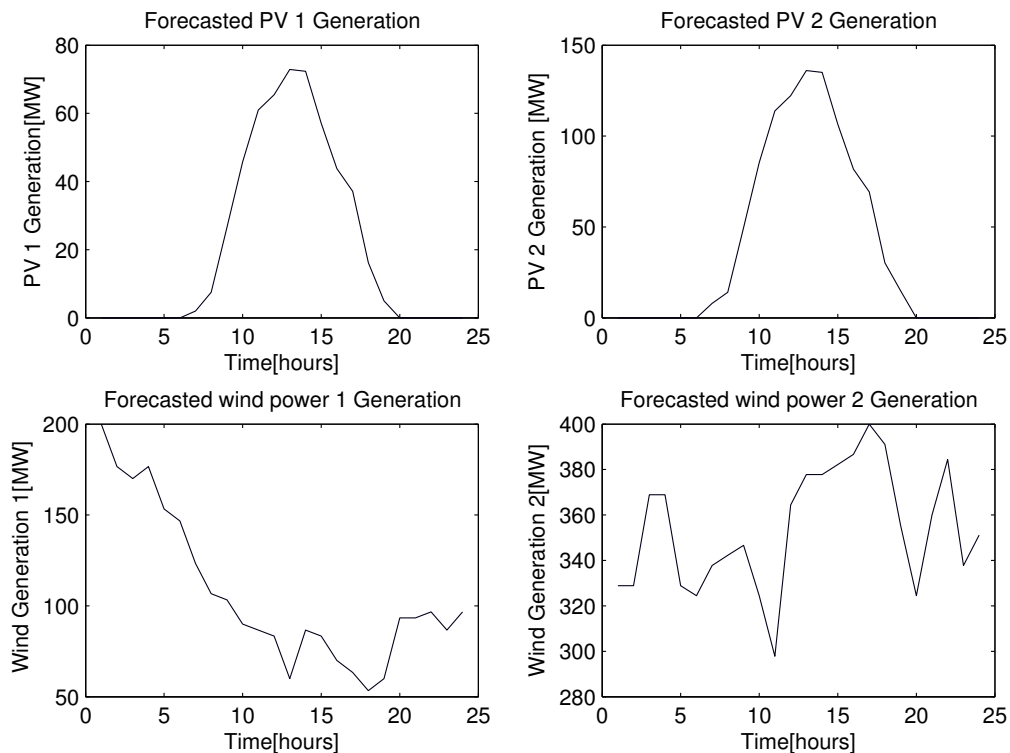
Figure 3.2. Forecasted load demand and RES generation.

The intermittent and variable RES information for the PV and wind power generators is given in Table 3.1 and Table 3.2 respectively, and the details of the transmission line data can be found in [65].

The details of the 32 thermal generator coefficients, capacity and ramp rates are provided in Table 3.3. There are 32 thermal generators which are connected to different buses on the IEEE 24 RTS network as shown in [85]. The details of the hourly demand requirements are shown in Table 3.4.

3.4.1.1   Comparison of traditional DED and proposed DED with RES obligation

In order to compare the traditional DED with the proposed model, it is important to make a distinction between the traditional model and the proposed model in Section II. For the traditional model, the

Table 3.1. PV solar irradiance profile for site 1 and 2.

Description	PV 1	PV 2
K_c (W/m^2)	150	150
Ω (W/m^2)	1000	1000
β	0.5	0.600
κ_1	0.8	1.2
κ_2	4.13	5.4
σ_1 (W/m^2)	150	140
σ_2 (W/m^2)	900	980

Table 3.2. Wind speed profile for site 1 and 2.

Description	Wind 1	Wind 2
κ	1.70	2.0
σ (m/s)	6.653	5.0

Sigmoid function in (3.8), which represents the RO requirement, is ignored. Moreover, the traditional DED model is a single objective function optimisation problem. This means that the maximisation objective function is also ignored. Therefore, the only function involved in the traditional DED problem is the cost function for the thermal generators, the spinning reserve and the cost paid to IPPs for PV and wind power generation. The traditional DED is solved maintaining the spinning reserves as the maximum capacity of the largest generator. For the proposed model, we solve the DED with two conflicting objective functions; one which aims to minimise the total operating cost and the other which maximises the RES penetration level. A comparison of the RES penetration level between the classical DED and proposed model is shown in Figure 3.3.

From Figure 3.3, the RES penetration level for the traditional DED is lower than the Pareto optimal point, which means that the achieved RES penetration for the traditional DED is less than the required 10% obligation. As a result, a penalty is imposed on the traditional DED which results in a higher operating cost in comparison to the Pareto end point 2 as shown in Table 3.5. The impact of RES obligation is shown by the second anchor point which shows a consistent 10% RES obligation. A

Table 3.3. Thermal generator parameters.

Unit	No.	Pmin	Pmax	a_g	b_g	c_g	RU	DR
G1	5	2.40	12	0.025	25.5	24.4	48	60
G2	4	4.00	20	0.012	37.6	117.8	31	70
G3	6	0.00	50	0	0.5	0	60	60
G4	4	15.20	76	0.009	13.3	81.1	39	80
G5	3	25.00	100	0.006	18	217.9	51	74
G6	4	54.24	155	0.005	10.7	142.7	55	78
G7	3	68.95	197	0.003	23	259.1	55	99
G8	1	140.00	350	0.002	10.9	177.1	70	120
G9	2	100.00	400	0.002	7.5	311.9	51	100

Table 3.4. Forecasted demand.

Hour	Load (MW)	Hour	Load (MW)	Hour	Load (MW)
1	1495.2	9	2369.8	17	2460.3
2	1557.8	10	2480.3	18	2474.7
3	1532.7	11	2561.4	19	2461.0
4	1546.1	12	2419.8	20	2591.1
5	1620.6	13	2435.0	21	2624.7
6	1737.1	14	2371.3	22	2546.4
7	1872.2	15	2508.0	23	2309.4
8	2246.3	16	2662.7	24	1924.5

comparison of the thermal and RES generation is made in Table 3.5 which shows the 0.98% increase in operating cost between the Pareto optimal solution and the traditional DED.

The traditional DED RES penetration level is affected by the RES generation cost. Table 3.6, shows the changes in RES energy cost from 100%, 50% to 10%.

It is important to note that the maximum RES injected is achieved when the energy cost is reduced
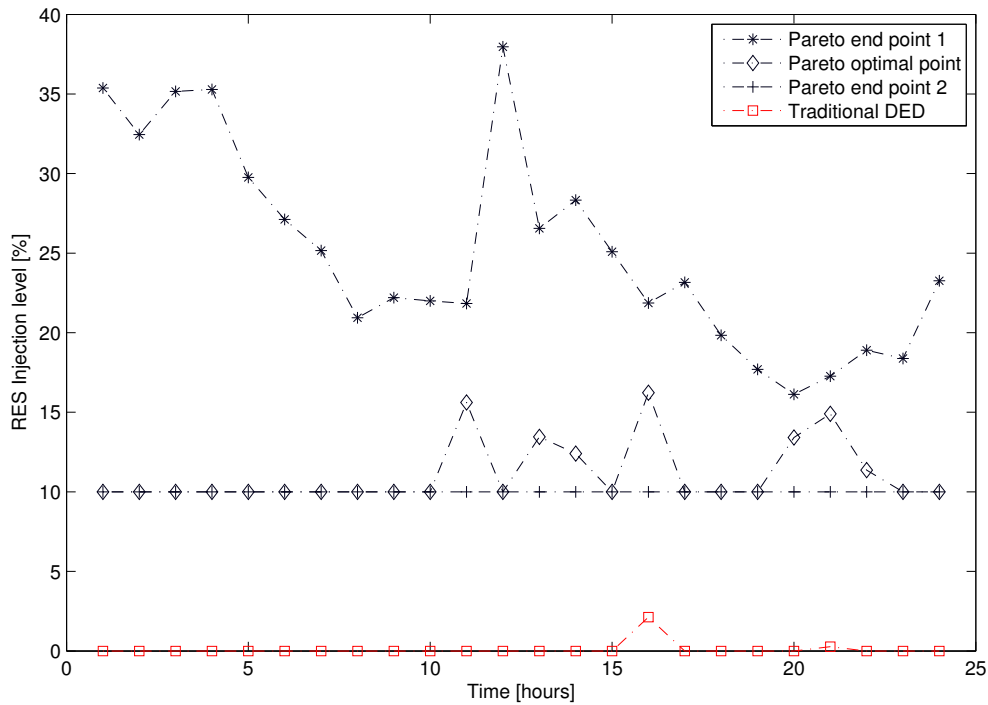
Figure 3.3. Hourly RES injection level between traditional DED and proposed model.

by 90%, which results in 20.85% of RES penetration. The maximum RES achieved for the Pareto solution shown in Figure 3.3, is 25% for the first end point which is 4% more than the traditional DED even with the reduction in RES energy cost. This demonstrates the effectiveness of the proposed model compared to the traditional DED.

3.4.1.2   Pareto frontier solution

In order to find the Pareto frontier for the two objective functions presented in Section II, the first step is to find the minimisation and maximisation point of the two functions in order to normalise the overall function. These two points are called the Pareto anchor points. Table 3.7 presents the anchor points of the two objective functions.

The anchor points are evaluated by finding the letting λ_1 and λ_2 to be 0 and 1, which will provide the first anchor point for J_2 and when λ_1 and λ_2 are 1 and 0, then the second anchor point of J_1 provided as shown in Table 3.7. The Pareto frontiers are presented for the non-normalised and normalised Pareto solution in Figure 3.4.

Table 3.5. Comparison between Pareto optimal solution and traditional DED.

Description	Pareto point	Traditional DED
Thermal (MWh)	45992.61	51820.18
PV (MWh)	1441.55	56.51
Wind (MWh)	4449.65	7.11
SR (MWh)	15565.14	15565.14
RES inj (%)	11.14%	0.12%
Cost ($)	1166356	1077753.11
Penalty cost ($)	-	1177753.11

Table 3.6. Impact of RES penetration on energy cost changes.

Description	100% cost	50% cost	10% cost
Thermal (MWh)	51820.18	50064.19	41066.34
PV (MWh)	56.51	1098.67	1292.03
Wind (MWh)	7.11	720.94	9525.44
SR (MWh)	15565.14	15565.14	15565.14
RES inj (%)	0.12%	3.51%	20.85%
Cost ($)	1077753.11	1 039 575.94	944 719.63
Penalty cost ($)	1177753.11	1 139 575.94	-

The Pareto optimal point shown in Figure 3.4, corresponds to the total operating cost of $1,166,356 and RES energy of 5891.2 MW. The Pareto solution is any solution that lies on the Pareto front curve, the anchor or end points correspond to the scenario where maximum RES penetration is achieved at a maximum operating cost or where a minimal operating cost is achieved with low to minimum RES penetration. A compromise solution is any solution that is on the Pareto front curve where enough RES penetration is achieved at an optimal operating cost with adequate spinning reserves. The RES penetration level for the first anchor point, Pareto point and last anchor point are shown in Figure 3.5.

From the three Pareto points shown in Figure 3.5, all the points satisfy the RES obligation requirement

Table 3.7. Pareto anchor points.

Description	Objective: J_1 [$]	Objective: J_2 [MWh]
Minimisation point J^0	1,151,590	5188.4
Maximisation point J^{max}	1,587,000	12,463
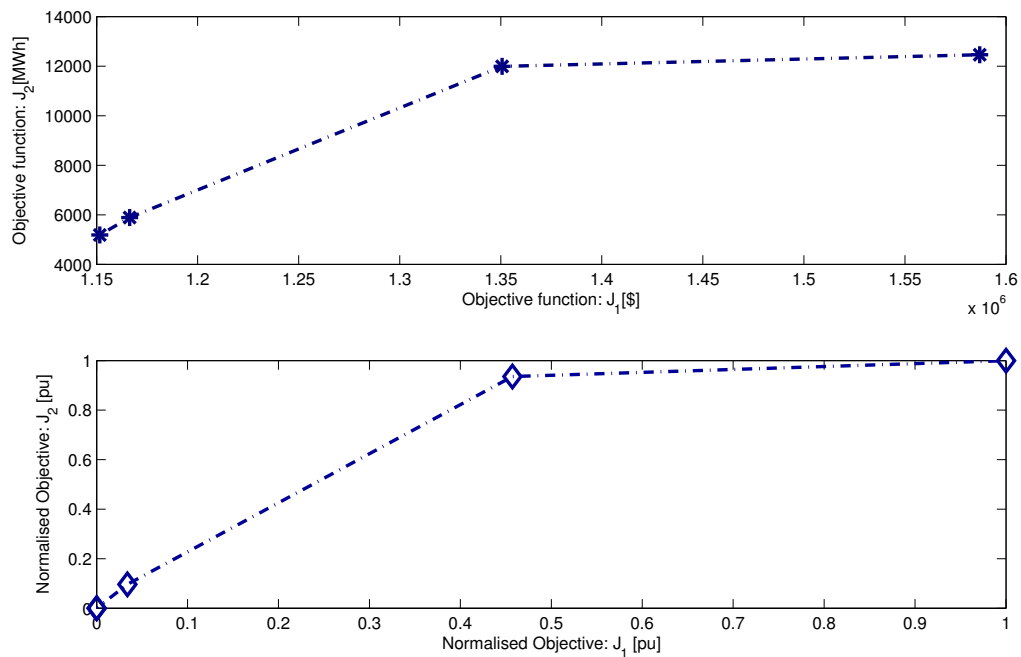
Figure 3.4. Normalised Pareto optimal solution for the IEEE 24 RTS system.

of 10%. In the first end point, a maximum of 38% of RES injection is achieved at 12h00 which corresponds to the maximum solar irradiance available. The overall average RES penetration achieved for the first anchor point is 25.07%. The optimal Pareto point chosen corresponds to the average RES injection level of 11.14% and in the last anchor point the achieved RES penetration level is 10%. It is important to note that the Pareto optimal solution shows the compromise between minimising the total operating cost while maximising the RES penetration and hence the RES penetration level has decreased in comparison to the first anchor point. In the last anchor point, the effectiveness of the proposed model is demonstrated by the achieved RES obligation of 10% with minimal operating cost.
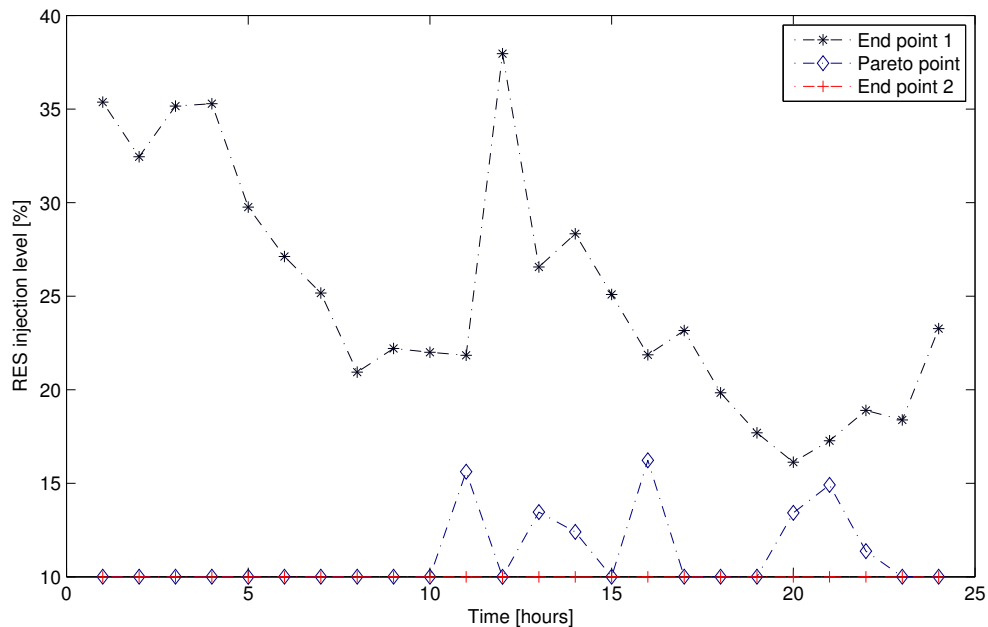
Figure 3.5. Pareto optimal solution for RES injection level of the anchor points and optimal point.

A comparison of the total energy generated over a 24-hour period for the thermal generators, RES generators and required spinning reserves is shown in Table 3.8. In all the Pareto points, the thermal

Table 3.8. Pareto optimal solution generation.

Description	End point 1	Optimal point	End point 2
Thermal Gen (MWh)	39420.85	45992.61	46695.42
PV Gen (MWh)	1479.71	1441.55	1441.55
Wind Gen (MWh)	10983.24	4449.65	3746.83
SR (MWh)	16295.7	15565.14	15565.14
PV Curtailment (MWh)	0	38.16	38.16
Wind Curtailment (MWh)	67.87	6601.47	7304.28

generator contributes the most energy as expected. In the first anchor point, more RES is generated and there is a small wind curtailment of 67.87 MWh and no PV curtailment. The average spinning reserve required is 31.41%. For one of the Pareto optimal points, the PV and wind curtailment is 38.16 MWh and 6601.47 MWh with the achieved RES injection level of 11.14%. The average spinning reserve required to guarantee continuity of power is 30% as shown in Table 3.8. For the last anchor point, the

average RES injection level achieved is 10%, which complies with the RES obligation requirement. The curtailment of RES and minimum spinning reserves is also presented. The Pareto optimal frontier demonstrates the effectiveness of the proposed model by achieving the RES obligation and minimising the total operating costs.

3.4.1.3   Impact of RO on the model operating cost

In this simulation study, the RO is varied from 5% to 50% at a step of 5%. The objective is to find the total RES penetration that can be achieved before any penalty can be imposed. The Pareto frontiers for each RES obligation are shown in Figure 3.6.
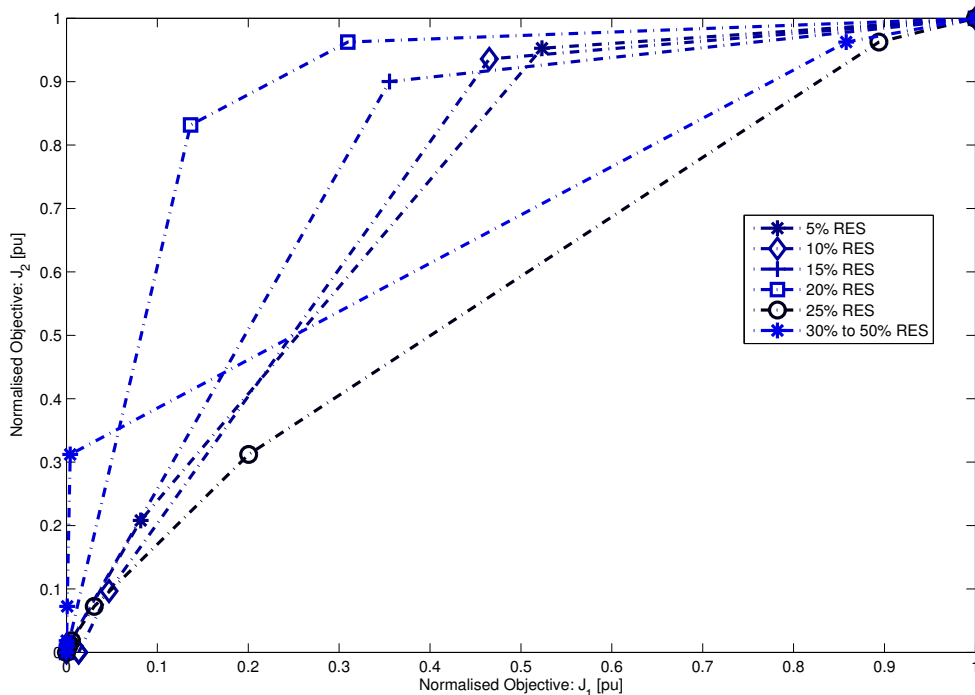
Figure 3.6. Pareto optimal solution for variation in RES penetration from 5% to 50%.

The impact of RES obligation is variable. The RES obligation is achieved for the 5% to 20% case and any RES obligation over 25% to 50% is not achieved. The limitation in this case is based on the available forecasted generation, which means that if more RES generators are added to the network, the limit will increase in the same proportion. From Figure 3.6, the Pareto frontier for 25% is the same as the Utopia line which means that anything over 25% will result in a dominant solution. The maximum RES penetration level is also indicated by the 20% RES Pareto front solution which forms the top limit for all the other Pareto curves. Therefore, from the normalised Pareto optimal solutions

Table 3.9. Pareto optimal solution for a variable RES penetration level.

Description	5%	10%	15%	20%	25%
Thermal [MWh]	49290	45993	44101	39888	39888
PV[MWh]	1215	1292	1292	1480	1480
Wind[MWh]	1379	3896	6491	10517	10517
SR[MWh]	15565	15565	15565	15565	15565
Cost[$]	84968	40998	40998	15257	15257

we observed that the Utopia line corresponds to a 25% RES penetration level. This also shows that any RES penetration over 25% is not attainable from the forecasted RES generation.

As expected, the total operating cost increases with the increase in RES obligation requirement due to the high RES energy cost. Table 3.9 shows the Pareto optimal point for the operating cost and the achieved RES penetration level for thermal and RES generators. When the RES obligation changes, generally the spinning reserve changes in the same proportion. The reason for such a change is the spinning reserve requirement imposed by constraint (3.19), which requires that the thermal generators must be able to sustain the total demand without RES generation. It should also be noted that the total operating cost increases as the RES penetration increases and the transmission thermal limits are respected in all scenarios.

3.4.2   IEEE 118-bus System

The IEEE 118-bus system consists of 118 buses, 186 transmission lines, 91 load sides, 54 thermal generators, 10 RES generators with 5 PV and 5 wind farms. The total demand over a period of 24 hours is 126,854 MWh. In this case study, a RES obligation is maintained at 10% in order to investigate the impact of adding RES generators to the network. Moreover, an optimal RES obligation is investigated to attain the optimal cost of operating an energy mix that consists of thermal generators and RES generators. The ten RES generators are made of 5 PV plants and 5 wind farms with the following sizes: 500 MW, 200 MW, 150 MW, 140 MW and 260 MW for the wind farms; whilst the PV farms are made up of 75 MW, 140 MW, 300 MW, 28 MW and 66 MW. The total installed capacity of the RES generator is 1859 MW. A penalty of $100,000 is imposed if the RES obligation is not achieved. Table 3.10 and 3.11 show the site parameters for PV and wind plants respectively.

Table 3.10. PV solar irradiance profile for site 1 to 5.

Description	PV 1	PV 2	PV 3	PV 4	PV5
K_c (W/m^2)	150	150	140	160	160
Ω (W/m^2)	1000	1000	950	1100	1050
β	0.5	0.6	0.5	0.5	0.5
κ_1	0.8	1.2	0.8	1.6	0.9
κ_2	4.13	5.4	4.13	5.8	4.5
σ_1 (W/m^2)	150	140	150	140	160
σ_2 (W/m^2)	900	980	930	970	900

Table 3.11. Wind speed profile for site 1 to 5.

Description	Wind 1	Wind 2	Wind 3	Wind 4	Wind 5
κ	1.70	2.0	1.90	2.8	2.5
σ (m/s)	6.7	5.0	7.2	5.4	7

Figure 3.7, shows the forecasted curves for demand and RES generation for the IEEE 118-bus system.

It is important to note that during winter seasons in South Africa wind speed can reach rated speed during the day in coastal areas which makes the forecasted wind power depicted in Figure 3.7 possible [81].

3.4.2.1   Pareto frontier solution

The RES obligation is maintained at 10% and the energy cost for wind and PV plants is given in [86]. As part of the Pareto solution, Table 3.12 shows the anchor points and one of the points on the Pareto frontier curve.

The Pareto point in Table 3.12, shows the trade-off between achieving maximum RES penetration at a high operating cost or a scenario of low-RES penetration at a minimum operating cost. Therefore, any solution on the Pareto front will realise a non-dominant solution. Figure 3.8, shows the Pareto frontier curves for non-normalised and normalised.
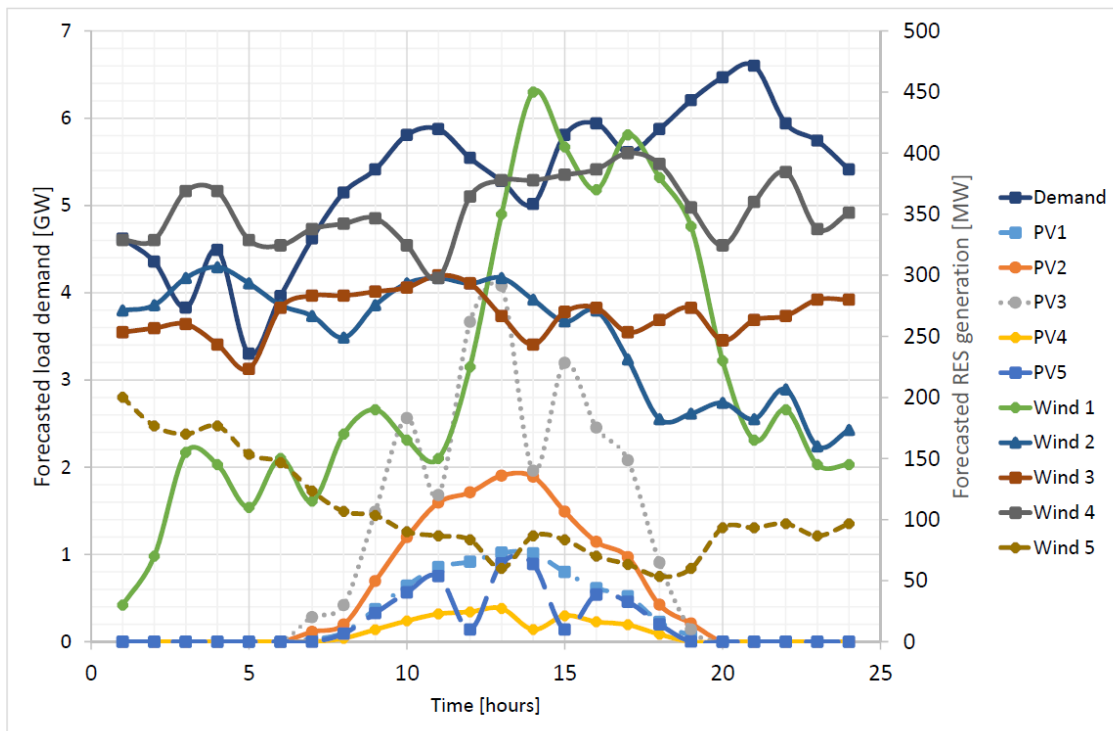
Figure 3.7. Forecasted demand and RES generation for IEEE 118-bus system.

Table 3.12. Pareto anchor points.

Description	Objective: J_1 [$]	Objective: J_2 [MWh]
Minimisation point J^0	3,038,231	13,043
Pareto point	3,041,191	13,087
Maximisation point J^{max}	4,703,000	32,115

In Figure 3.8, the minimum point corresponds to the RES obligation requirement of 10% which demonstrates the effectiveness of the proposed model. A 10% RES obligation is achieved, and the total operating cost is $3,038,231. The RES penetration levels for the two end points and one of the Pareto points are shown in Fig 3.9.

From Figure 3.9, the average RES penetration level for the first anchor point is 25.46% and the minimum average RES penetration corresponds to the last anchor point which is 10.07%. In addition to the anchor points shown in Figure 3.9, a single point in the Pareto frontier curve depicted shows an
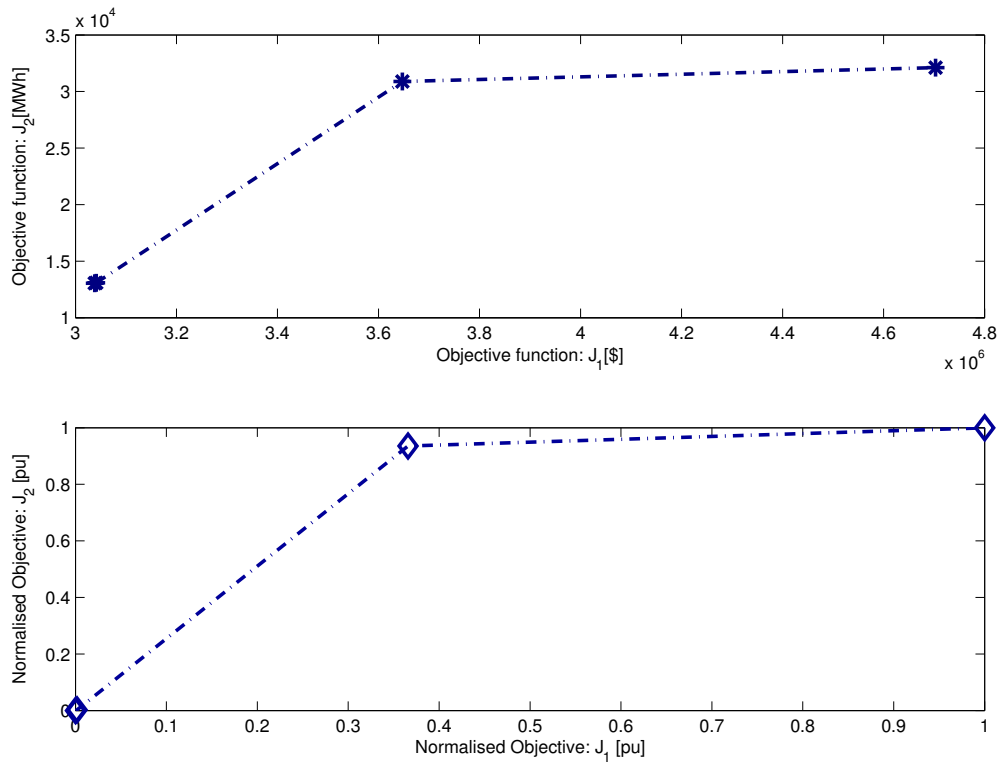
Figure 3.8. Pareto frontier solution for IEEE 118-bus system.

average RES penetration level of 10.31%; this means the RES obligation is attained for this scenario. Table 3.13 shows the achieved generation for thermal and RES generators, the minimum spinning reserves required, the curtailment of RES generators and the achieved RES penetration for each Pareto point.

The RES penetration achieved on the first anchor point demonstrates the typical Pareto solution compromise, which means that for a maximum RES penetration level, the total operating cost is also high. On the contrary, for the first end point, where more RES generation is injected, there is no curtailment for PV generators and a small curtailment for wind generators. This curtailment corresponds to transmission line limit. A significant curtailment is shown for the other Pareto points, however, in all Pareto curves the RES obligation is still attained. This demonstrates the effectiveness of the proposed model which means that a solution that rests anywhere on the Pareto frontier will realise an optimal solution with a compromise between operating cost and RES penetration level.
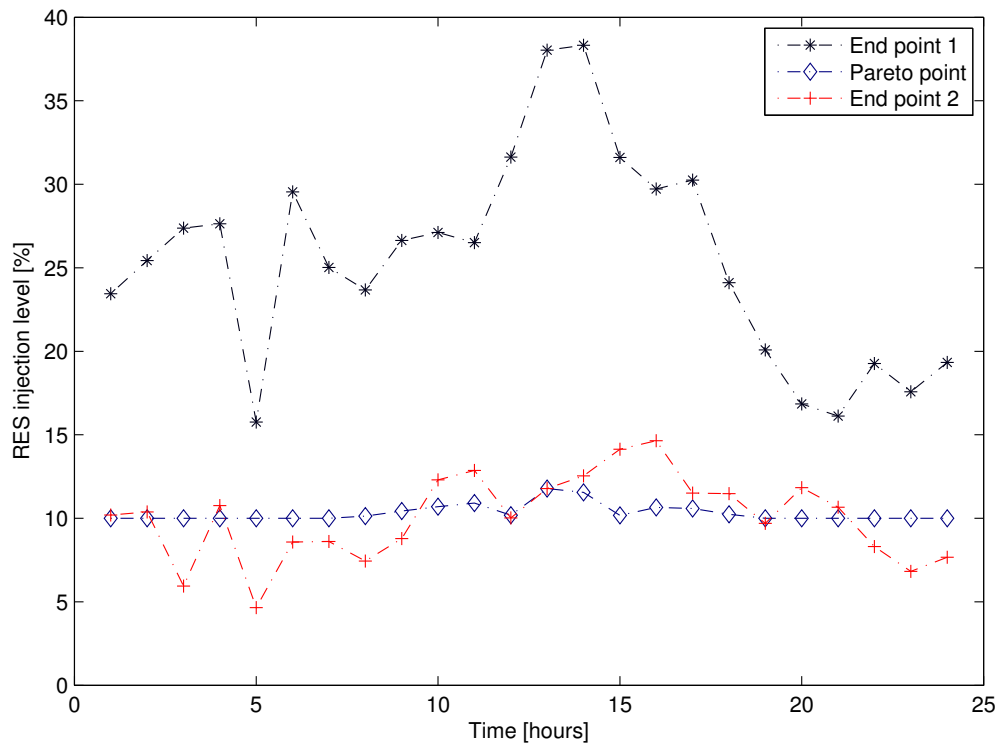
Figure 3.9. Pareto optimal solution for RES injection level of the anchor points and optimal point.

3.4.2.2   Impact of RO on the model operating cost

In this scenario, the impact of varying RES penetration level is investigated to ascertain the maximum RES penetration that can be attained for the forecasted RES generation. As mentioned in the previous case study, the RES penetration level is varied from 5% to 50% at a step of 5%. It is important to note that the task of selecting an adequate solution from a set of optimal solutions is difficult, therefore, to overcome this challenge a sequence of Pareto optimal solutions is presented in Figure 3.10 for different RES penetration levels.

The different Pareto front optimal solutions presented in Figure 3.10, show the impact of RES penetration level. Firstly, we observed that the maximum RES penetration achieved for the IEEE 118-bus system corresponds to the 25% RES penetration Pareto frontier. This means any Pareto optimal solution that is less than 25% RES penetration is attainable without the need for penalty. The 25% penetration level is the Utopia line for the bi-optimisation problem. It was also observed that the 20% RES penetration level is the top Pareto optimal solution that covers all the other Pareto solutions, which

Table 3.13. Pareto optimal solution generation.

Description	End point 1	Pareto point	End point 2
Thermal Gen (MWh)	95096	114125	114169
PV Gen (MWh)	3788	1324	1324
Wind Gen (MWh)	28327	11762	11719
SR (MWh)	38934	38056	38056
PV Curtailment (MWh)	0	2464	2464
Wind Curtailment (MWh)	435.3	17000	17044
RES injection (%)	25.46	10.31	10.07
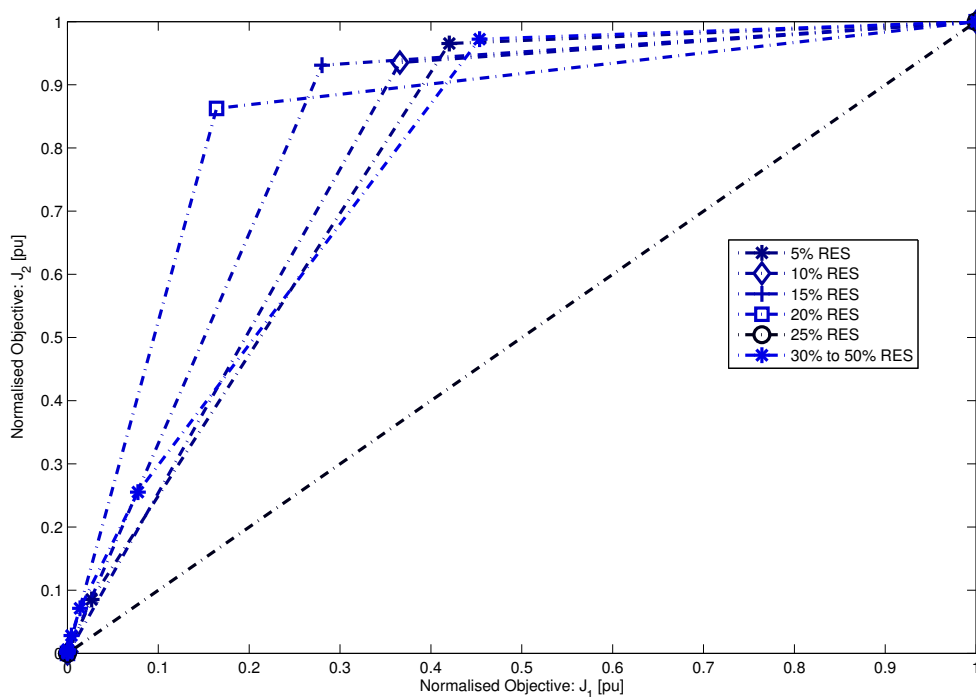
Figure 3.10. Pareto optimal solution for variation in RES penetration from 5% to 50%.

means an optimal Pareto solution for the forecasted RES generation lies in the range of 20% to 25% and any solution over 25% of RES penetration is unattainable due to the limitation in the forecasted RES generation.

3.5   DISCUSSION

In Section 3.4, we presented a case study that investigated the impact of RES penetration from a RO point of view. Three case were presented; in the first case a comparative study between the classical SCED and the proposed RO is investigated. Then the impact of varying the RES energy cost is investigated and compared to the RO model to better appreciate the proposed model robustness to attain the RO. In the second case study a Pareto optimal solution is presented which shows a compromise between maximising the RES energy penetration and minimising the total operating cost while maintaining the renewable energy quota. The final case study shows the impact of varying the RES obligation on the sensitivity of the model. We vary the obligation target from 5% to 50% with a step of 5% to show its impact on the total operating cost and the RES penetration level.

The impact of increasing RES penetration level using renewable obligation policy framework it is better appreciated when we compared the classical SCED. Figure 3.3 shows a comparison between classical SCED and the RO SCED model. The RO model shows a Pareto optimal solution for the end points and optimal point, i.e., minimum, optimal and maximum Pareto point. The RO model can meet the required renewable energy quota compared to the classical SCED model. The classical model shows poor performance in terms of RES penetration and this is due to the cost associated with procuring RES energy which is higher than the traditional thermal generator energy cost. It is interesting to note that for the RO model, the cost of RES is not an important factor in achieving the RES penetration. This is due to the penalty imposed for not achieving RES which is much higher compared to the RES energy cost, and hence in all cases the RO is achieved. To overcome the impact of RES energy cost, Table 3.6 shows the RES penetration level for different energy cost reduction, i.e., from nominal to 90% RES energy cost reduction. Note that in these simulation studies, the RO is set as 10%. It is clear from the simulation results that RES obligation is achieved only when the RES energy cost is reduced by 90%. The first case study demonstrates the importance of including a penalty cost in the RO model by ensuring that the renewable energy quota is achieved. Therefore, the RO models presented in Section II is dependent on the penalty cost which mean that if the penalty cost is low then the RES quota is ignored, and if it high then the RES obligation is achieved based on the available resource and the line thermal limits. This part of the model demonstrates a useful tool for policy makers to encourage energy mix. When we compare the total operating cost of the classical SCED and the proposed RO model we notice that the proposed model operating cost is lower than the classical SCED cost and this is due to the penalty cost imposed for not achieving the RO quota. However, when the RES energy cost is reduced by 90%, the classical SCED operating cost becomes

competitive and the renewable energy quota is achieved. This means that for the RES to be competitive on the classical model, its energy cost must be lower than the thermal generators.

The Pareto optimal solution presented in Section 3.4 shows that there is not a single solution to the model but several optimal solutions. This is clearly demonstrated by Figures 3.6 and 3.10 for the IEEE 24 RTS and 118-bus system. This means that if the first objective function is set to zero, then the overall optimisation problem changes to a maximisation of RES energy penetration that can be achieved without any curtailment. The solution to this problem corresponds to the first end point of the Pareto frontier curve. On the contrary, if the second objective function is set to zero, then the aim simply turns into minimising the total operating while achieving the minimum RES quota set out by the SO and this point is also known as the Pareto end point. These two points are the anchors of the Pareto frontier curves and all the points that lie on the curve forms the Pareto frontier as demonstrated in Figures 3.4 and 3.9. The impact of varying RO is illustrated by the Pareto frontiers shown in Figures 3.6 and 3.10 for the two test systems. The variation in the Pareto frontier curves is due to different RO requirements. For example, if we consider Figure 3.6 for IEEE 24 RTS system, we can observe that the RO is achieved from 5% all the way to 25% of RES penetration. The 25% Pareto frontier forms a Utopia line which shows the maximum RES that can be achieved without any penalty. A RES penetration level over 25% is shown in the same figure which is far less than the RES penetration of all Pareto frontier curves. This demonstrates the effectiveness of the proposed RO model to meet different RES quota obligation.

To summarise the finding of Section 3.4, a RO model leads to higher RES penetration while minimising the total operating cost and spinning reserves. The RO model shows that the only limiting factor to maximum RES penetration is the available resource and transmission thermal limit. Although the CO_2 emission reduction is not quantified in this study, we can infer that the RO model has a potential to decrease CO_2 emission and significantly reduce the operating cost of thermal generators.

3.6   CONCLUSION

A new DED model with RES obligation is presented which integrates RES generation to maximise the RES penetration while minimising the total operating cost and the spinning reserves. The approach presented determines the optimal RES penetration level that minimises the operating cost and spinning reserves while providing continuity of power supply. A bi-optimisation problem is presented that minimises the operating cost and maximises the RES energy penetration. The formulation shows a

trade-off between maximum RES penetration and minimum operating costs. Generally, the proposed model has the advantage of achieving a maximum RES penetration based on the RES obligation and minimising the required spinning reserves and total operating costs. In all the case studies presented, the power transfer flow is respected. The results of the case studies demonstrate the robustness of the proposed optimisation model in terms of RES obligation requirement and optimal operating cost and a trade-off between economical operation and maximum RES penetration.

CHAPTER 4   MULTI-OBJECTIVE ECONOMIC DISPATCH WITH RESIDENTIAL DEMAND RESPONSE PROGRAMME UNDER RENEWABLE OBLIGATION

In this chapter, the renewable penetration is improved by incorporating demand response. Residential customers are paid an incentive for participating in the demand response programme. The mathematical model of the demand response model under renewable obligation is presented.

4.1   INTRODUCTION

In recent years there has been a great deal of attention on the optimal demand and supply side strategy. From the supply side the focus has been on reducing conventional generators by increasing the penetration level of renewable energy sources (RES). While on the demand side several programmes have been introduced to create customer awareness of utilising energy in an efficient manner. The intermittency and stochastic nature of RES such as wind and photovoltaic generators makes it difficult for their integration in the power system. This means that the RES generators cannot be completely regulated by producers throughout the day as they are weather dependent and an increase of RES in power systems requires a robust system. Moreover, the need for capacity margins during peak hour demand coupled with the inherent limited ramping capacity of thermal generators affect the system security whenever the RES generators decrease their output power due to meteorological conditions. To tackle this challenge, the system operator takes the advantage of demand side strategy by either shifting or cutting down the load to balance the RES production. Therefore, it is essential to evaluate the effectiveness of demand response strategy in relation to increasing RES penetration without affecting the system reliability and security.

4.1.1   Literature review

Demand side management (DSM) has two fields that focus on demand management, i.e., energy efficiency (EE) and demand response programmes (DRP). EE concentrates on retrofitting electrical equipment with more energy efficient equipment while DRP focuses on demand management through price-based or incentive-based demand reduction programmes. Both programmes are used to encourage the customers to use electricity prudently. Although a comparison between EE and DRP shows that DRP is more cost-effective in terms of capital expenditure, and as a result it is the most common demand management strategy utilised. DRP takes the advantage of load flexibility patterns to increase the efficient operation of power system. For example, flexible load from residential customers such as electric water heaters can be shifted to low demand period which improves the system performance and allows the system operator (SO) to schedule an optimal energy mix at a least operating cost. Flexible demand is therefore, defined as the potential to modify the consumption profile by varying power consumption, time of operation and the activation time of electrical equipment [51].

Demand response has two components, i.e., tariff and incentive-based instruments that are used to encourage electricity end-users to respond either to changes in electricity prices over time or provide an incentive to customers for reducing their electricity use. The main idea behind all price-based DR is to encourages electricity end-user to take the advantage of the electricity prices in different hours to adjust their flexible loads and move them to low demand periods. The types of price-based demand response are (i) time-of-use (TOU) pricing, (ii) critical peak pricing, (iii) peak load pricing; and (iv) real-time pricing.

On the contrary the incentive-based demand response offers customers incentives in addition to their retail electricity rate for achieving demand reduction on the flexible loads when the system reliability is required or when electricity prices are too high. The types of incentive-based demand response are (i) direct load control (DLC), (ii) interruptible service, (iii) demand bidding/buy back, (iv) emergency demand response programme (EDRP), (v) capacity market programme; and (vi) various ancillary service markets. The demand response is applied to all customers base, i.e. industrial, commercial and residential, and it is normally implemented on non-critical loads that are reducible and deferrable.

A significant amount of research has been conducted in the combined field of dynamic economic dispatch (DED) and DRP which focuses on different types of customers, e.g., residential, commercial

and industrial [87], [88]. A day ahead stochastic economic dispatch with price-based demand response is implemented in [89] where maximum wind energy is added into the grid by encouraging the customer to shift their demand profile which improves the utilisation of the wind energy and reduces the total operating cost. The main disadvantage with this type of price based DRP is the direct dependence of the customer behaviour to voluntarily decrease the demand and it fails to show the impact of direct or indirect load rebound effects [90], [91] due to the DRP implementation. A more robust approach that provides the system operator (SO) with more control and predictability of the demand is the incentive-based demand response. In the US alone, it is estimated that an incentive based DRP can realise up to 93% of the peak load reduction [92]. This direct approach of controlling the customer demand by incentives has resulted in a great deal of interest in researchers. In [93], [94], a stochastic unit commitment with incentive based DRP is presented and a price quantity package for incentive based DRP is reported in [95]. Authors in [96] consider a robust optimisation approach to economic dispatch with renewable energy sources and incentive DRP. A DR approach which considers EDRP and DLC based price elasticity and linear responsive loads i.e. power, exponential and logarithmic models are presented in [97]. A combined DED and DR is used to determine an optimal incentive for customers considering different responsive loads.

In [98], a deep neural network for incentive based DRP is reported where the uncertainties in price and demand are studied by deep learning and neural network. This is to ensure that an optimal incentive price is achieved for the energy demand balance and to improve the grid reliability. A combined dynamic economic emission dispatch (DEED) and DRP for industrial customers is presented in [99] where a game theory demand-based response programme is used to find an optimal hourly incentive that can be offered to customers that participate in load curtailment. The model presented in [100] finds an optimal incentive for customers in order to provide maximum relief to the power system by providing customers incentives for participation throughout the day.

Ref. [46] presents the impact of applying both price-based and incentive-based DR on demand-price elasticity concept while incorporating the customer benefit. In the study, the demand is categorised as flexible load in a micro-grid with residential and commercial customers and the impact of different price and incentive-based schemes are investigated. In [101], a DR scheduling model is presented for smart residential community. The residential loads are classified into different categories based on their demand response capability, i.e., interruptible load, controllable loads and deferrable loads, and thereafter the load is reduced from peak to peak-valley without bringing any customer discomfort. The

integration of distributed generators (DG) is also included to better manage the demand shifting. This study did not incorporate the load rebound effects which results from deferrable load shifting from peak demand period to low demand period.

In South Africa, the main electricity supplier has developed a large-scale residential load management (RLM) programme which is aimed specifically at the residential sector [102]. The electric water heaters also known as geysers account for about 30% and 50% of the electricity consumption in a household [103] and the load can be classified as deferrable. Moreover, the utility's residential customers consume around 20% to 25% of the total electricity generated with their peak period amounting to 35%. The RLM programme involves the connection of ripple control units to electric water heaters which allows the units to be switched on and off remotely by the system operator.

Although all the studies have focused on providing a combined benefit from demand and supply side, the disadvantages with their proposed methods are: (i) the level of customer discomfort caused by regular demand reduction, (ii) the inability of the theoretical DRP models to include the load rebound effects that result from demand reduction programmes due to arbitrary control of flexible load. The literature review shows that residential flexible loads under DR with DLC is performed during periods of high electricity cost and in [51] the authors did not show the impact of load increase outside of the peak period and this implies that the flexible load is reducible. Reference [104] did not quantify the demand reduction due to deferrable loads in their models. In cases where storage is used [105], [106] the authors assume that the cost of electricity from storage is lower than the utility low tariff price which implies that the flexible load during peak hours is automatically supplied by the storage system. Although this may be a benefit, it is important to note that there are cases where the cost of storage is higher than that of the utility and this is not shown in the literature. The use of DG and RES to offset the electricity prices is also proposed by other authors. This approach is generally acceptable since the flexible load can be supplied by RES or DG, however, there is also a challenge with this approach since RES is intermittent and may not be available during peak period or the generation may be inadequate to supply the demand. Lastly, most DRP with flexible residential loads in the literature assume that the deferrable loads do not have load rebound effects and this is mainly due to the lack of real data.

4.1.2   Research Objectives

To address the challenges, this chapter aims to develop a combined demand and supply side economic dispatch model. This includes the renewable obligation policy framework to maximise RES penetration

and deferring residential flexible demands to period of low electricity price. A renewable obligation policy aims to ensure that the deferrable demand can be supplied from RES during peak hours by ensuring that a quota of RES generation is achieved. The customer discomfort level is minimised by limiting the demand reduction to electric water heaters. All participating residential customers have a smart home energy management system (HEMS) which incorporates a DLC unit connected to the electric water heaters that allows remote switching. The main contributions of this chapter are summarized as follows:

1. A multi-objective economic dispatch model is presented which integrates deferrable demand within a real DLC DRP intermittent renewable energy under renewable obligation;

2. Real data from a South African DRP are taken in the optimisation model so that the system operator can decide whether a substation needs to respond to the DR request;

3. The application of the real DRP data avoids traditional inaccurate approaches in assuming the arbitrary controllability of deferrable load and can cover actual load rebound effect.

4.2 RESIDENTIAL LOAD MANAGEMENT FRAMEWORK

RLM is a utility programme that is focused on residential customers with the objective of reducing and shifting the customers flexible load during peak demand periods. The flexible load considered in the programme is the electric water heater.

The residential customers are generally connected at the end of the power grid, while large-scale wind and PV plants are normally connected to the transmission power network as shown in Figure 4.1.

On the residential demand side, all the customers participating in the DRP use a DLC unit which is integrated to the two-way smart metering system to send real-time status of the electric water heater. The customers are aggregated together on each participating substation. A municipality distribution system operator (DSO) acts as a demand aggregator and facilitates the communication between the SO and the customers. The real-time data is used by the utility to manage real-time demand on the power system. In the RLM programme implemented in South Africa, the residential customers participate on a voluntarily basis. However, in this proposed model an incentive is paid to participating customers. In fact, the SO uses DRP as a tool for load shifting and pays an incentive proportional to demand reduction achieved. The customers can choose to participate in the programme during peak demand
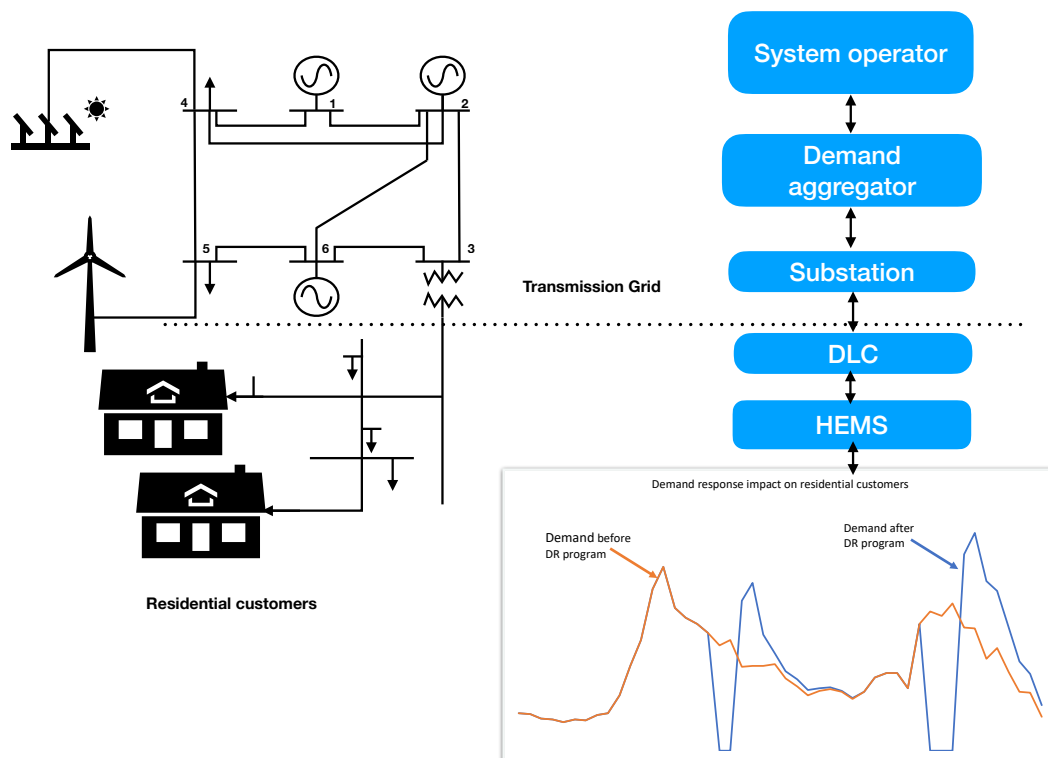
Figure 4.1. Typical RLM programme structure based on an arbitrary 6 bus network.

periods where electricity price is high. If the consumers chose to participate in the programme the demand is reduced and deferred to low demand period and the customers receive an incentive. On the contrary, if the customer declines to participate then the customer pays high electricity price associated with peak demand. All the real-time demand information is managed through a HEMS.

The utility owns all the thermal generators while the RES is owned by independent power producers (IPPs). The system operator is responsible for controlling and dispatching all generators to meet the demand and achieve RO. The DSO is responsible for managing the residential participation to the DRP programme through the substation DLC system. The demand is modelled like negative generation with the minimum and maximum load changes based on customer participation level [107]. The main objective from the SO point of view is to dispatch all the generators to meet the demand while minimising the cost for thermal generators and achieving a RO with minimum power fluctuations from RES generators by utilising demand response.

4.3   PROBLEM FORMULATION

In this section a mathematical model of a renewable obligation model that incorporates the DRP for residential customers is presented. In Section 4.3.1 the RO model is presented and then in Section 4.3.2 the RLM model is presented and finally in Section 4.3.2.3 the modelling or RES is presented.

4.3.1   Renewable obligation

The main purpose here is to minimise the total operating cost for the system operator thermal generators while maintaining a percentage of renewable energy in the energy mix.

4.3.1.1   Objective functions

The total operating cost includes two terms. The first term is the cost of operating thermal generators and the cost paid to IPP for RES generators. The second part is the penalty function that ensures that a minimum renewable obligation is maintained in the dispatch period to guarantee the required energy mix.

$$\varphi_1 = \sum_{t=1}^{T} \left(\sum_{g=1}^{N_G} C_g(P_{g,t}) + \sum_{r=1}^{N_R} C_r(P_{r,t}) + \sum_{m=1}^{N_M} C_m(P_{m,t}) + \sum_{v=1}^{N_V} C_v(P_{v,t}) \right) + \Upsilon \tag{4.1}$$

where $C_g(P_{g,t})$ is the generator fuel cost function which is a quadratic equation, and $C_r(P_{r,t})$ is the spinning reserve operating cost and $C_m(P_{m,t})$, and $C_v(P_{v,t})$ are the cost function for wind and PV generators, respectively, as shown in (4.2) to (4.5).

$$C_g(P_{g,t}) = \sum_{g=1}^{N_G} \left(a_g P_{g,t}^2 + b_g P_{g,t} + c_g \right) \tag{4.2}$$

$$C_r(P_{r,t}) = \sum_{r=1}^{N_R} \rho_r P_{r,t} \Delta t. \tag{4.3}$$

$$C_m(P_{m,t}) = \sum_{m=1}^{N_M} \zeta_m P_{m,t} \Delta t. \tag{4.4}$$

$$C_v(P_{v,t}) = \sum_{v=1}^{N_V} \tau_v P_{v,t} \Delta t. \tag{4.5}$$

The notation Υ is the second part of the total cost which is a renewable obligation part of the model shown in (4.6).

$$\Upsilon = \gamma \sum_{t=1}^{T} \left(\alpha \left(\sum_{g=1}^{N_G} P_{g,t} + \sum_{s=1}^{N_S} P_{s,t} + \sum_{m=1}^{N_M} P_{m,t} + \sum_{v=1}^{N_V} P_{v,t} \right) - \left(\sum_{m=1}^{N_M} P_{m,t} + \sum_{v=1}^{N_V} P_{v,t} \right) \right)^+ \tag{4.6}$$

where γ is the penalty imposed to the thermal generators for not achieving the required renewable obligation, α is the renewable obligation requirement in percentage. The notation $\Upsilon(\cdot)^+$ is the sigmoid function which is equal to γ if the RES obligation is unattained and 0 otherwise. The penalty γ is normally provided by the energy regulator as an annual value. This penalty value can be changed to a daily penalty value corresponding to daily economical dispatch of generators.

4.3.1.2   Maximise renewable energy penetration

The second objective function is to maximise the injection of renewable energy into the grid. It is worthy to note that the second objective on the maximum renewable energy is not completely covered by the minimisation of renewable obligation violation cost in the first objective function. This is because at times the renewable energy obligation can be met in that case no penalty is paid, however, the amount of renewable energy power scheduled to the grid may not be maximal. With the second objective function the amount of dispatched renewable energy has to be maximised to overcome the limitation of merely meeting the obligation without maximising the RES energy penetration. In addition to the total operating cost in (4.1), the maximization of RES penetration is shown in (4.7).

$$\varphi_2 = \sum_{t=1}^{T} \left(\sum_{m=1}^{N_M} P_{m,t}\Delta t + \sum_{v=1}^{N_V} P_{v,t}\Delta t \right) \tag{4.7}$$

4.3.1.3   Constraints

The system constraints is divided into five parts, the power balance constraint (4.8), the system ramping rates (4.9) to (4.12), the generator limits (4.13) to (4.16), spinning reserve constraints (4.17) to (4.20)

and the network transmission capacity constraints (4.21) to (4.22).

$$\sum_{g=1}^{N_G} P_{g,t} + \sum_{m=1}^{N_M} P_{m,t} + \sum_{v=1}^{N_V} P_{v,t,} = \sum_{b=1}^{N_B} P_{b,t} \ \forall t \tag{4.8}$$

$$P_{g,t} - P_{g,t-1} \leq UR_g \Delta t \ \forall t \tag{4.9}$$

$$P_{g,t-1} - P_{g,t} \leq DR_g \Delta t \ \forall t \tag{4.10}$$

$$P_{r,t} - P_{r,t-1} \leq UR_g \Delta t \ \forall t \tag{4.11}$$

$$P_{r,t-1,} - P_{r,t} \leq DR_g \Delta t \ \forall t \tag{4.12}$$

$$P_{g,t} \leq min(P_{g,max}, P_{g,t-1} + UR_g \Delta t) \ \forall t \tag{4.13}$$

$$P_{g,t} \geq max(P_{g,min}, P_{g,t-1} - DR_g \Delta t) \ \forall t \tag{4.14}$$

$$P_{m,t} \leq P_{m,t,gen} \ \forall t \tag{4.15}$$

$$P_{v,t} \leq P_{v,t,gen} \ \forall t \tag{4.16}$$

$$P_{g,t} + P_{r,t} \leq P_{g,max} \ \forall g,t \tag{4.17}$$

$$0 \leq P_{r,t} \leq SRR_{r,max} \ \forall t \tag{4.18}$$

$$\sum_{r=1}^{N_R} P_{r,t} \geq SSRR \ \forall t \tag{4.19}$$

$$\sum_{g=1}^{N_G} P_{g,t} + \sum_{r=1}^{N_R} P_{r,t} \geq \sum_{b=1}^{N_B} P_{b,t} \ \forall t \tag{4.20}$$

$$-P_{l,max} \leq P_{l,t} \leq P_{l,max}, \ \forall l,t \tag{4.21}$$

$$P_{l,t} = \sum_{g=1}^{N_G} G_{l,g} P_{g,t} + \sum_{m=1}^{N_M} F_{l,m} P_{m,t} + \sum_{v=1}^{N_V} H_{l,v} P_{v,t} - \sum_{b=1}^{N_B} D_{l,D} P_{b,t} \tag{4.22}$$

The maximum spinning reserve requirement $SRR_{r,max}$ is equal to the maximum thermal generator capacity, and the system spinning reserve requirement (SSRR) is equal to 30% of demand $P_{b,t}$; where $G_{l,g}$, $F_{l,m}$, $H_{l,v}$, and $D_{l,D}$ denote the generator shift factor (GSF) coefficient between line l and thermal generator, wind farms, PV plant, and system demand at each bus. The transmission line power $P_{l,t}$ of line l at time interval t is calculated using DC power flow.

4.3.2   Residential load management

The programme considers voluntary participation by residential customers to reduce and shift their demand. However, in this case the DRP model assumes an incentive is paid to participating customers. The load reduction request from the utility can be anytime of the day and particularly when the demand is high.

4.3.2.1   Demand response programme model

The price-based DR objective function presented in (4.23) is known as the customer utility function which aims to minimise the discomfort level due to the lack of electricity.

$$\varphi_3 = \sum_{t=1}^{T} \sum_{b=1}^{N_B} \left(\left(\lambda_t^R - \xi_{b,t}^c \right) \left(P_{b,t}(1 - u_{b,t}) + \tilde{P}_{b,t} u_{b,t} \right) \right) \Delta t + \sum_{t=1}^{T} \sum_{b=1}^{N_B} \Delta P_{b,t} u_{b,t} \xi_{b,t}^i \tag{4.23}$$

Equation (4.23) refers to the total cost associated with minimising the customer discomfort level which measures the benefit the consumer achieves by using electricity during time period t, λ_t^R is the TOU price of electricity while $\xi_{b,t}^c$ is the benefit or willingness of the customer to buy electricity for performing tasks requiring electricity. For simplicity, the benefit for the consumer is assumed to be constant and time independent which implies that the residential load is deferrable since the task can be performed at any time during the day.

To encourage residential customer participation, an incentive is introduced to the model to quantify the impact of demand reduction and demand deferred as a result of the incentive and the residential customers are incentivized only during peak hours which is assumed to correspond to high demand period.

The incentive price paid to customers is $\xi_{b,t}^i$ and $\Delta P_{b,t}$ is the difference between the actual demand at the participating DRP bus b before and after the demand reduction.

$$\Delta P_{b,t} = P_{b,t} - \tilde{P}_{b,t} \tag{4.24}$$

The DLC switching status $u_{b,t}$ is a binary variable that is equal to 1 if the RLM is implemented at bus b in time t and 0 indicating that no RLM is implemented.

4.3.2.2   Constraints changes

The only changes in the constraints are due to the change in demand which is replaced by in (4.25); the constraints affected by the demand reduction are (4.8), (4.19), and (4.20). The change of constraint (4.19) is due to the fact that SSRR is equal to 30% of demand $P_{b,t}$ that guarantee enough spinning reserves.

$$P_{b,t} = \sum_{b=1}^{N_B} \left(P_{b,t}(1 - u_{b,t}) + \tilde{P}_{b,t} u_{b,t} \right) \ \forall t. \tag{4.25}$$

The two cost functions can be added together to form a new objective function as shown in (4.26).

$$\min \varphi_{TC} = \varphi_1 + \varphi_3 \tag{4.26}$$

4.3.2.3 Implementation steps for RES selection and output power estimation

The step-by-step approach for selecting RES location and estimate RES output are as follows.

1. Collect 1-year data for wind speed [81] and solar irradiance [82] related to each wind and PV site.

2. Pre-data processing: remove measurement errors and outliers.

3. Formulate a histogram of the wind speed and solar irradiance data.

4. Calculate the average wind and solar power density from the real data.

5. Fit the histogram with the best PDF or multimodal PDF, i.e., Weibull and bimodal Weibull.

6. Estimate the initial parameters of the PDFs.

7. Calculate the wind and solar power density of the histogram which also includes the PDF.

8. Calculate the sum of wind power density and solar power density.

9. Estimate the PDF parameters using least square method in excel solver by finding the best parameters that match the wind and PV power density curves.

10. Calculate the wind and solar CDF functions based on the estimated parameters.

11. Forecast wind power and PV output power

A flow chart representing a step-by-step approach is shown in Figure 4.2.

4.4 MULTI-OBJECTIVE OPTIMISATION APPROACH

There are generally several approaches that can be utilised to solve a multi-objective problem in the literature. These methods are typically, the weighted sum [108], global criterion [109] and ε-constraint [110] to mention a few. In this chapter, ε-constraint method is used to change the multi-objective optimisation problem into a single objective problem. The reason for selecting this method originates from the fact that it is efficient for solving non-convex and non-linear problems such as the one presented. A single objective function is considered in the ε-constraint methods while the other objectives are changed into constraints as shown in (4.27).

$$\begin{aligned} \min \quad & \varphi_{TC} \\ \text{s.t.} \quad & \varphi_2 \geq \varepsilon \\ & \text{eqs. } (4.8) - (4.22) \end{aligned} \qquad (4.27)$$

The constraints are increased from the minimum value to the maximum to generate a Pareto front. The minimum and maximum values of the constrained objective function are calculated by maximising
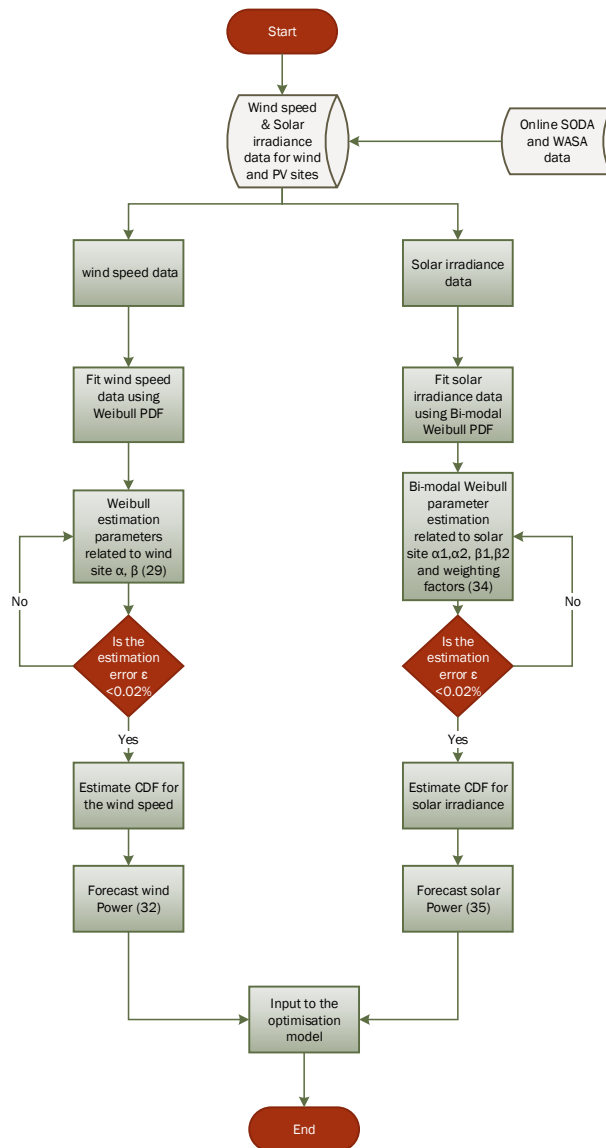
Figure 4.2. A step-by-step approach to estimating wind and PV PDF parameters and output power.

and minimising those functions. Thereafter, the ε-constraint bounds increase from the minimum to the maximum function.

There are different methods used in the literature that assist in selecting the best compromise solution. For example, in [110] a fuzzy set approach is used to select the best solution by using a linear membership function. The membership function is assigned to the objective function which varies from 0

to 1 for measuring each Pareto optimal solution. In [109] a VIKOR technique is used for specifying the preferred solution and then ranking all Pareto solution to the ideal solution. A preference-based approach similar to [108] is used for the best compromise solution in a Pareto optimal set. To select the best compromise solution, the SO is the main decision maker. All decisions are implemented considering demand reduction, renewable obligation requirements, spinning reserve allocation, operating cost and RES penetration level. The SO determines the allowable values for both the demand reduction operating costs and the maximum RES penetration level. To this end, the SO selects the minimum lower bounds related to maximising RES penetration and upper limit for minimising the total operating cost. These upper and lower bounds assist the SO to select the best compromise solution on a Pareto optimal set.

4.5 NUMERICAL CASE STUDIES

The modified IEEE 30-bus and IEEE 118-bus test systems are used to validate the proposed DRP model over a 24-hour time horizon using a temporal resolution of 60-minutes. The historical data of RES generators is collected over a period of a year from January 1st 2018 to December 31st 2018 and it can be found in [81], [82]. The system load is obtained from a real RLM study performed in SA [111] which also includes the total number of electric water heaters used, the capacity and the temperature range of the storage tank. The modified IEEE 30-bus system has 6 thermal units and 41 transmission lines. The system data for IEEE 30-bus can be found in [112], which includes all the ramp rates, thermal transmission limits and quadratic cost coefficients for the thermal units.

The modified IEEE 118-bus system consists of 54 thermal generators and 186 transmission lines. The system detailed data of units and network parameters can be found in [83]. A total of 10 RES generators (5 PV and 5 wind farms) are added to the network on buses 1, 33, 38, 52, 58, 75, 96, 102 and 117. The transmission line flow limit is simulated using DC power flow at a sampling interval of 60-minutes. In all the simulation studies, a RES penetration level of 10% is used as a benchmark. In the case where RES penetration level is not achieved a penalty of $100,000 per day is imposed. In addition, the system spinning reserve required is based on 30% of the maximum demand and the spinning reserve of each generator is equal to the maximum generator capacity.

The DSO is responsible for implementing the RLM switching at the substation based on SO DRP requirement. An incentive of $40 per MWh is paid to participating customers for achieving demand reduction. The utility sell electricity to all customers based on the TOU tariff scheme, which is divided

into three periods, i.e., peak, off-peak, and valley. The electricity price is $200/MWh, $50/MWh and $100/MWh for the TOU period. The customer willingness to buy electricity is $120/MWh. In this study, peak period is classified as 07:00 to 09:00 in the morning, 18:00 to 20:00 in the evening; the valley period is from 09:00 to 18:00 and from 20:00 to 21:00 and remaining period is classified as off-peak.

The simulation is conducted on a notebook with an Intel Core i5 at 2.70 GHz and 8 GB of RAM. The optimisation model is a mixed integer quadratic programming (MIQP) problem and it is built in IBM ILOG CPLEX. The tolerance gap in the CPLEX solver is set to 0.02%. To show the effectiveness of the DRP RO model, the effects of operating cost, spinning reserve allocation, incentive cost, substation participation to RLM programme, RES penetration increase, peak RES increase or decrease, peak demand reduction, demand deferred to other time periods and total demand reduction are analysed. The DRP RO model is tested on the modified IEEE 30-bus system considering the following cases.

1. A base case scenario which considers the proposed model without the implementation of DRP DLC;

2. The implementation of the proposed model with DRP DLC; and

3. Comparison of the base case to the proposed DRP DLC model.

Thereafter, IEEE 118-bus system is also used to test the model on a large scale and the sensitivity of the model to RES penetration against DRP DLC in terms of spinning reserve, total demand reduction and increase in RES penetration.

4.5.1   Implementation steps

The step-by-step approach for implementing the stochastic RO model for a combined energy and reserve dispatch is as follows.

1. Input demand before and after RLM, 24-hour RES output data, TOU tariff, incentive cost for DRP participation and customer willingness cost of electricity.

2. DSO provides daily demand reduction forecast for participating substations to SO.

3. Formulate ε-constraint optimisation model.

4. Evaluate RO and DRP requirements.

5. Provide an optimal Pareto set.

6. Implement preference-based approach to select the best compromise solution using lower and upper boundaries provided by the SO.

7. Schedule RO and DLC to participating substations according to the best compromise solution.

The overall implementation flow chart is shown in Figure 4.3.
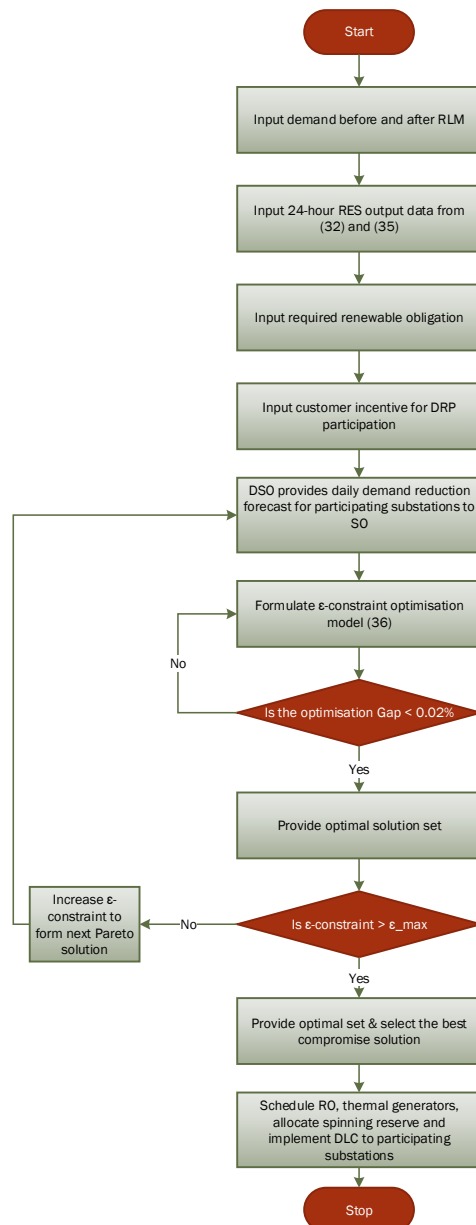
Figure 4.3. Optimisation algorithm for solving multi-objective DRP-RO model with Pareto optimal set and preference-based approach for selecting the best compromise solution.

Table 4.1. Thermal generator parameters.

Unit	Pmin	Pmax	a_g	b_g	c_g	RU	DR
G1	50	350	0.0070	7	240	60	60
G2	50	250	0.0095	10	200	60	60
G3	50	150	0.0090	8	220	60	60
G4	50	350	0.0090	11	200	60	60
G5	50	450	0.0080	10.5	220	60	60
G6	50	500	0.0075	12	190	60	60

4.5.2 Modified IEEE 30-bus

The modified IEEE 30-bus test system has a total demand before and after RLM of 26822.5 MW and 26501.3 MW. The integrated PV and wind farms are connected to buses 7, 15, 22, and 24, i.e. two PV plants and two wind farms. The sizes of the PV and wind farms are 75 MW, 140 MW, 300 MW and 500 MW with an installed capacity of 1015 MW. The parameters of thermal units and RES generators are listed in Tables 4.1 - 4.3 respectively [86].

Table 4.2. PV solar irradiance profile for site 1 and 2.

Description	PV 1	PV 2
K_c (W/m^2)	150	150
Ω (W/m^2)	1000	1000
β	0.5	0.600
κ_1	0.8	1.2
κ_2	4.13	5.4
σ_1 (W/m^2)	150	140
σ_2 (W/m^2)	900	980

The RLM programme is applied to load buses, also referred to as substations. The substations participating in the RLM programme are located on buses 10, 14, 23 and 26. The total demand before and after the implementation as well as the forecasted RES penetration is shown in Figure 4.4.

Table 4.3. Wind speed profile for site 1 and 2.

Description	Wind 1	Wind 2
κ	1.70	2.0
σ (m/s)	6.653	5.0
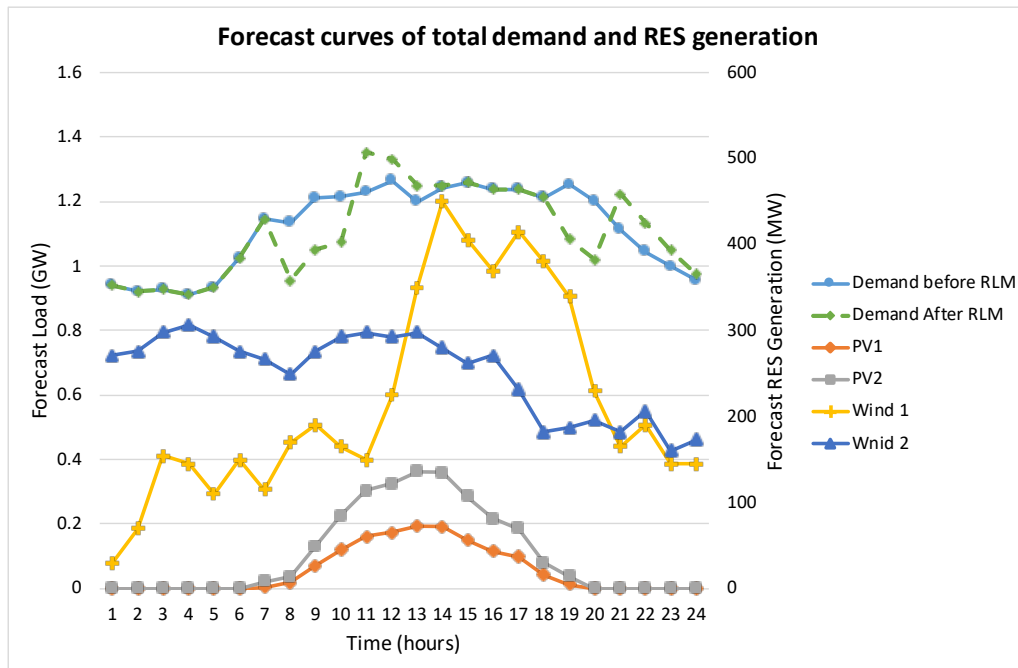
Figure 4.4. Forecasted demand and RES generation before RLM is implemented.

4.5.2.1   Normal operation without demand response

In this case the normal operation without demand response is investigated in terms of total operating cost, maximum achieved RES penetration and the allocated spinning reserves. In the first case, a Pareto front is used to select the best compromise solution for the multi-objective optimisation problem. The minimum and maximum values of the two objective functions are calculated and thereafter, the ε-constraint method is used to generate multiple solutions related to the changes of the ε-constraint. Table 4.4 shows the Pareto optimal set for different RES penetration level. The italic values refer, to the minimum and maximum values used in formulating the Pareto set. To select, the best compromise

Table 4.4. Pareto optimal set under renewable obligation of 10%.

RES (MWh)	TC ($)	SR (MW)
7934.70	*313,880.00*	*8168.10*
7983.70	313,880.00	8215.90
8053.70	313,890.00	8283.00
8115.30	313,910.00	8341.00
8149.30	313,930.00	8370.90
8158.00	313,940.00	8377.10
8158.00	313,940.00	8377.10
8160.80	313,940.00	8379.90
8241.00	313,980.00	8389.80
8241.00	**314,520.00**	**8456.80**
8592.30	*1102400.00*	*30983.00*

solution from a Pareto optimal set, the SO is the main decision marker. In this case the lower and upper boundaries related to the total operating cost and RES penetration level are set to $400,000 and 8200 MWh. From the SO boundaries, the best compromise solution is highlighted in bold as depicted in Table 4.4. A detailed analysis of the best compromise solution for a 24-hour dispatch period is shown in Figure 4.5.

The generation from thermal units makes up the largest contribution and followed by RES generators. The total operation costs for supplying electrical demand is $314,520. The thermal units generate 18581.5 MWh (69.28%) and RES generators contribute 8241.01 MWh (30.72%) to the total demand. A maximum of 8456.80 MW is allocated for spinning reserve services.

4.5.2.2 Implementation of incentive based DRP

The demand on the IEEE 30-bus test system is divided into deferrable, firm and reducible loads. The demand before and after the RLM is depicted in Figure 4.4. In this case, the impact of DLC is evaluated considering the operation costs, spinning reserve allocation, substation participation level, incentive paid to customers, total RES and thermal generation levels and the achieved demand reduction. A Pareto optimal set is shown in Table 4.5 as well as the best compromise solution according to the SO. The best compromise solution is highlighted in bold and corresponds to RES penetration level of
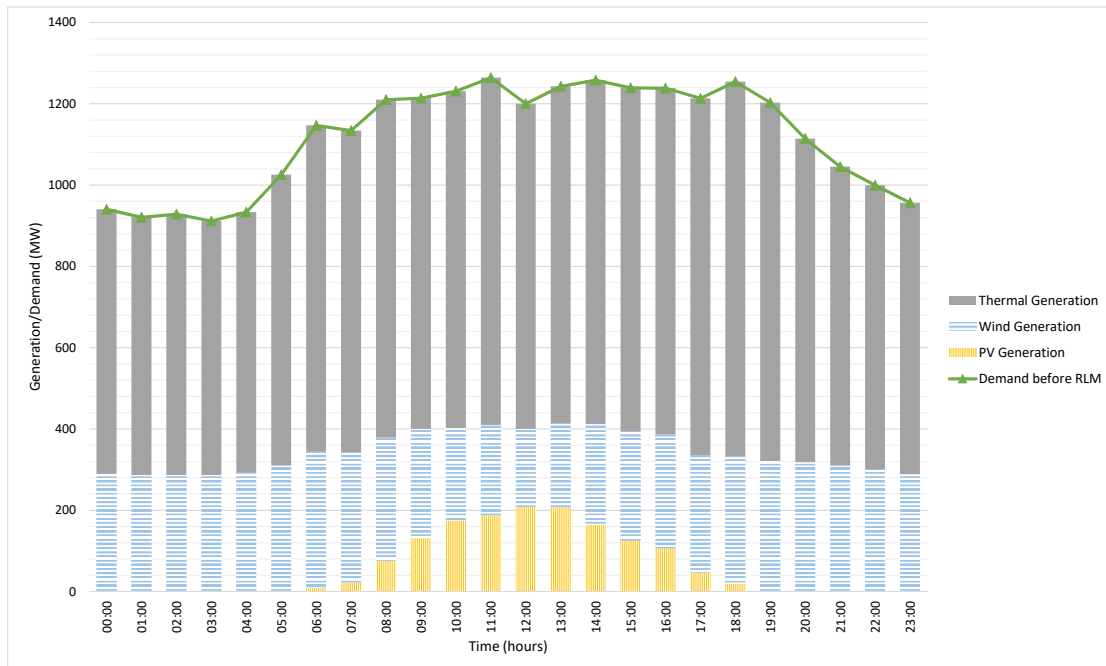
Figure 4.5. Demand and generation for 24-hour dispatch period considering 10% RES penetration level.

8296.30 MWh and total operation cost of $246,670.00.

When DRP is implemented on the substations, the total demand reduced during peak hour period is 830 MW while the demand deferred from peak to valley and off-peak is 509.72 MW. The difference between the peak demand reduction and deferred load is 321.12 MW which is the actual achieved demand reduction due to DLC implementation. This is properly shown in Figure 4.6 where the RES and thermal unit generation makes up the hourly demand. From Figure 4.6 the morning peak corresponds to the time when wind power is available and PV production is not a low and this is like evening peak period. The total generation from thermal and RES units over a 24 our period is 18205 MWh (68.69%) and 8296.34 (31.31%) while the spinning reserve allocation is 8424.79 MW. The substations contributing to RLM programme are active during peak hours which means they have reduced their loads. In total throughout the peak period the RLM substation are actively participating in the programme. This results in a total incentive of $12,844.8 MW to all the customers participating in the RLM.

Table 4.5. Pareto optimal set under renewable obligation of 10% and DLC.

RES (MWh)	TC ($)	SR (MW)
7951.30	245,640.00	8080.20
7987.60	245,640.00	8116.60
8044.00	245,650.00	8173.20
8095.20	245,670.00	8224.40
8111.20	245,680.00	8240.40
8112.20	245,680.00	8241.30
8113.60	245,680.00	8242.70
8134.50	245,720.00	8263.50
8174.60	245,840.00	8303.30
8296.30	**246,670.00**	**8424.80**
8592.30	1,091,700.00	31381.00

The reduction in demand during peak-demand period assists in lowering the system stress on the flexible units to supply peak demand and reduce the overall operating costs. Moreover, the increase in demand during valley period contributes to lowering the power production of highly loaded base load generating units.

4.5.2.3   Comparison between base scenario and DRP DLC scenario

In this case study a comparison of Section 4.5.2.1 and Section 4.5.2.2 results is conducted. In the first case a Pareto front curve for the two scenarios is presented in Figure 4.7 which shows the two curves based on whether the DLC is implemented or not. From Figure 4.7, the Pareto front curve where DRP is implemented is below the curve where there is no DLC programme. In this case, DRP is implemented to improve the system flexibility by ensuring that more RES can be injected in the power system. For the DRP Pareto front, more RES is injected at a low cost compared to the normal case without DRP. This shows that the DLC programme increases RES penetration compared to the normal RO penetration model without DLC. It also illustrates the importance of demand flexibility as an important tool to improve fluctuations in RES generation by allowing more RES penetration.

Table 4.6 shows a detailed comparison of the base scenario RO model and the DLC RO model.
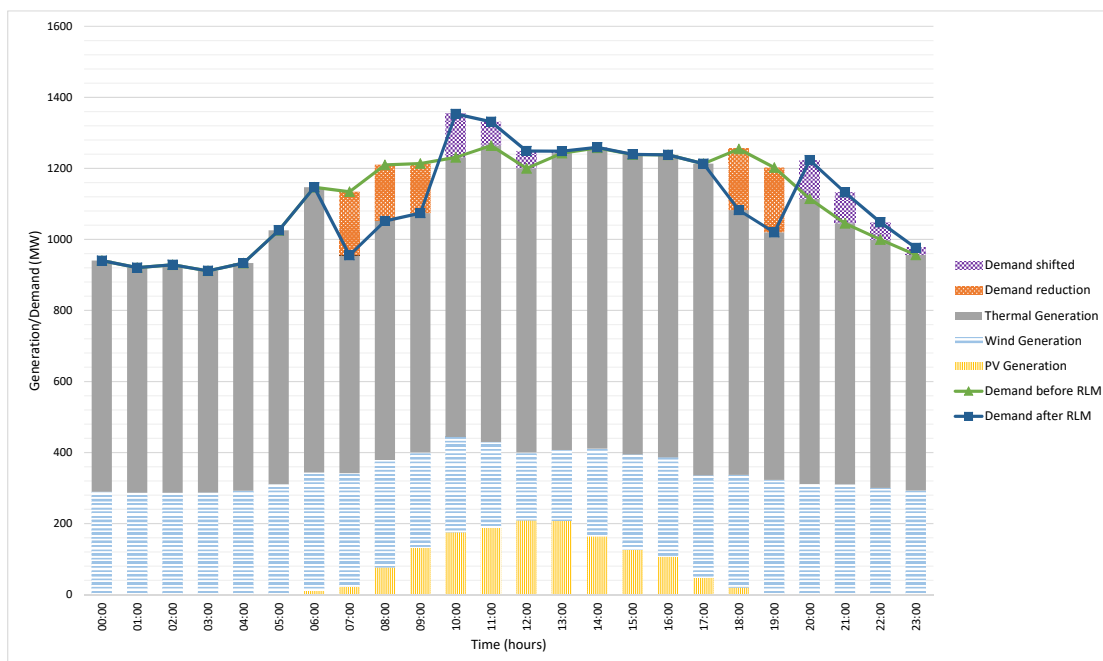
Figure 4.6. Demand and generation for a 24-hour dispatch period under 10% RES penetration and DLC.

To analyse the influence of DRP-DLC programme on the normal RO optimisation model, this section evaluates the optimisation results as given in Table 4.6 which provides the optimisation results in different scenarios. According to the results in Table 4.6, the demand before and after RLM is shown as 321.12 MW which means that the implementation of DLC has significantly decreased the load demand. This can be seen by the thermal unit output power over the dispatch period. In the first case where no DLC is implemented, the overall thermal unit production is higher than the DLC case by 2.03%. This shows that the demand flexibility has reduced the need for an increase in thermal unit production. The same analysis can be extended to the allocation of spinning reserve requirements for the two scenarios. As clearly shown in Table 4.6, the base scenario has a higher requirement for spinning reserve compared to the DLC case. The introduction of DLC reduces the spinning reserve allocation by 0.38%. This leads to a reduction in the thermal unit ramping requirements as a result of managing RES penetration fluctuations.

RES penetration level increase from base scenario to DLC scenario by 0.67%. This is mainly attributed
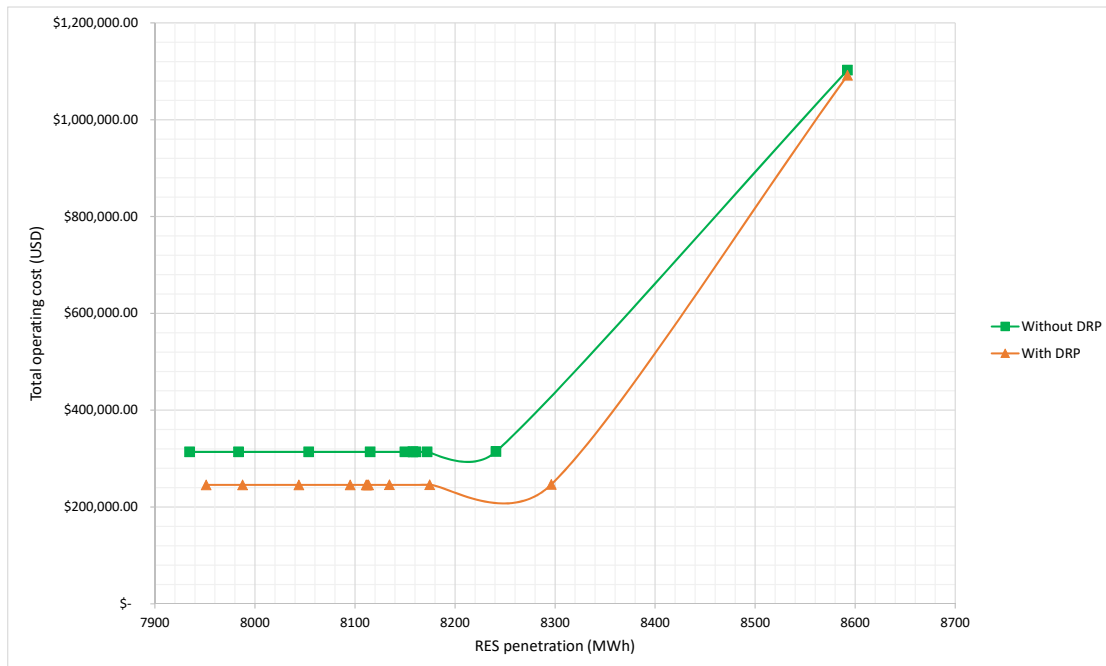
Figure 4.7. Pareto front comparison between a DLC and non-DR programme.

by deferring load from peak period to valley period where PV production is at the highest. This is also attributed by the low energy cost of RES compared to thermal units. More importantly, the flexibility of demand response has increased the RES penetration. In fact, demand flexibility is acting a temporary spinning reserve storage which in turn assists in improving network reliability and security associated with an increased RES penetration.

The overall benefit of DLC is shown by a significant decrease in the total operation cost between the two scenarios. Due to the reduced production of thermal units and minimised allocation of spinning reserves the overall cost is also decreased for the DLC scenario. The reduction is operating cost also includes an incentive that is paid to the participating customer. The overall cost reduction is 21.57% lower than the base case scenario. These benefits are not only limited to demand reduction or the total operating cost, but also includes a significant reduction in thermal generation capacity requirements which also corresponds to a reduction in power flow congestion. This ultimately increases the utilisation of RES units and it may speed up the integration of RES generators to power systems.

Table 4.6. A comparison of base case and DRP case

Description	Without DRP	With DRP	Delta
Daily demand (MW)	26822.5	26501.3	321.12
Thermal Gen (MWh)	18581.5	18205	376.5
RES Gen (MWh)	8241.01	8296.34	-55.33
SR (MW)	8456.80	8424.79	32
DR (MW)	0	321.12	-321.12
Peak RES Gen (MWh)	1774.03	1779.61	-5.581
Incentive ($)	0	12,844.80	-12,844.8
TC ($)	314,520	246,670	67,850

4.5.3   IEEE 118-bus test system

In this case study a large-scale power system is used to test the performance of the proposed DRP RO mode on the IEEE 118-bus system. The system base line load is found from [83] and real data from the RLM programme is used on load bus 2, 12, 18, 32 and 59. The total demand before and after the implementation of RLM is 126,854 MW and 125,830.20 MW. The sizes and parameters of the RES generators can be found in [86] and the total installed capacity is 1859 MW. The RES output power is same as the one shown in Figure 4.4.

The two cases, which were studied in Sections 4.5.2.1 and 4.5.2.2 are also performed for the large-scale system. Table 4.7 shows a comparison between the two cases studies. The overall performance of a large-scale test system shows no deviation from a small network since the results are consistent with previous system.

For example, in Table 4.7, the flexibility due to demand reduction is shown to increase the overall RES penetration while decreasing the production of thermal units. In total, the thermal units reduce their production by 2.14% while the RES penetration is increased by 3.49%. This is consistent with the previous test system. The reduction in thermal unit production is also followed by the reduction in spinning reserve allocation of 0.81%.

The implementation of the DLC programme has a positive impact on the operation cost. The overall

Table 4.7. A large-scale comparison of base case and DRP case

Description	Without DRP	With DRP	Delta
Daily demand (MW)	126854	125830.2	1023.78
Thermal Gen (MWh)	96895,69	94825.8	2069.89
RES Gen (MWh)	29958.00	31004.48	-1046.48
SR (MW)	38056	37749.07	306.93
DR (MW)	0	1023.78	-1023.78
Peak RES Gen (MWh)	6500	6500	0
Incentive ($)	0	40,951.20	-40,951.20
TC ($)	2,288,000	1,926,400	361,600

operating costs are reduced by 15.8% while an incentive of $40,951.20 is paid to participating customers. The total demand reduction before and after the RLM implementation is 1023.78 MW. Figure 4.8, shows the overall demand before and after the implementation of the RLM programme. In this case study, there is no increase in RES production during peak hours as it remains the same.

4.6 CONCLUSION

This chapter proposes a demand response programme with renewable obligation with the aim of maximising renewable penetration level while shifting and reducing flexible load. The proposed model uses real data from a residential load management programme implemented in South Africa to test the effectiveness of demand response on increasing renewable energy level in the network. To show the effectiveness of the proposed mode, a 30-bus system is used to evaluate the maximum increase in renewable penetration due to demand reduction. A comparative study is used to illustrate the effectiveness of the proposed model in terms of the operating cost, peak load reduction, deferred load, spinning reserve allocation and incentive paid. The conclusion related to all the key indicators are as follows:

1. The proposed optimisation model helps the system in scheduling renewable energy sources and thermal units while allocating enough spinning reserves. The proposed model introduces demand response to improve the level of renewable energy penetration while minimising the system total operating cost.

2. For the large-scale network, demand response is used to increase the overall renewable energy
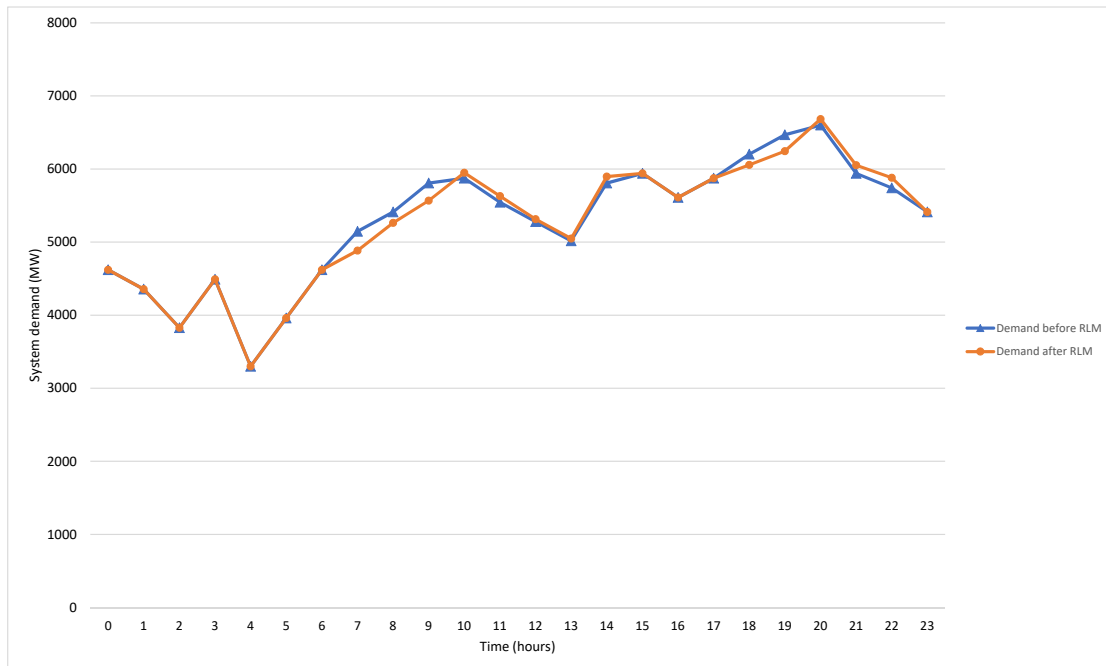
Figure 4.8. Comparison of demand before and after the implementation of RLM for a large-scale network.

       penetration by as much as 3.49% and the total operating cost is reduced by 15.8%. Transmission constraints are reduced.

3. A comparison of the normal renewable obligation model and demand response model shows that demand response is an effective tool to achieve system at a level of reliability at a minimum operating cost.

The current renewable obligation and demand response model does not take into consideration the uncertainty of renewable energy sources as well as real-time electricity prices. Therefore, the future research will include uncertainty in renewable energy source modelling, and the demand/supply bid curves in modelling the impact of demand response on renewable penetration.

CHAPTER 5   MULTI-OBJECTIVE STOCHASTIC ECONOMIC DISPATCH WITH MAXIMAL RENEWABLE PENETRATION UNDER RENEWABLE OBLIGATION

In this Chapter, the deterministic renewable obligation model is extended to stochastic in order to handle the uncertainty of renewable energy sources.

5.1   INTRODUCTION

The intermittent nature of renewable energy sources (RES) has created a challenge for their integration into the conventional power system. This increase in stochastic RES generators has escalated the cycling cost of thermal generators and has resulted in high operating costs. Consequently, it is very important to include the stochastic nature of wind and photovoltaic (PV) power plants to reduce uncertainty in generation scheduling and allow a smooth integration into the power system. As part of the integration of RES generators to the power system it is important to quantify the level of RES penetration to adequately operate the power system within its operational limits. A typical quantity-based instrument used to quantify the level of RES penetration in the grid is known as a renewable obligation (RO). It refers to the minimum renewable energy quota to be adhered to without imposing any penalty for non-compliance. A useful tool used to quantify the dispatch of intermittent energy sources is the classic economic dispatch. Economic dispatch is a power system operation problem which optimises the generation resources within each dispatch interval.

In general, there are two policy frameworks that are commonly used to boost the penetration of RES

[86]. A tariff-based instrument is the feed-in tariff (FIT), which provides an economic incentive for generating electricity using RES. A quantity-based instrument requires electricity suppliers to comply to a minimum renewable energy quota. This is known as RO in the UK or renewable purchase obligation (RPO) in other parts of the world. The RO allows electricity suppliers to buy a specified amount of their electricity sales from renewable sources. For each renewable energy sale, a renewable obligation certificate (ROC) is issued to demonstrate compliance to RES quota. Normally, a single ROC is equivalent to 1 MWh of renewable energy production. If the RES quota is not achieved, a penalty is payable by the generation companies. This approach of RO is used to support large scale generation of RES by fast tracking the integration of RES in the power system. This type of policy framework requires that a certain percentage of energy is attributed to RES and under this agreement a penalty is imposed for non-compliance. Moreover, the renewable energy quota is measured annually. This policy framework guarantees the use of renewables in the electricity generation as the RES target is dependent on the countries renewable energy policy and is administrated by the system operator (SO).

The increased level of RES penetration is normally approached from a dynamic economic dispatch (DED) point of view. In [113], [114], a DED with wind and PV injection is considered using the method of penalising the under and over estimation of the RES generators. The method used in approximating the under and over estimation of RES penetration considers the Weibull probability density function (PDF) for wind generation and a bimodal Weibull or Beta PDF for PV generation. The conventional DED has made great strides in approximating the level of RES penetration in the grid. It, however, has a limitation since it does not include the uncertainty of renewable generation and system demand. This has led to two main approaches adopted by many researchers for including uncertainty which are robust optimisation and stochastic programming.

The addition of large-scale intermittent energy sources such PV and wind generators has adversely affected thermal generators performance in the power system. Their integration has increased the cycling costs of thermal generators [115]. This has led to an overall increase in maintenance cost of thermal generators [116]. To lower the variability and uncertainty of RES integration, both robust and stochastic optimisation framework are used for optimal scheduling of RES and thermal generators [117].

In the robust optimisation approach studied in [118], the aim is to scale down the ramping and cycling

rates of thermal generators. This is performed to reduce the total operating costs associated with high RES penetration using a chance constraint approach. In [119], a DED problem with wind penetration is changed into a robust optimisation model and further transformed into a deterministic problem. The purpose of the model is to lessen the uncertainty of the wind power generation and improve the different levels of adjustable uncertainty budget. An adaptive robust optimisation is presented in [120], where a multi-period economic dispatch is used to model the uncertainty related to temporal and spatial correlations of wind power generators. In [121], [122] the stability of the power system is analysed using robust optimisation considering a high level of wind generation. Although robust optimisation has been applied to circumvent the challenges of uncertainty of wind and PV generators, the main disadvantage is that it only considers the worst case in the analysis of RES penetration level. The robust optimisation framework increases the operating cost that affects the optimal dispatch scheme. This is especially the case when a multi-objective optimisation problem is considered. It is generally unable to coordinate the multi-objective with a single min-max-min mathematical model [123].

In contrast to robust optimisation, the stochastic programming approach uses a large number of scenarios to handle uncertainty in RES generation. In scenario generation method the stochastic variables are identified by the location, environmental parameters and renewable energy type. The analytical method includes fast Fourier transform method (FFTM), multi-linear simulation method (MLSM) and point estimation method (PEM) [33]. On the other hand, simulation methods such as Monte Carlo simulation (MCS) are used for PV and wind scenario generation, however, they are computationally inefficient compared to Latin hypercube sample (LHS). A two-stage stochastic DED is presented in [124], where the system variability is modelled in terms of uncertainty in wind generation and demand. The model is solved using a stochastic decomposition algorithm to take the uncertainty of wind generation and apply it to real-time applications. In [125], a stochastic unit commitment model is given for long-term generator allocation and dispatch which considers the uncertainty related to the load forecast errors and intermittent wind generation patterns. A multi-stage stochastic DED problem in [126] presents a multi-area transmission constrained problem. The uncertainty model is related to the multi-area RES production with the aim of increasing the dispatch storage. An integrated wind-thermal and energy storage self-scheduling model is demonstrated in [127] for energy and spinning reserve market. This study uses a three-stage stochastic framework to show the benefit of energy storage in the spinning reserve market. Authors in [128] presented a two-stage DED for a multi-wind farm generation considering copula correlation among the different wind farm sites. The solution is obtained by decoupling the stochastic variables and reformulating the problem as a deterministic DED. In [129],

a dynamic carbon emission trading scheme is proposed for reducing carbon emission of thermal power generators by coordinating PV and wind generators in the energy mix to meet the Chinese carbon emission reduction targets.

A combined wind-thermal stochastic generation is presented in [130], from the utility's perspective. The model presented minimises the dispatch of thermal generators in each dispatch horizon while taking into consideration the uncertainty of wind generation and pool market. An optimal decomposition technique is utilised to solve the problem in real time. The uncertainties of wind generation and market electricity prices are modelled by a scenario generation approach. In [131], a stochastic scheduling DED model with multiple time resolution is presented for a high RES injection problem. The problem is presented in twofold, firstly a unit commitment problem is solved, and thereafter an economic dispatch model is solved for short term operations.

The literature reviewed shows that it is possible to integrate RES to the power system considering both the stochastic and robust optimisation framework while minimising RES curtailment. However, there is still a need for a detailed and optimal framework which considers renewable integration from the RO point of view. In this chapter, we extend on a renewable obligation framework presented in [86] by introducing the stochastic nature of RES. This is done to quantify the level of RES generated daily while minimising the expected system operating costs. In addition, the proposed model aims to maximise the level of RES energy produced without the need for curtailment [132]. In this model, the scenarios for wind and PV output power are created to realise a RES quota from the SO perspective. The generation companies are subjected to penalties imposed by the SO, if they do not meet a minimum set out obligation. The battery energy storage system (BESS) is added to the model to leverage on the storage of excess energy from the RES to the BESS and it is only used in times of low-RES production and high demand. Moreover, it is also used to reduce the spinning reserves of the thermal generators. The contributions are listed below;

1. A novel stochastic multi-objective RO model is presented for joint scheduling of power dispatch and maximising RES penetration.

2. A stochastic multi-objective RO model is changed into a single objective function using weighting factor approach.

3. A preference-based approach is used to select an optimal solution from a Pareto Front set.

4. A BESS unit is introduced to support thermal generators in spinning reserve allocation.

Department of Electrical, Electronic and Computer Engineering   75
University of Pretoria

The contents of this chapter are organised into six sections. In Section 5.2 a renewable obligation framework is presented for the proposed stochastic model. In Section 5.3, the stochastic DED model is developed which includes PV, wind, BESS and conventional generators in the energy mix. In Section 5.4, a scenario generation method for wind and PV uncertainty is presented. Additionally, a scenario reduction method is presented and as well as a method for reducing redundant inactive constraints for a stochastic security constraint economic dispatch (SCED). In Section 5.5, the feasibility and efficiency of the proposed method are investigated on two test systems. Finally, in Section 5.6 the conclusions are drawn.

5.2   RENEWABLE OBLIGATION POLICY FRAMEWORK

The RO policy is focused on increasing the level of renewable energy in the overall electricity production. The fundamental premise behind any RO policy is to encourage investment in renewable energy by ensuring that renewable energy production is included in the electricity production portfolio of the country. Typically, the renewable target is set on an annual basis and increases gradually per annum. The generation companies have the choice of building their own RES as a strategy to achieve the RO target. Alternatively, they can also choose to buy ROC from third party companies. If they fall short of meeting the required RO, they are required to pay a penalty associated with the RES target deficit. This penalty is measured on every MWh of renewable energy produced. There are several technologies that are considered in the RO target, i.e., offshore wind and onshore wind, PV plant, tidal wave electricity generation, concentrated solar power generation, and geothermal generation. All the technologies have different ROC rating with the emerging technologies such as tidal energy having the highest ROC rating per MWh produced [133].

In the open market, where generation companies are competing against each other, RES can be at a disadvantage due to its inherent nature of variability and uncertainty associated with power production. The RO ensures that RES is included in the energy mix thus increasing the level of RES in the grid. The general framework proposed is such that the SO is responsible for optimal dispatching of all generators, and the RES generators are given first preference over thermal generators. Generation companies provide forecasts to the SO with a 1-day lead time. The SO is responsible for optimally scheduling the available power to meet the system demand. In addition, the SO also ensures the renewable target is attained daily by continuously monitoring the energy production and providing feedback to generation companies. A typical policy framework for a renewable obligation model is shown in Figure 5.1.
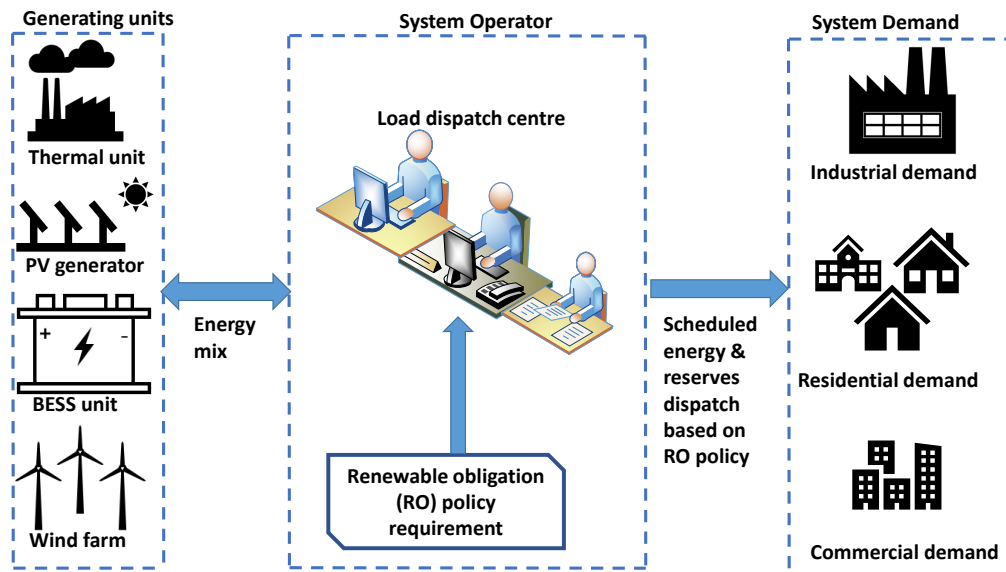
Figure 5.1. Renewable obligation policy framework for optimal energy mix and reserve allocation.

In Figure 5.1, the generation mix is made up of thermal, PV, wind, and BESS generating units. The policy framework is made up of three main components, i.e., the generation companies, the regulator or SO and the customers. The generators produce clean energy and the SO ensures that the renewable quota is achieved while maximising RES penetration and optimally scheduling energy and allocating the minimum spinning reserves.

5.3   PROBLEM FORMULATION

The approach considered in this chapter treats wind and solar power as non-dispatchable. The following assumptions are made for the formulation of the DED problem with RES obligation. All the RES (wind and solar) must be consumed first and the thermal generators must reduce their generation capacity to give preference to RES generators. The dispatch period considered in all the case studies is fifteen minutes. All RES is non-dispatchable and cannot be used as part of spinning reserves unless they have storage. The SO is responsible for dispatching all the generators including RES and BESS generators. The thermal and BESS generators can be used for spinning reserve. All the RES and BESS generators are owned by independent power producers (IPP).

5.3.1 Objective function

The objective is made up of two objective functions, i.e., the fuel cost minimisation with RO and the RES maximisation function. The objective functions are as follows:

$$\min J_1 = \mathbb{E}\{C_T\} \tag{5.1}$$

$$\max J_2 = \mathbb{E}\{E_{RES}\} \tag{5.2}$$

5.3.1.1 Minimisation of the total operating cost C_T

The expected operating cost $\mathbb{E}\{C_T\}$ in (5.3) is made up of two terms. The first term is the total operating cost of each generating unit, that is, thermal generators, RES generators and BESS. For each scenario, the operating cost is multiplied by the probability of that scenario occurring. The second term is related to the renewable obligation policy framework which ensures an adequate energy mix.

$$\mathbb{E}\{C_T\} = \sum_{\omega=1}^{N_\Omega} \sum_{t=1}^{T} \pi_\omega \left(\sum_{g=1}^{N_G} C_g(P_{g,t,\omega}) + \sum_{m=1}^{N_M} C_m(P_{m,t,\omega}) + \sum_{v=1}^{N_V} C_v(P_{v,t,\omega}) + \sum_{s=1}^{N_S} C_s(P_{s,t,\omega}) \right. \tag{5.3}$$
$$\left. + \sum_{r=1}^{N_R} C_{r,\omega}(P_{r,t,\omega}) \right) + \Gamma$$

The second term of the RO model is presented by the notation Γ which is shown in (5.4).

$$\Gamma = \gamma \sum_{\omega=1}^{N_\Omega} \sum_{t=1}^{T} \pi_\omega \left(\alpha \left(\sum_{g=1}^{N_G} P_{g,t,\omega} + \sum_{m=1}^{N_M} P_{m,t,\omega} + \sum_{v=1}^{N_V} P_{v,t,\omega} + \sum_{s=1}^{N_S} P_{s,t,\omega} \right) - \left(\sum_{m=1}^{N_M} P_{m,t,\omega} + \sum_{v=1}^{N_V} P_{v,t,\omega} \right) \right)^+ \tag{5.4}$$

The second term of the expression in (5.3) is the sigmoid function $\Gamma(\cdot)^+$ which is equal to γ if the renewable target is not achieved and 0 otherwise; α is the required RO in percentage which means that a portion of the total scheduled output power must come from RES. The penalty cost is represented by γ, which is the cost imposed for not achieving the RES obligation requirement and π_ω is the probability of each scenario. The generator cost function is a quadratic equation as shown in (5.5) where the units for the cost coefficients are $\$/MWh^2$, $\$/MWh$, and $\$/h$ and the generator spinning reserve cost is a linear function as shown in (5.6).

$$C_g(P_{g,t,\omega}) = \left(\frac{1}{n_0} \right) \sum_{g=1}^{N_G} \left(a_g + b_g P_{g,t,\omega} + c_g P_{g,t,\omega}^2 \right) \tag{5.5}$$

$$C_r(P_{r,t,\omega}) = \rho_r P_{r,t,\omega} \Delta t \tag{5.6}$$

Note $n_0 \Delta t = 1$ hour where $n_0 = 4$ and $\Delta t = 0.25$. This notation is introduced to ensure that the model can be applicable to any sampling period as long as it satisfies $n_0 \Delta t = 1$ hour. The cost functions for wind and PV generators are shown in (5.7) [86] and (5.8) [134], respectively, and the operating cost for BESS generating unit is shown in (5.9) [135].

$$C_m\left(P_{m,t,\omega}\right) = \zeta_m P_{m,t,\omega}\Delta t. \tag{5.7}$$

$$C_v\left(P_{v,t,\omega}\right) = \varphi_v P_{v,t,\omega}\Delta t. \tag{5.8}$$

$$C_s\left(P_{s,t,\omega}\right) = \tau_s P_{s,t,\omega}\Delta t. \tag{5.9}$$

The costs of PV, wind and BESS comprise of a direct cost related to the SO buying energy from the IPP, where ζ_m is the wind energy cost in $\$/MWh$, φ_v is the PV energy cost in $\$/MWh$ and τ_s is the BESS energy cost in $\$/MWh$.

5.3.2   Maximisation of the renewable energy penetration

The second objective function is the maximisation of the expected renewable energy into the grid. It is worth noting that the second objective of the maximum renewable energy is partially covered by the minimisation of RO violation cost in the first objective function. If the renewable energy obligation can be met, then no penalty is imposed. The amount of renewable energy power scheduled to the grid may not be maximal. With the second objective function the amount of dispatched renewable energy has to be maximised to overcome the limitation of merely meeting the obligation without maximising the RES energy penetration. The second objective function is shown in (5.10).

$$\mathbb{E}\{E_{RES}\} = \sum_{\omega=1}^{N_\Omega} \sum_{t=1}^{T} \pi_\omega \left(\sum_{m=1}^{N_M} P_{m,t,\omega}\Delta t + \sum_{v=1}^{N_V} P_{v,t,\omega}\Delta t \right) \tag{5.10}$$

5.3.3   Constraints

The DED problem under investigation has five constraints which are considered as hard or soft constraints. These constraints are:

1) Real power balance which represents the sum of all generating units, i.e., the thermal generators, wind power generators and PV plant generators that should meet the forecast demand as given in (5.11).

$$\sum_{g=1}^{N_G} P_{g,t,\omega} + \sum_{m=1}^{N_M} P_{m,t,\omega} + \sum_{v=1}^{N_V} P_{v,t,\omega} + \sum_{s=1}^{N_S} P_{s,t,\omega} = \sum_{b=1}^{N_B} P_{b,t} \quad \forall t, \forall \omega \tag{5.11}$$

The BESS stores excess energy and returns the energy back into the grid. In this chapter, positive $P_{s,t,\omega}$ indicates the discharging mode and negative $P_{s,t,\omega}$ indicates the charging mode.

$$P_{s,t,\omega} = P_{s,t,\omega}^d x_{s,t,\omega} - P_{s,t,\omega}^c y_{s,t,\omega} \quad \forall t, \forall \omega \tag{5.12}$$

where $P_{s,t,\omega}^d$ and $P_{s,t,\omega}^c$ are the discharging and charging power of the battery, and $x_{s,t,\omega}$ and $y_{s,t,\omega}$ are binary variables that ensure that discharging and charging do not take place at the same time as shown in (5.13) [136], [137].

$$x_{s,t,\omega} \mid y_{s,t,\omega} = \begin{cases} 1, & \text{if battery is charging;} \\ 0, & \text{if battery is discharging.} \end{cases} \tag{5.13}$$

2) Generator ramp rate and BESS stored energy. This is only applicable to thermal generators. The ramp up and ramp down units are in MW/h as given in (5.14).

$$P_{g,t,\omega} - P_{g,t-1,\omega} \leq UR_g \Delta t \quad \forall g, \forall t, \forall \omega \tag{5.14a}$$

$$P_{g,t-1,\omega} - P_{g,t,\omega} \leq DR_g \Delta t \quad \forall g, \forall t, \forall \omega \tag{5.14b}$$

$$P_{r,t,\omega} - P_{r,t-1,\omega} \leq UR_g \Delta t \quad \forall r, \forall t, \forall \omega \tag{5.14c}$$

$$P_{r,t-1,\omega} - P_{r,t,\omega} \leq DR_g \Delta t \quad \forall r, \forall t, \forall \omega \tag{5.14d}$$

$$E_{s,min} \leq E_{s,t,\omega} \leq E_{s,max} \quad \forall t, \forall \omega \tag{5.14e}$$

$$E_{s,0,\omega} = E_{s,t_f,\omega} \quad \forall t, \forall \omega \tag{5.14f}$$

3) Generator limits. The generator limits are applicable to thermal, RES and BESS generators. Equations (5.15) and (5.16), show the thermal generator limits. Since $P_{m,t,\omega}$ and $P_{v,t,\omega}$ flow from wind and PV systems into the grid, respectively, they are represented by (5.17) and (5.18). The top limit is the forecasted wind power generation and solar power generation at time t, and scenarios ω, respectively. They both include the amount of power flow to the network and the remaining amount, which is either consumed locally or curtailed due to line capacity limit. The BESS limits are shown in (5.19) and (5.20). Equation (5.21), ensures that the charging and discharging of the battery cannot happen at the same time. The energy balance of the battery that considers the amount of charged or

discharged energy and the relevant charging or discharging efficiency is given in (5.22).

$$P_{g,t,\omega} \leq min(P_{g,max}, P_{g,t-1,\omega} + UR_g) \ \forall t, \forall \omega \tag{5.15}$$

$$P_{g,t,\omega} \geq max(P_{g,min}, P_{g,t-1,\omega} - DR_g) \ \forall t, \forall \omega \tag{5.16}$$

$$P_{m,t,\omega} \leq P_{m,t,gen,\omega} \ \forall t, \forall \omega \tag{5.17}$$

$$P_{v,t,\omega} \leq P_{v,t,gen,\omega} \ \forall t, \forall \omega \tag{5.18}$$

$$0 \leq P^d_{s,t,\omega} \leq P^d_{s,max} \ \forall t, \forall \omega \tag{5.19}$$

$$0 \leq P^c_{s,t,\omega} \leq P^c_{s,max} \ \forall t, \forall \omega \tag{5.20}$$

$$x_{s,t,\omega} + y_{s,t,\omega} \leq 1 \ \forall t, \forall \omega \tag{5.21}$$

$$E_{s,t,\omega} = E_{s,t-1,\omega} - \frac{P^d_{s,t,\omega} \Delta t y_{s,t,\omega}}{\eta_d} + \eta_c P^c_{s,t,\omega} \Delta t x_{s,t,\omega} \tag{5.22}$$

4) Spinning reserve constraints.

$$P_{g,t,\omega} + P_{r,t,\omega} \leq P_{g,max} \ \forall g, \forall t, \forall \omega \tag{5.23}$$

$$0 \leq P_{r,t,\omega} \leq SRR_{r,max} \ \forall t, \forall \omega \tag{5.24}$$

$$\sum_{r=1}^{N_R} P_{r,t,\omega} \geq SSRR \ \forall t, \forall \omega \tag{5.25}$$

$$\sum_{g=1}^{N_G} P_{g,t,\omega} + \sum_{r=1}^{N_R} P_{r,t,\omega} + \sum_{s=1}^{N_S} P_{s,t,\omega} \geq \sum_{b=1}^{N_B} P_{b,t} \ \forall t, \forall \omega \tag{5.26}$$

where $P_{r,t,\omega}$ is the reserve contribution of unit g during time interval t and scenario ω. Constraint (5.24) represents the maximum reserve contribution for each generator where $SRR_{r,max}$ is the maximum contribution of unit g to the spinning reserve requirement (SRR). Constraint (5.25) is the minimum total system spinning reserve requirement (SSRR) for each time interval, and (5.26), simply means that the sum of the total generation, spinning reserve and BESS generators must be able to support the demand without RES generators.

5) Network transmission constraints. For the economic dispatch problem, only the active power of the transmission line under RES forecast is considered as shown in (5.27).

$$-P_{l,max} \leq P_{l,t,\omega} \leq P_{l,max}, \ \forall l, \forall t, \forall \omega \tag{5.27}$$

The transmission line power of line l at time interval t and scenario ω, which will be calculated by a nonlinear power flow for small size power systems, and DC power flow for large size power system is shown in (5.28).

$$P_{l,t,\omega} = \sum_{g=1}^{N_G} G_{l,g} P_{g,t,\omega} + \sum_{m=1}^{N_M} F_{l,m} P_{m,t,\omega} + \sum_{v=1}^{N_V} H_{l,v} P_{v,t,\omega} + \sum_{s=1}^{N_S} Q_{l,s} P_{s,t,\omega} - \sum_{b=1}^{N_B} D_{l,D} P_{b,t} \tag{5.28}$$

where $G_{l,g}$, $F_{l,m}$, $H_{l,v}$, $Q_{l,s}$ and $D_{l,D}$ denote the active power transfer coefficient factor between line l and thermal generator, wind farms, PV plant, BESS system and loads. The overall objective function is summarised as follows in (5.29).

$$\min J = (1 - \vartheta)J_1 - \vartheta J_2 \tag{5.29}$$

where ϑ is the weighting factor that converts the multi-objective functions into a single objective function, and a Pareto front is obtained by varying ϑ from 0 to 1. The objective function (5.29) is subject to constraints (5.11) - (5.28).

5.3.4 Formulation of multi-objective optimisation model

The proposed multi-objective optimisation model presented in the previous section is presented in its compact form as follows:

$$\min J(x) = \{J_1(x), J_2(x), \cdots, J_k(x)\} \; \forall k \in K \tag{5.30}$$

$$\text{s.t } h_i(x) = 0; \forall i \in N_I \tag{5.31}$$

$$g_j(x) \leq 0; \forall j \in N_J \tag{5.32}$$

where $J_1(x)$ to $J_k(x)$ represent multiple objective functions in (5.1) and (5.2), the value of K is 2, and x is the output vector which consists of an optimal dispatch solution for thermal and RES generators. The equality constraint in (5.11) is indicated by (5.31) and the inequality constraints from (5.14) to (5.28) is denoted by (5.32).

5.4 SCENARIO GENERATION FOR WIND AND PV GENERATORS

The principles of these techniques are explained in the following subsections.

5.4.1 Scenario generation using Latin hypercube sampling

The generation power of PV and wind turbine depends on the environmental input. The variation of wind speed is a key factor for the evaluation of wind turbine output. As for the PV generation, the variation of solar irradiance is used to determine the output power of a PV plant. The uncertainty of wind power comes from the stochastic nature of wind speed while that of PV depends on external weather conditions such as clouds. The forecast errors of the RES generators are taken as random variables with specific PDF [138]. Afterwards, LHS method [139] is used to generate scenarios. The associated PV and wind power output scenarios are as follows.

$$P_{v,t,} = P_{v,t,f} + \Delta P_{v,t,e} \tag{5.33}$$

$$P_{m,t} = P_{m,t,f} + \Delta P_{m,t,e} \tag{5.34}$$

where $P_{v,t,f}$ and $P_{m,t,f}$ are forecasted value of the output wind and PV power and PV from the autoregressive moving average (ARMA) model and $P_{v,t,e}$ and $P_{m,t,e}$ are the prediction error of the output wind and PV power at time t which is defined by the ARMA(1,1) [140], [141].

$$\Delta P_{v,t,e} = \phi_v \Delta P_{v,t-1} + e_{v,t} + \theta_v e_{v,t-1} \tag{5.35}$$

$$\Delta P_{m,t,e} = \phi_m \Delta P_{m,t-1} + e_{m,t} + \theta_m e_{m,t-1} \tag{5.36}$$

where ϕ and θ are the auto-regressive and moving average parameters, which are obtained by minimising the mean square error of the ARMA model from the historical data of RES output power. The PDF of wind forecast error is considered as a Weibull distribution function. While a normal distribution function is used for the PV power forecast error. Moreover, for scenario generation purposes the empirical PDF and cumulative distribution function (CDF) from historical data are used. The RES data profiles are taken from [142] for a period of 2018.

The LHS method in [33], [143], is the method used to create scenarios of RES generation. Firstly, the PDF of the two uncertain variables are defined and their respective correlation matrix are created. LHS are used to generate different outcomes of dependent variables from different PDFs [144]. The following steps are employed to create 1000 scenarios of even probability.

1. Step 1: A Latin cube with the same number of independent variables is defined using the inverse cumulative distribution function (ICDF) of the normal variable with zero mean and a standard deviation of one to map the independent random variable of the sample to a value.

2. Step 2: The independent normal variables are formed from the Latin cube.

3. Step 3: The dependency to the independent normal variables is added using the Cholesky transformation which results in dependent variables. This means that when a normal CDF is applied to a normal random variable, the result is a uniform distribution between zero and one which still maintains the dependency between the variables.

4. Step 4: In the final step, the dependent uniform distributions are mapped using the ICDF to their original PDF, which results in dependent random variables.

5.4.2 Scenario reduction

In order to reduce the number scenarios, the initial scenarios are approximated by finite scenarios of even probabilities. The scenario reduction determines a scenario subset and assigns new probabilities to the preserved scenarios so that the corresponding reduced probability measure is the closest to the original measure in terms of probability distance. The probability distance trades off scenario

probabilities and distance of scenario values, and the Kantorovich distance of probability distribution is used for scenario reduction [42], [145]. The scenarios can be reduced using forward or backward reduction algorithm as described in [146]. The final reduced scenarios with their respective probability are used in the stochastic programming model as shown in Figure 5.2.
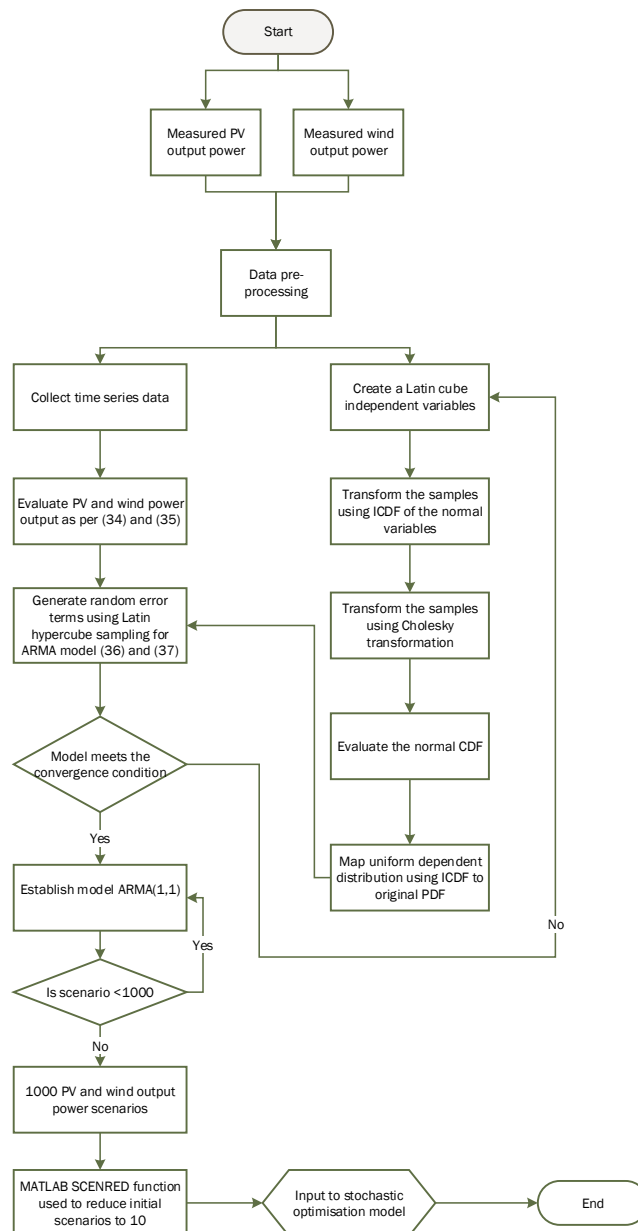
Figure 5.2. The process of generating scenarios from historical data using ARMA and LHS process to generate 1000 scenarios and then reducing the scenarios to 10 for stochastic optimisation model.

5.4.3   Line capacity constraint reduction

The SCED increases the number of constraints based on the number of scenarios, number of transmission lines involved and the time horizon considered. Generally, the constraints increase when the problem is extended to the stochastic SCED model. Most security constraints are inactive and as a result do not affect the optimal solution. It is important to identify these inactive constraints; these can be eliminated to reduce the problem complexity. Authors in [147], identified an effective method of eliminating the inactive constraints without affecting the original optimal solution. The inactive constraints are only related to the system demand and transmission line parameters, and if the security constraint is inactive, then it is applicable as long as the system demand does not change.

Theorem 1 [147]. For a SCED optimisation problem with a feasible region $S = \{x \in R \mid Ax \leq b\}$, there exists a relaxed feasible region such that the kth constraint $A_{l,t,\omega}^{k} x \leq b^{k}$ is inactive and can be omitted in S and provided a new optimisation model $max\ A_{l,t,\omega}^{k} x \leq b^{k}$ is feasible if $A_{l,t,\omega}^{k} \leq P_{l,max}$.

A new problem is formulated as follows.

$$A_{l,t,\omega}^{k} = max \sum_{g=1}^{N_G} G_{l,g} P_{g,t,\omega} + \sum_{m=1}^{N_M} F_{l,m} P_{m,t,\omega} + \sum_{v=1}^{N_V} H_{l,v} P_{v,t,\omega} + \sum_{s=1}^{N_S} Q_{l,s} P_{s,t,\omega} - \sum_{b=1}^{N_B} D_{l,D} P_{b,t} \qquad (5.37)$$

The objective function in (5.37) is subject to a power balance constraint (5.11) and generator limit constraints (5.15) to (5.21). The optimal solution is compared to the upper bound in (5.27) and if the optimal solution is smaller than the upper bound, then the lth transmission line at time t and scenario ω is considered inactive and can be removed from the optimisation model [42].

5.5   NUMERICAL CASE STUDIES

The proposed optimisation model is applied to the IEEE bus test systems, i.e., the modified IEEE 30 and 118-bus systems. The historical data of RES generators and system load are obtained from Elia Group using a temporal resolution of 15-minutes [142]. The RES data is collected over a period of a year from January 1st 2018 to December 31st 2018. The integrated PV and wind farms are connected to buses 7, 15, 22, and 24. The modified IEEE 30-bus system has 6 thermal generators and 41 transmission lines. The ramp rates and quadratic cost coefficients are taken from [112]. The BESS system is connected to buses 26 and 28 respectively. The second IEEE 118-bus system consists of 54 thermal generators and 186 transmission lines. Ten additional RES generators are added to the system on buses 1, 33, 38, 52, 68, 75, 96, 102 and 117. In the second test system, a combination of five PV and five wind systems is used. The BESS generators are added to buses 9 and 11. The details of the IEEE 118-bus system can be found in [83]. The fixed demand at each bus is the portion

of the total capacity at each sampling period. The transmission line flow limit is simulated by using DC power flow and a sampling interval of 15 minutes is considered due to the intermittency of RES generators. The optimisation problem is solved over a 24-hour period. In the simulation studies, all the uncertainty is generated from 1000 scenarios which are further reduced to 10 scenarios and are solved using a deterministic approach. In all simulation studies, a RES penetration level of 10% is used as a benchmark and if the obligation is unattained, a penalty of $100,000 per day is imposed on generation companies by the SO. In addition, the system spinning reserves requirement is based on 30% of the maximum thermal generator capacity and the spinning reserves requirement of each generator is equal to the maximum generator capacity.

The optimisation problem presented in Section 5.3 is a mixed integer quadratic programming (MIQP) problem. The scenarios are generated and reduced using MATLAB [144], [145] and the optimisation model has been implemented using IBM ILOG CPLEX optimisation studio [148] on a quad-core 3 GHz desktop computer. The MIQP model is implemented by CPLEX using optimisation programming language (OPL). The main advantage of using CPLEX is the ease of software syntax to the mathematical representation of the optimisation problem. In order to show the effectiveness of the RO model the effects of the operating cost under RO target are analysed, the reduction in spinning reserve allocation due to BESS operating units and the impact of RES penetration on the overall energy mix. In all comparisons a RO target of 10% is used as a benchmark, and the RO model is tested on the IEEE 30-bus system to illustrate the effectiveness of the model by considering the following cases:

1. A comparison of the proposed stochastic RO model to the deterministic model to show the impact of RES intermittency on the key comparison parameters;

2. The impact of varying the RO target from 5% to 50% at a step of 5% on the overall energy mix and total operating cost;

3. The impact of using different penalty costs to measure the RES penetration level; and

4. The impact of changing the transfer limit on the overall RES penetration level.

Thereafter, IEEE 118-bus system is also used to test the model on a large-scale test system to measure the effectiveness of the proposed stochastic RO model.

5.5.1   Implementation steps

The step-by-step approach for implementing the stochastic RO model for a combined energy and reserve dispatch is provided as follows.

1. Generate 1000 scenarios of wind and PV output power based on the scenario generation algorithm in Section 5.4.1.

2. Due to the high computation requirement for large scenario sets, the fast-forward reduction algorithm in [146] mentioned in Section 5.4.2 is applied to reduce the original 1000 scenarios to 10 scenarios.

3. Formulate the deterministic based joint energy and reserve scheduling under RO framework using the reduced scenarios as the input to the model.

4. Using the inactive constraint theorem presented in (5.37) the preliminary optimisation problem is solved, which reduces the number of inactive line capacity constraints that are related to the system demand and transmission line parameters.

5. Set the weighting factor in (5.29) to zero and solve the reformulated optimisation problem.

6. The reformulated MIQP is solved using dynamic search in CPLEX which is a search strategy for mixed integer programming (MIP) problems using the OPL parameter "MIPSEARCH".

7. Increase the weighting factor from 0 to 0.1 and solve the reformulated optimisation problem; iterate until the weighting factor is equal to 1.

8. Output the Pareto optimal set solution.

9. Applying the preference-based approach to select the best compromise solution using lower and upper boundaries of RES penetration and total operating costs.

10. Implement the best compromise solution and provide the optimal RO dispatch strategy.

The overall implementation flow chart is shown in Figure 5.3.

5.5.2   Case study 1: IEEE 30-bus deterministic renewable obligation

In this section, the new model benefits are demonstrated by comparing the deterministic to the stochastic model. In order to compare the proposed model, the total operating cost, actual RES penetration level and the reduction in spinning reserves due to an increase in BESS penetration are used for comparison. The sizes of the PV plants are 500 MW and 275 MW and the size of the wind farms are 300 MW and 350 MW. The two BESS generators are rated at 15 MWh each and the charging and discharging
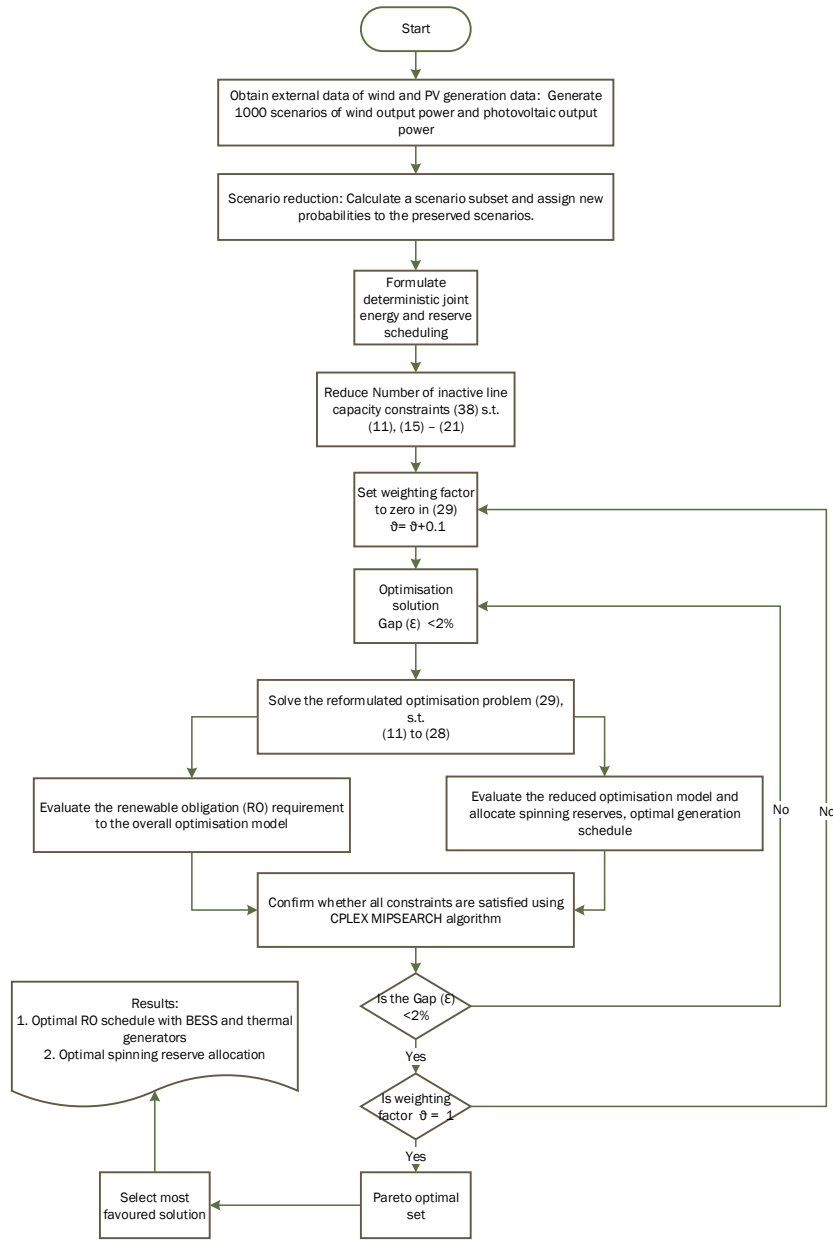
Figure 5.3. Optimisation algorithm for solving multi-objective stochastic RO model with Pareto optimal set and preference-based approach for selecting the best compromise solution.

efficiency is considered as 90%. The total installed capacities of RES and BESS generators are 1425 MW and 30 MWh, respectively. All the transmission line thermal limits are maintained at 100%. The IPP costs of energy for PV are 1.5 $/MWh and 3.0 $/MWh, and the costs of energy for wind are 1.3 $/MWh and 4.0 $/MWh and finally the costs for BESS are 1.36 $/MWh and 1.31 $/MWh, respectively [149]. Table 5.1 shows the thermal generator data. The daily forecasted demand and the power transfer

Table 5.1. Thermal generator data.

Unit	Pmax	Pmin	a_g	b_g	c_g	RU	DR
G1	350	50	240	7.00	0.0070	60	60
G2	250	50	200	10.0	0.0095	60	60
G3	150	50	220	8.00	0.0090	60	60
G4	350	50	200	11.0	0.0090	60	60
G5	450	50	220	10.5	0.0080	60	60
G6	500	50	190	12.0	0.0075	60	60

thermal limit of each transmission line is shown in Figure 5.4. The ARMA model for wind and PV
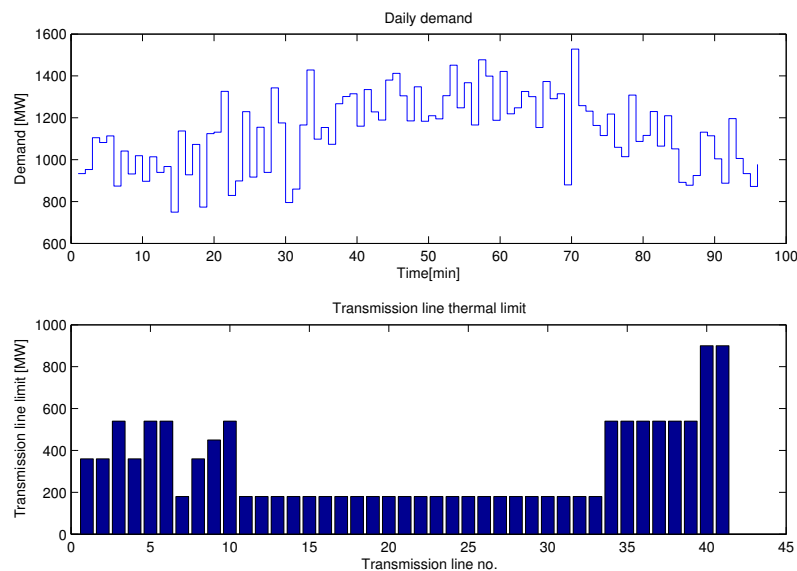
Figure 5.4. Forecasted demand and transmission line thermal limit for IEEE 30-bus system.

output power is given in Table 5.2. All the fifteen minute data for demand and RES output power are obtained from EirGrid [142]. Figures 5.5 – 5.12, shows the RES output power for 1000 generated scenarios and the 10 reduced scenarios, respectively.

5.5.2.1 Solver parameter relaxation

A pre-solved relaxation parameter is used which performs the reduction with tight tolerances ($1e^{-10}$) than the default simplex tolerance ($1e^{-6}$) and offers more compact matrix and identifies obvious infeasibility much quicker. This is applied to the MIQP for root relaxation in order to perform

Table 5.2. ARMA model for wind and PV output power.

Description	ϕ	θ
Wind 1	1.0	0.634012
Wind 2	0.968057	0.278895
PV 1	0.986552	-0.155482
PV 2	0.989746	0.072684
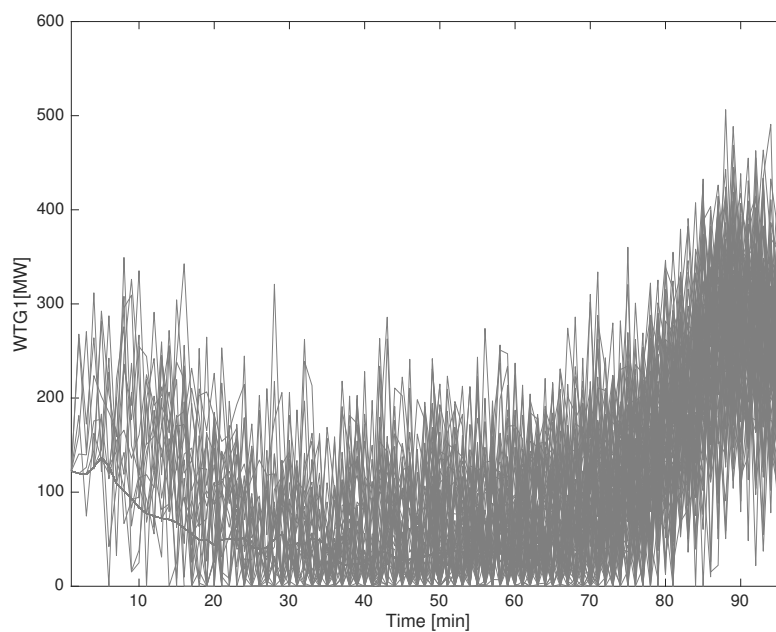
Figure 5.5. Forecasted wind power plant 1 with 1000 generated scenarios.

preliminary reduction, elimination, substitution and coefficient modification in solving the optimisation model. Moreover, a dynamic search algorithm is used for solving a MIQP using a parallel mode switch parameter, and the continuous optimiser is set to solve the initial relaxation using dual simplex optimiser for root relaxation under the CPLEX OPL environment. The impact of implementing the relaxation parameter reduces the computing time and minimises the memory required to solve the optimisation model. Typically, the root relaxation computing time takes between 4 to 6 s while the overall root, branch and cut computing time is between 9 to 10 s compared to the default parameter setting which is between 30 to 60 s for the modified IEEE 30-bus system. In the MIQP model, a relative optimal solution gap parameter is set to 2%, which ensures that the relative tolerance on the
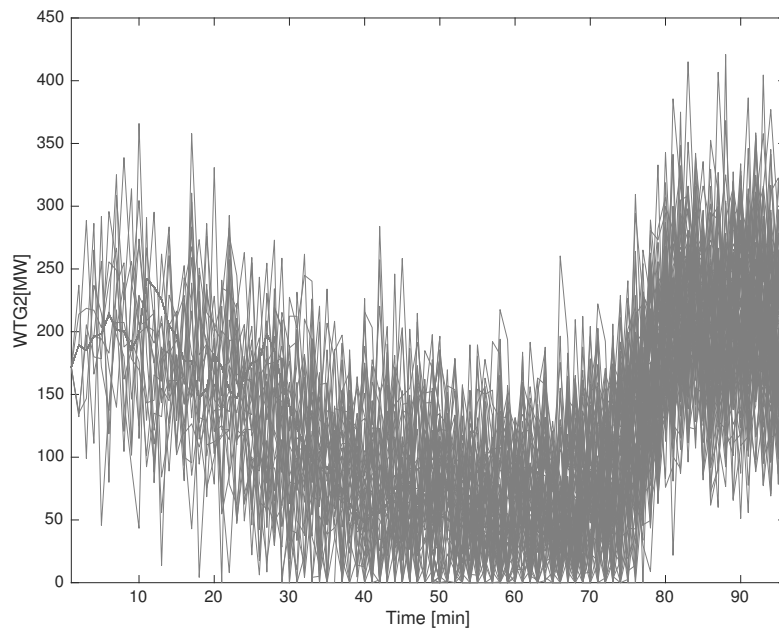
Figure 5.6. Forecasted wind power plant 2 with 1000 generated scenarios.
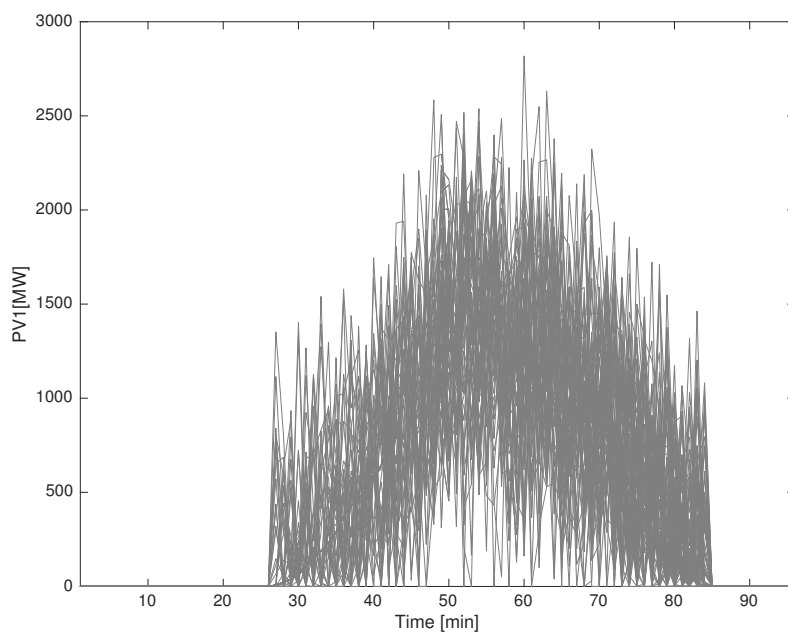
Figure 5.7. Forecasted PV plant 1 with 1000 generated scenarios.

gap between the best integer objective and the obtained objective falls below the 2% tolerance, this 2% error is good enough for the power dispatch purpose. When this tolerance is reached, the optimisation
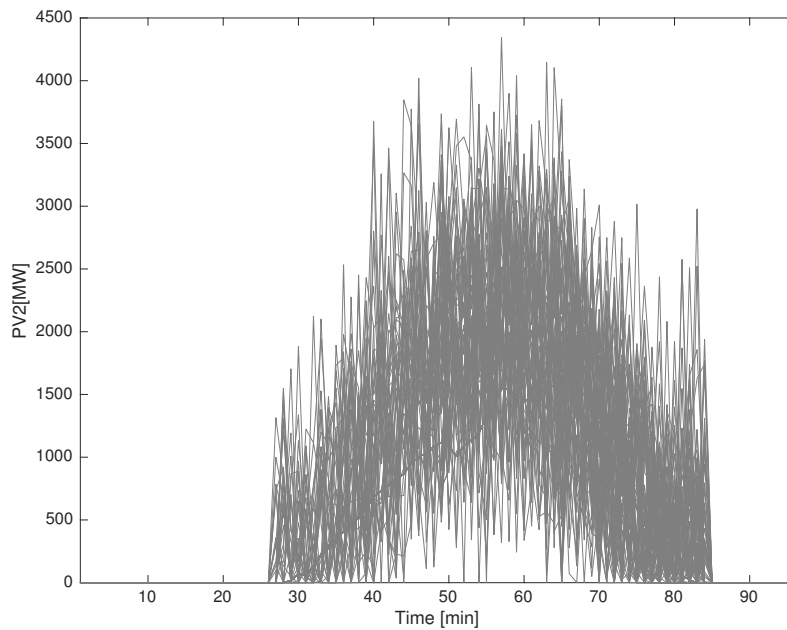
Figure 5.8. Forecasted PV plant 2 with 1000 generated scenarios.
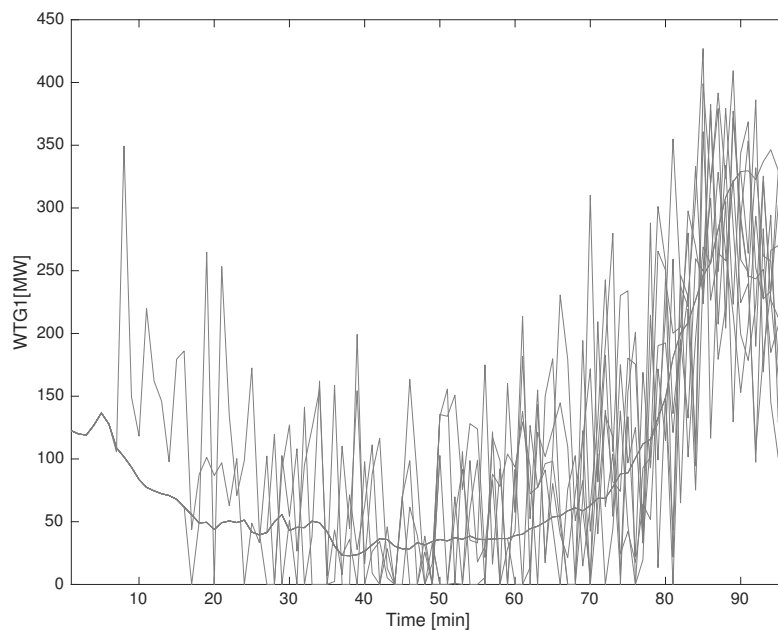
Figure 5.9. Forecasted wind power plant 1 with 10 scenarios.

model terminates; however, under default settings, this parameter is set to 0.0001% which means that

the optimisation model will continue the search until the relative solution gap falls below 0.0001%. The
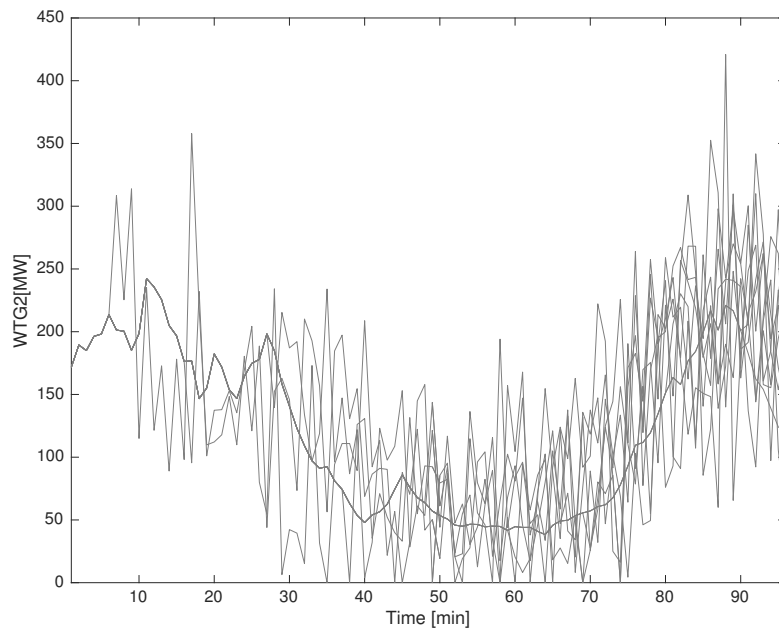
Figure 5.10. Forecasted wind power plant 2 with 10 scenarios.
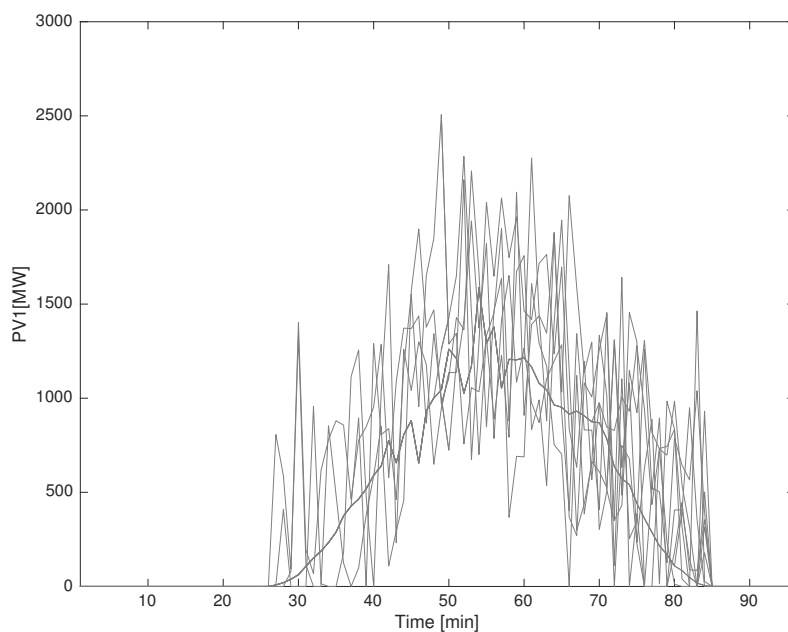
Figure 5.11. Forecasted PV power plant 1 with 10 scenarios.

proposed parameter relaxation allows the optimisation model to reach an acceptable optimal solution

much faster and saves memory compared to the default setting parameter.
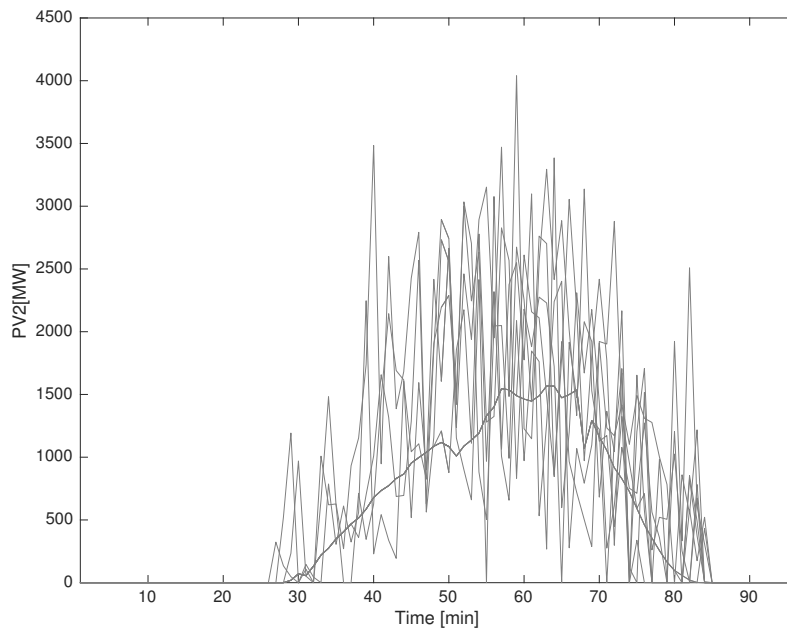
Figure 5.12. Forecasted PV power plant 2 with 10 scenarios.

5.5.2.2   Comparison of a stochastic and deterministic RES obligation model

In order to quantify the effectiveness of the proposed model, a benchmark base case simulation study is performed using the parameters in Table 5.1 and Table 5.2. The proposed model presented in Section 5.3, is compared to a deterministic version of the model. For the deterministic model, the total number of scenarios is equal to one which converts the stochastic model to a deterministic model. In both the deterministic and stochastic model, the RO is set as 10%. A comparison in terms of the reduction in thermal energy production, an increase in RES production, a reduction in spinning reserve and an increase in battery storage due to excess RES production is provided in Table 5.3.

A comparison of the deterministic to the stochastic model indicates that in both models, the RES obligation requirement is attained, with the deterministic achieving a maximum of 45.84% of RES penetration. For the stochastic model, the mean RES obligation is 39.57%. The best and worst RES penetration levels are 46.74% and 30.04% respectively, which is above the RES obligation of 10%. There is an increase of 0.9% in RES penetration when a stochastic model is used. The stochastic solution presented in Table 5.3 corresponds to a single end point of the Pareto optimal solution when the RES energy is maximised, and the total cost is minimised. Figure 5.13 shows a comparison of the normalised Pareto front for the stochastic and deterministic model.

Table 5.3. Comparison between Pareto optimal solution and traditional DED.

Description	Stochastic			Deterministic
	Best	Mean	Worst	
Thermal (MWh)	58445	66125	76245	59144
PV (MWh)	31964	25894	17147	28954
Wind (MWh)	18890	17156	15533	20908
BESS (MWh)	-515	-391	-140	-222
SR (MWh)	50490	45432	35861	51885
RES (MWh)	50854	43050	32679	49865
RES (%)	46.74	39.57	30.04	45.84
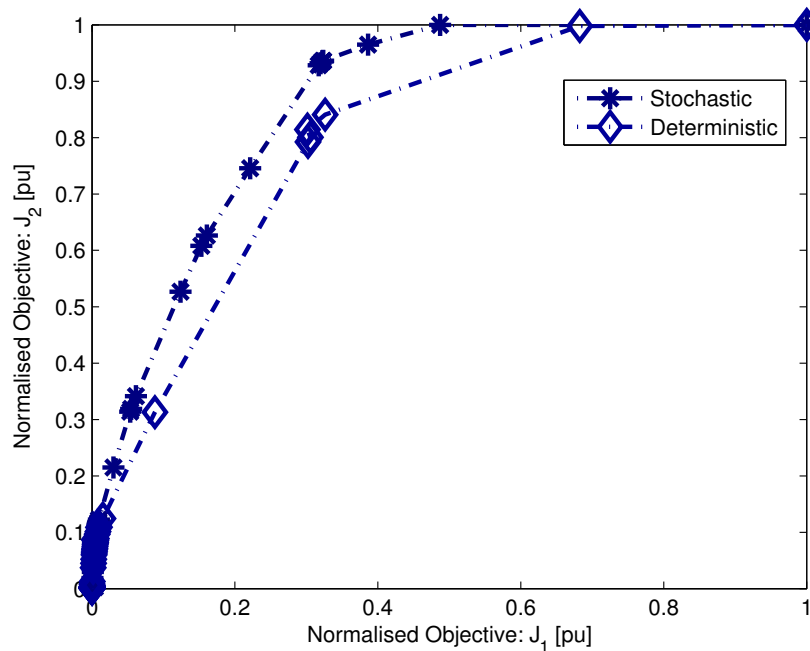
Figure 5.13. Comparison of stochastic and deterministic Pareto front.

The maximum and minimum operating cost for the stochastic model is \$829,910 and \$415,555 respectively while the total operating cost for the deterministic model is \$499,280 and \$320,030 respectively. When comparing the results shown in Table 5.3 between the stochastic and deterministic model, it can be inferred that modelling the intermittent nature of the RES generators increases the

total operating cost whilst increasing the RES penetration and the required spinning reserves. The stochastic model increases the operating cost by 66% compared to a deterministic model. On the contrary, the stochastic model provides higher RES penetration and more precise solution for different scenarios. This means that solving a stochastic optimisation model provides better insight for the SO which provides the most likely scenarios in comparison to the deterministic approach.

5.5.2.3   The impact of renewable obligation requirement on the model sensitivity

In order to understand the impact of the RO parameter on the proposed model, the RO is varied from 5% to 50% at a step of 5%. This means the RES penetration level increases with each step change and the thermal and BESS system must increase their generation to support the demand while the spinning reserve will also increase with the increase in RES penetration. The Pareto frontiers for each RES obligation are shown in Figure 5.14.
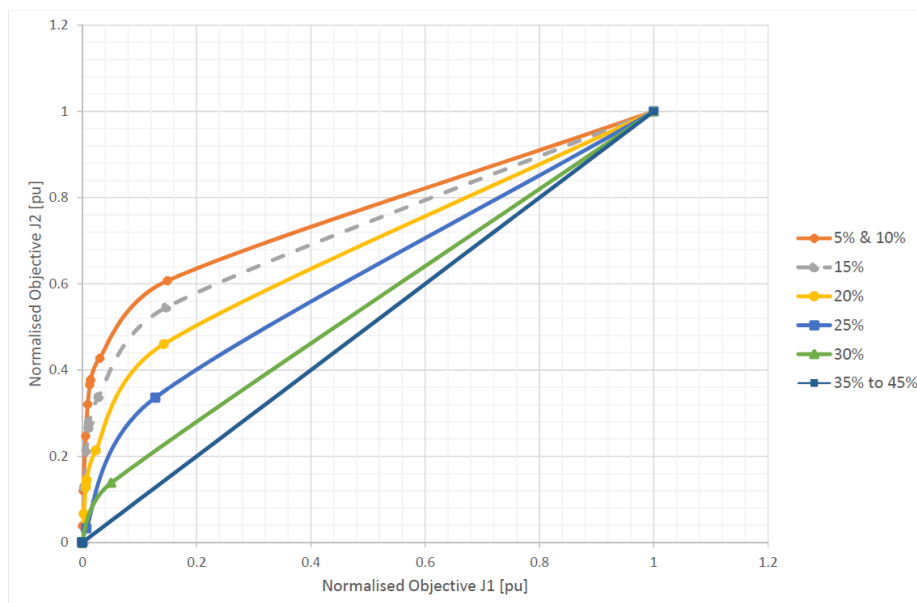
Figure 5.14. Pareto optimal solution for different RO target varying from 5% to 50%.

The impact of the RES obligation is variable. Figure 5.14 shows the Pareto fronts for different RES penetration levels. The RES obligation is attained for a RES obligation of 5% to 45% and any RES obligation over 46% is unattained due to the transmission thermal limit. It is important to note that the Pareto front from 35% to 45% forms a Utopia line, which means that anything over 45% will result in a dominant solution that cannot be achieved and thus a penalty will be imposed. Figure 5.15 indicates the average operating cost and RES penetration level for the stochastic model.
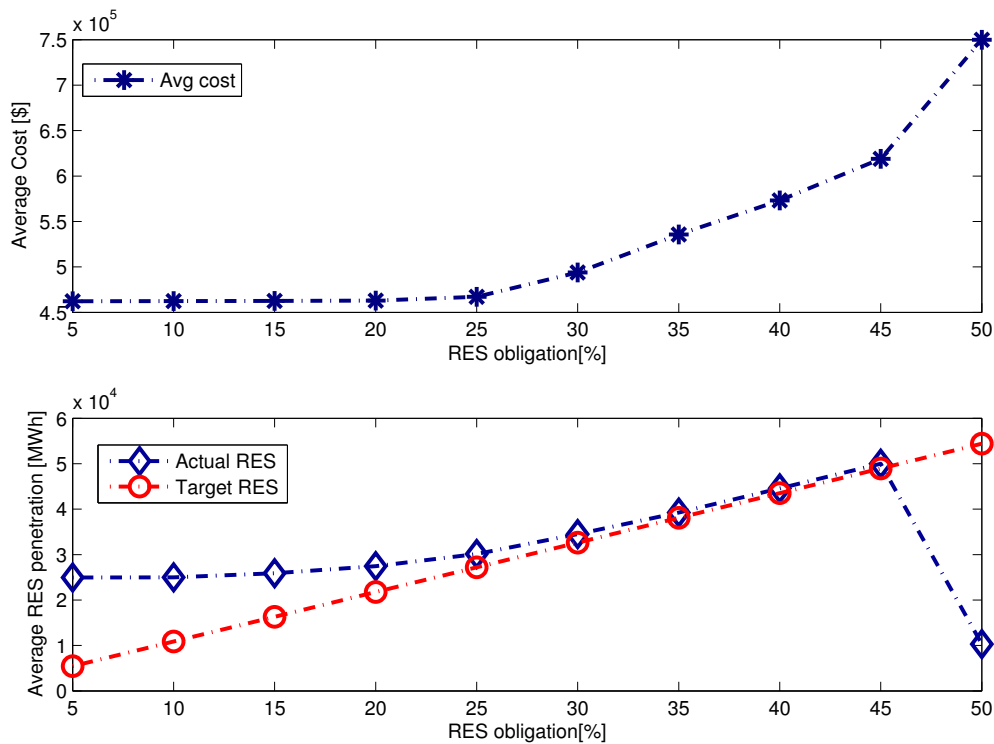
Figure 5.15. Expected average operating cost for different Pareto front and different RES penetration level.

From Figure 5.15 it is observed that the total operating cost increases with the increase in RES obligation requirement. The RES penetration level is achieved at all points except for when the obligation is set to 50%, which corresponds to the highest operating cost.

The impact of the weighting factor on the optimal solution is shown in Table 5.4. When the weighting factor is zero, the optimisation model in (5.29) changes into a minimisation of the expected operating cost which consists of thermal generating units, RES, BESS and spinning reserve allocation cost. The thermal generators produce more power, followed by wind and PV generators, and BESS units produce the least. The spinning reserve allocation respects constraint (5.25) which ensures that a minimum of 30% of the total production is always covered by thermal generators and BESS units. The maximum RES achieved is 46.75% which occurs when the weighting factor is 1. It can also be seen that for the maximum RES penetration scenario, excess RES energy is injected to the BESS units. This complies with the requirements of using BESS as a storage for excess RES energy injection as well as minimising spinning reserves from thermal generators. In this scenario, more spinning reserves are

Table 5.4. Demand and supply for different weighting factor with the RO set to 10%.

ϑ	Gen (MWh)	RES (MWh)	SR (MW)	BESS (MWh)	TC ($)
0.00	97626.00	10878.00	32901.00	280.49	415560
0.10	96081.00	12422.00	32902.00	281.45	372851.8
0.20	92827.00	15672.00	32919.00	285.30	329881.6
0.30	87749.00	20754.00	32929.00	280.69	286331.8
0.40	84820.00	23696.00	32919.00	269.10	242215.6
0.50	83022.00	25500.00	32905.00	263.36	197720
0.60	82641.00	25905.00	32927.00	238.45	153021
0.70	82580.00	25976.00	32931.00	228.29	108278.8
0.80	80837.00	27971.00	34353.00	-23.92	63263.2
0.90	73819.00	35152.00	35137.00	-186.67	16080.2
1.00	58448.00	50860.00	50530.00	-523.51	-50860

allocated from thermal generators than any other scenario. This implies that when RES is maximised, the SO must allocate more spinning reserves to overcome the intermittency nature of RES generators. If the end points are selected as the optimal solution to the multi-objective function problem, then the solution becomes bias as it only complies to a single requirement, i.e., the maximisation of the expected RES penetration or minimisation of the expected operating costs under RO. For example, the first end point provides the least expected operating cost with the least RES energy penetration, while the last end point gives a high RES energy penetration and high operating costs. An optimal solution must provide a compromise between minimising the expected operating cost and maximising the expected RES energy penetration. Based on the preference-based approach, the SO is the main decision marker. The SO can select the best compromise solution considering lower boundaries related to maximising RES penetration and upper boundaries for minimising the total operating cost.

Figure 5.16 shows the Pareto front of the stochastic RO model when the RES quota is set to 10% with the optimal solution indicated by point A.

The lower and upper boundaries are selected as 30,000 MWh and $600,000. The Pareto optimal point provides a solution that realises a compromise in the expected operating cost and the expected RES
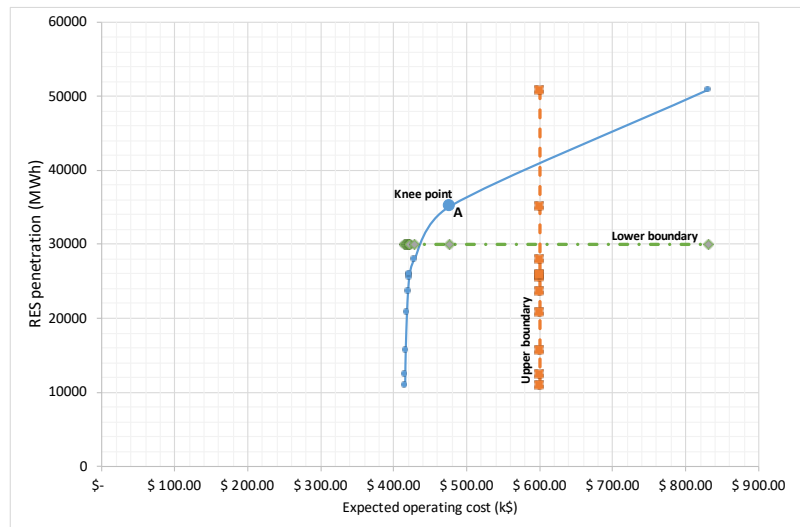
Figure 5.16. Pareto front optimal solution point 'A' with RO target set to 10%.

penetration. The knee point shown as A in Figure 5.16 corresponds to the weighting factor of 0.9 in Table 5.4. This point indicates a fair trade-off between minimising the expected operating costs while maximising the expected RES penetration in the grid and matches with the SO boundaries; any point away from the knee point will realise a non-compliant solution, in either direction. Although the minimum RES quota is achieved in the RO model the second objective function aims to maximise the expected RES penetration over and above the minimum RO requirement.

5.5.2.4   Importance of multi-objective functions

The RO model only focuses on setting a minimum quota in terms of renewable energy that must be achieved daily according to (5.3). The limitation with the RO model is that it only aims to achieve the minimum stipulated RO and does not increase renewable energy over the stipulated quota, hence, there is a need to add an objective function that maximises the RES penetration. This function is shown in (5.2) and (5.10) as a RES energy objective function. It is important to note that although objective function achieves the RES obligation, it does not maximise the level of RES penetration. This is shown in Table 5.4, which indicates the Pareto optimal points for different weighting factors. For example, if a weighting factor of 0 is considered the operating cost is minimised and the RO is achieved, however, the RES is not maximised. When the weighting factor is increased gradually, the impact of objective function starts to increase the RES penetration over and above the RO quota in (5.3).

5.5.2.5   The impact of penalty cost on the model sensitivity

In this simulation study, the RES obligation penalty cost is varied in two steps, i.e., $1000 and $10,000 per day to quantify its impact on the RES penetration level which is varied from 10% to 20%. Figure 5.17 illustrates the two RES penetration levels when penalty is varied. For example, when the RES
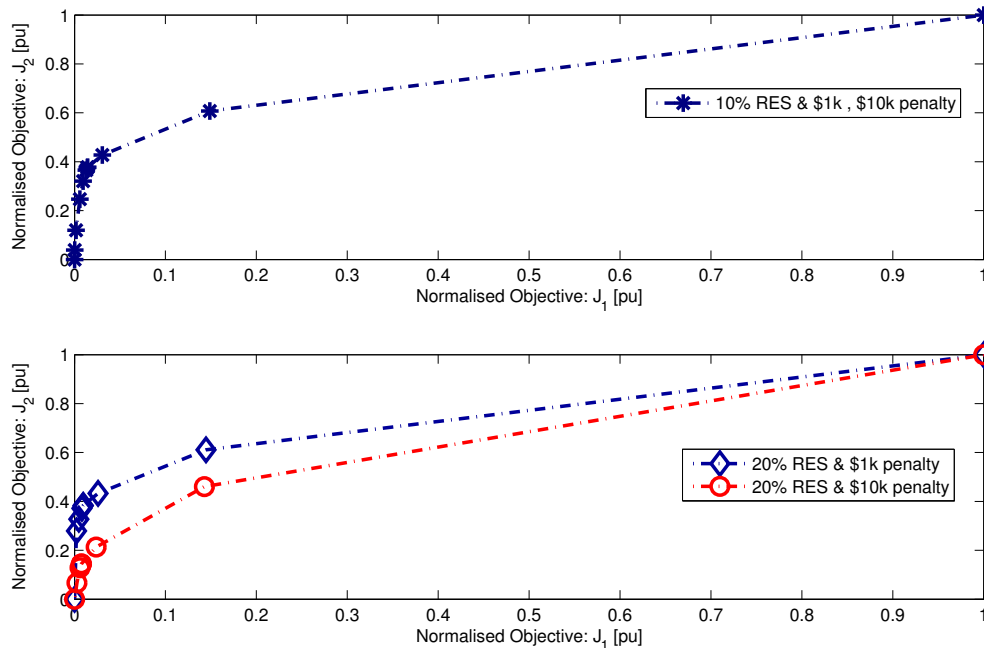
Figure 5.17. Average expected operating cost and RES penetration level.

obligation is 10% and the penalty is varied from $1000 and $10,000, the RES obligation is attained without any penalty. However, when the RES obligation is increased to 20% while varying the penalty, then the RES penetration is achieved only when the penalty is $10,000 which results in an average RES penetration level of 27,463 MWh compared to 26,439 MWh of RES when the penalty is $1000. The total operating costs for the two scenarios when RES obligation is 20% are $462,862.7 and $462,941.8, respectively for the $1000 and $10,000 penalty. The operating cost increases because in the first case when the penalty is $1000, it is acceptable to not attain the RES obligation since the operating cost is minimal. The optimal solution presented shows that the proposed model is robust and can achieve RES penetration while considering the minimal operating cost for different RES obligation penalty cost.

5.5.2.6   The impact of transfer limits on RES penetration level

Initially, the transfer limits of the transmission line as shown in Figure 5.18 are divided into five transfer limits which are 180 MW, 360 MW, 450 MW, 540 MW and 900 MW and the RES penetration achieved is 46.74%. In order to show the effect of transfer limits on the RES penetration, two cases are considered; the transmission transfer limit is increased and decreased by 10% respectively. The optimal RES penetration level under different transfer limit is depicted in Figure 5.18.
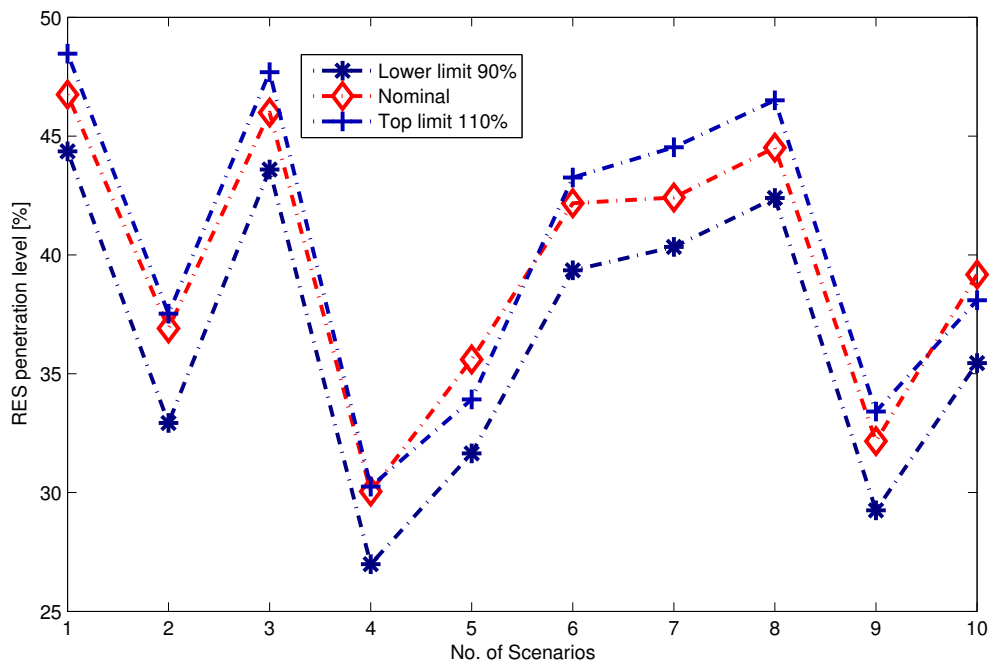
Figure 5.18. Impact of different transfer limits on RES penetration.

The impact of transmission limit is variable, which means that it may lead to an increase in total operating cost as well as the RES penetration when the limit is increased. However, when the limit is reduced, RES penetration level also decreases. This arises due to scheduling changes of the individual units. Specifically, the reduction in outputs of some units results in more RES penetration, while an increase in output of other units results in a decrease in RES penetration and spinning reserves as well as the total operating cost. The impact of increasing the transfer limit increases the operating cost and RES penetration level. On the other hand, the decrease in thermal limits leads to a decrease in total operating costs and RES penetration level.

5.5.3   Case study 2: IEEE 118-bus system

In the second case study, the proposed model is tested on a large-scale bus system. The system data for the IEEE 118-bus is from [83] and this system consists of 54 thermal generators and 186 transmission lines. The total thermal power installed is 12156 MW and the peak demand is 12147 MW. The sizes of the five wind farms are 250 MW, 1050 MW, 350 MW, 320 MW and 1600 MW, while the sizes of the five PV plants are 200 MW each. The two BESS generators are rated at 35 and 40 MWh with the charging and discharging efficiency of 90%. The proposed model is used for calculating the total operating cost and RES penetration level.

5.5.3.1   Computational efficiency of the proposed model

This section explores the computational efficiency of the IEEE 118-bus system, due to the stochastic nature of the model presented in Section 5.3, there are generally many constraints that are inherent because of the number of scenarios. For example, the total number of line capacity constraints is the multiple of the time period (96), total number of transmission lines (186) and the number of scenarios (10). For the IEEE 118-bus system, the total number of transmission constraints is 357,120. When the inactive constraint reduction theorem presented in [147] is applied, the total number of inactive constraints is identified as 87%. The new transmission line constraints are reduced to 46,426 which reduces the solving time to 60 s.

In the first case the total number of line capacity constraints is considered, and the time taken to solve the problem using parameter relaxation is 130 s compared to 60 s when the line constraints are reduced. In both cases, the RES obligation is attained, and the total operating cost is \$4,500,900 with a standard deviation of 0.2%. From observations made, the computational efficiency shows that the proposed method can be utilised in scheduling RES, thermal and BESS units in a large-scale bus system.

5.5.3.2   Impact of RES obligation on model sensitivity

The impact of RES penetration on the model sensitivity is investigated in the IEEE 118-bus system. The total number of RES generators is increased from 4 to 10. The computed results are shown in Figure 5.19 when varying the RES penetration from 10% to 50%. As can be seen in this figure, the total operating cost increases with the increase in RES penetration level. It is important to note that the total operating cost of the 30-bus system is considerably lower than that of the 118-bus system which is to be expected since the demand has increased, and the network size is larger. The RES penetration level is achieved until 30% and any requirement over that results in a penalty. The reason for this limitation is due to the transfer limit on the transmission lines.
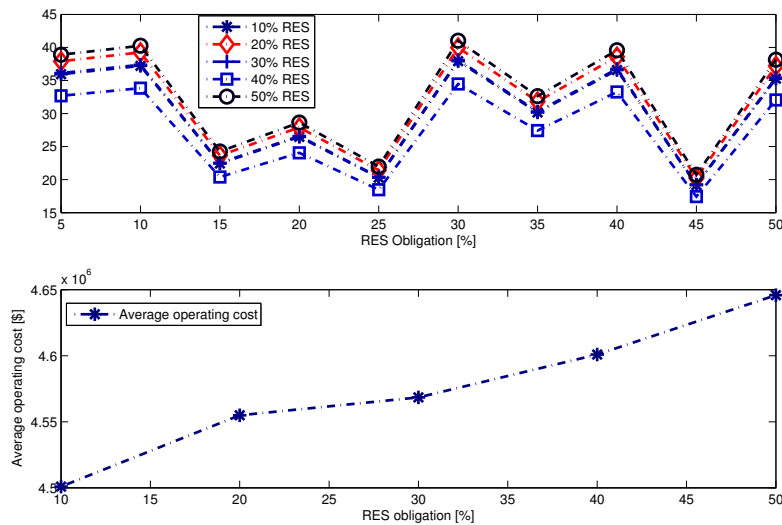
Figure 5.19. Average RES penetration and average operating cost for IEEE 118-bus system.

The average RES penetration achieved for the different obligation starting from 10% to 50% is 30.15%, 32%, 30.5%, 27.4% and 32.6% respectively. The highest operating cost occurs at 50% RES obligation which is \$4,645,909, which corresponds to the RES penetration of 32.6% when the obligation is 50%.

5.5.3.3   Impact of BESS on spinning reserves and RES obligation

In this case study, 10 scenarios are considered for the evaluation of the proposed model. The achieved expected operating cost is \$4,376,923.81 and the achieved maximum RES injection level is 34.47%, while the total reduction in spinning reserves is 0.19% and the BESS generation is -1132 \$MWh\$. This means that throughout the dispatch period the BESS is charging up with minimum discharge. The stochastic model proposed is better in the approximation of the RES penetration level. Table 5.5 shows a comparison of the IEEE 118-bus generation for thermal, BESS, RES and the spinning reserves. The average operating cost achieved for the deterministic model is \$4,017,379.10.

5.6   CONCLUSION

This chapter proposes a stochastic economic dispatch model with renewable obligation requirement to maximise renewable energy penetration. The system operator is responsible for scheduling energy and spinning reserve under the renewable obligation framework. This framework aims to allocate the required renewable energy as part of an optimal energy mix strategy that reduces greenhouse gas emission. A dynamic scenario generation algorithm is used to characterise the intermittent nature

Table 5.5. Comparison of stochastic and deterministic RES penetration for IEEE 118-bus.

Description	Stochastic			Deterministic
	Best	Mean	Worst	
Thermal (MWh)	669433	741970	843566	790605
BESS (MWh)	-1132	-1874	-3095	-1272
SR (MWh)	370973	304732	208720	194101
RES (MWh)	352153	279979	178020	230981
RES (%)	34.47	29.83	17.43	22.61

of wind and photovoltaic output power and thereafter a scenario reduction algorithm is used in the renewable obligation model to schedule an optimal dispatch energy and allocate spinning reserves. To show the effectiveness of the proposed model, a 30-bus network with 6 thermal generators and 4 renewable energy sources is used to show the impact of high renewable energy penetration. Four cases were used to illustrate the effectiveness of the proposed renewable obligation model; in the first case a comparison of the deterministic and stochastic renewable obligation was performed based on the system operating costs, the reduction in spinning reserve allocation due to battery energy storage system and the achieved renewable energy penetration level. The comprehensive benefit of the four models were evaluated and thereafter we showed that the stochastic renewable obligation model is the most effective model in terms of the key measurement parameters. The sensitivity analysis was used to investigate other key parameters and the applicability of the proposed model. Our conclusion are as follows:

1. A benchmark renewable obligation target of 10% was used for the energy mix and output power of renewable energy sources was simulated using historical data. The simulated results show that higher renewable obligation can be achieved over and above the target.

2. The key indicator for any renewable obligation programme is the energy produced from renewable energy sources, which is used to issue renewable obligation certificates to all qualifying generation companies. The simulation studies show that it is possible to achieve high renewable penetration at a reasonable operating cost using the Pareto front approach.

3. A penalty is normally paid by generation companies for any renewable obligation shortfall; the simulation studies shows the different penalty factors used to validate the effectiveness of the

proposed model and show the limitation and application in practical problems.

4. The maximum renewable penetration level is also limited by the available transmission thermal limits on the 30-bus network.

5. In a large 118-bus network, the computational effectiveness is improved by reducing the inactive transmission limit and a maximum of 87% inactive transmission constraints are reduced.

The current renewable obligation model does not take into consideration the trading of renewable obligation certificates. Therefore, the future research will include the risk associated with trading renewable obligation certificates in the secondary market.

CHAPTER 6   RISK-CONSTRAINED STOCHASTIC ECONOMIC DISPATCH WITH DEMAND RESPONSE UNDER RENEWABLE OBLIGATION

In this chapter, the deterministic demand response model is extended to stochastic model to handle all the RES uncertainty.

6.1   INTRODUCTION

The variable and stochastic nature of renewable energy sources (RES) such as wind and photovoltaic generators makes it difficult for their integration in the power systems. This means that RES generators cannot be completely regulated by producers throughout the day as they depend on weather conditions. Therefore, it is not easy to know the level of power production with certainty, however, this can be forecasted with some level of accuracy. The increased level of RES in power systems requires a robust demand side and supply side strategy from the viewpoint of the system operator. The need for capacity margins during peak hour demand coupled with the inherent limited ramping capacity of thermal generators affect the system security whenever the RES generators decrease their output power due to meteorological conditions. To tackle this challenge, the system operator takes advantage of the demand side strategy by either shifting or cutting down the load to balance the RES production. Therefore, it is essential to carry out a joint strategy for RES penetration and demand response [141] to allow the system operator to optimally dispatch power while meeting a specific renewable obligation for energy mix and minimising the risk of profit loss. A useful tool to quantify the dispatch of thermal and RES generators is the classical dynamic economic dispatch (DED). This tool can be used together with demand response to quantify the level of RES penetration that can meet the required renewable

obligation while minimising the risk of profit loss for thermal generators.

An important aspect that helps in the increase of RES penetration is demand response (DR). There are two main categories for DR programmes, namely, the price-based demand response (PBDR) and incentive based demand response (IBDR) [150]. The PBDR uses time-varying tariff structure for the sale of electricity to customers. The tariff structure is often divided into three parts, namely, peak, standard and off-peak hour rates; while a two-part tariff with only peak and off-peak rates can also be found in many places. The use of PBDR helps in reshaping the demand profile by moving peak load to off-peak and reducing the operating costs. The main disadvantage of this DR strategy is that it depends on the voluntary participation of customers and cannot be directly controlled by the system operator [42]. On the contrary, the IBDR pays participating customers for reducing their demand when requested by the system operator. This is most conveniently done using direct load control (DLC) during periods of high demand and high electricity prices. The main advantage of using the IBDR comes from the ability of the system operator to control the system reserves to create flexibility of the system by increasing or curtailing demand. In [93] and [94], a stochastic unit commitment with IBDR is presented and a price quantity package for IBDR is reported [95]. Authors in [96] consider a robust optimisation approach to economic dispatch with RES and IBDR. A demand reduction approach is presented in [97] where emergency demand response programme (EDRP) and DRP are considered using price elasticity and linear responsive loads.

A detailed comparison of different demand response paradigms is presented in [151] for the integration of renewable energy sources and deferrable demand considering the reserve requirements. The authors show that coordinating flexible demand with renewable energy can increase RES penetration and show that the conventional way of defining demand elasticity has to be adapted for deferrable loads. Reference [152] presents a demand response model integrated to a day-ahead scheduling of electricity and natural gas using stochastic unit commitment problem. In their model, they show that using demand response can enhance the coordination of gas and electricity and reduce demand uncertainty.

In [153] a hybrid power plant is constructed considering the DR aggregator and wind power aggregator to limit the inherent stochastic nature of wind generator to take part in the electricity market. The model presented is a three-stage stochastic programming problem which participates in three electricity markets and the risk is managed by the conditional value-at-risk (CVaR). In [154] shows a risk-constrained bidding strategy for a hybrid power plant that participate in a joint operation of wind power

and energy storage to maximise its profit. Different bidding curves are presented for an optimal day-ahead market that maximises the expected profit for a coordinated operation of wind and compressed air storage system.

In the network that has a high level of RES penetration, the issues of capacity margins during peak hours are important for a reliable and continuously supply of energy. The literature reviewed shows that the inclusion of demand response with high RES penetration is possible, however, there is still a need for a detailed and optimal framework which considers the a risk constrained stochastic DED under a renewable obligation and demand response from the system operator's point of view who owns and operate the thermal generators. The proposed model in this chapter takes advantage of quantifying the level of financial risk to the system operator by incorporating a renewable obligation and demand response in its generation portfolio. A framework for renewable obligation and demand response is presented to increase the output power of RES generators by coordinating the operation of RES quota and DR. The contributions are listed below;

1. The development of a combined IBDR model with renewable obligation for joint operation to maximise the expected profit of generation companies while mitigating the uncertainties of RES generators;

2. The implementation and analysis of the proposed model on a renewable obligation framework; and

3. The inclusion of risk constrained model to minimise financial risk in the IBDR and renewable obligation framework.

The contents of this chapter are organised into four sections. In Section 6.2.1, we provide the problem formulation for the risk constrained stochastic DED with renewable obligation and IBDR. In Section 6.3, the solution approach for the risk-constrained model and in Section 6.4 the simulations and numerical studies are presented. In Section 6.4, the conclusion and recommendations are drawn.

6.2   PROBLEM FORMULATION

In this section a mathematical model of a renewable obligation policy framework from [86], [155] is extended to incorporate risk-based demand response to increase RES penetration. The model includes the penalty function that is imposed by the system operator to thermal generators when the RES quota is not achieved. Then an optimisation model is presented to include demand response by modifying a

renewable obligation model to allow for demand reduction while providing an incentive to residential customers that participated in the IBDR program. The financial risk of system operator is quantified to incorporate demand response and renewable obligation in the generation portfolio over a 24-hour period.

6.2.1   Renewable obligation framework

The main purpose here is to maximise the economic profit of system operator thermal generators while maintaining a percentage of renewable energy in the energy mix.

6.2.1.1   Objective functions

The main goal is to maximise the economic profit of the thermal generators which is defined as the difference between the revenue and total operating cost as shown in (6.1).

$$\text{Maximise } \mathbb{E}\{PF\} = \mathbb{E}\{RV\} - \mathbb{E}\{TC\} \tag{6.1}$$

where $\mathbb{E}\{PF\}$, $\mathbb{E}\{RV\}$, and $\mathbb{E}\{TC\}$ are the expected economic profit, the expected revenue of thermal generators, and the expected total operating costs respectively. The thermal generators sell power in the energy market and ancillary service market. In the ancillary market the RES companies pay the thermal generators for allocating the reserves for balancing the RES shortfall. This cost is paid despite whether the reserves are used or not. On the contrary, the thermal generators must buy energy from the renewable energy producers to ensure that a certain minimum quota is achieved. The revenue for the generation companies is calculated as follows.

$$\mathbb{E}\{RV\} = \sum_{\omega=1}^{N_\omega} \sum_{t=1}^{T} \sum_{g=1}^{N_G} \pi_\omega \left(P_{g,t,\omega} \Delta t \Upsilon_t + P_{r,t,\omega} \Delta t \vartheta_t \right) \tag{6.2}$$

where $P_{g,t,\omega}$ is the thermal generator output power of generator g at time t and scenario ω, Υ_t is the forecasted market price for electricity at time t, $P_{r,t,\omega}$ is the spinning reserve of thermal generator g at time t and scenario ω, and ϑ_t is the market price for spinning reserves at time t.

The total operating cost includes two main terms. The first term is the cost of operating thermal generators and the cost paid to IPP for RES generators. The second part is the penalty function that ensures that a minimum renewable obligation is maintained in the dispatch period to guarantee adequate energy mix.

$$\mathbb{E}\{J_1\} = \sum_{\omega=1}^{N_\omega} \sum_{t=1}^{T} \pi_\omega \left(\sum_{g=1}^{N_G} C_g(P_{g,t,\omega}) + \sum_{m=1}^{N_M} C_m(P_{m,t,\omega}) + \sum_{v=1}^{N_V} C_v(P_{v,t,\omega}) \right) + \Gamma \tag{6.3}$$

where π_ω is the probability of each scenario, $C_g(P_{g,t,\omega})$ is the generator fuel cost function which is a quadratic equation, and $C_m(P_{m,t,\omega})$ and $C_v(P_{v,t,\omega})$ are the cost function for wind and PV generators,

respectively, see (6.4) to (6.6).

$$C_g\left(P_{g,t,\omega}\right) = \sum_{g=1}^{N_G}\left(a_g + b_g P_{g,t,\omega} + c_g P_{g,t,\omega}^2\right) \tag{6.4}$$

$$C_m\left(P_{m,t,\omega}\right) = \sum_{m=1}^{N_M} \zeta_m P_{m,t,\omega}\Delta t \tag{6.5}$$

$$C_v\left(P_{v,t,\omega}\right) = \sum_{v=1}^{N_V} \varphi_v P_{v,t,\omega}\Delta t \tag{6.6}$$

The notation Γ is the second part of the total cost which is a renewable obligation part of the model shown in (6.7).

$$\Gamma = \gamma \sum_{\omega=1}^{N_\omega}\sum_{t=1}^{T}\pi_\omega\left(\alpha\left(\sum_{g=1}^{N_G}P_{g,t,\omega} + \sum_{m=1}^{N_M}P_{m,t,\omega} + \sum_{v=1}^{N_V}P_{v,t,\omega}\right) - \left(\sum_{m=1}^{N_M}P_{m,t} + \sum_{v=1}^{N_V}P_{v,t}\right)\right)^+ \tag{6.7}$$

where γ is the penalty imposed to the thermal generators for not achieving the required obligation, α is a renewable obligation requirement in percentage. The notation $\Gamma(\cdot)^+$ is the sigmoid function which is equal to γ if the RES obligation is unattained and 0 otherwise. The penalty γ is normally provided by the energy regulator as an annual value. This penalty value can be change to a daily penalty value to correspond to daily economical dispatch of generators. In addition to the total operating cost in (6.3), the renewable producers also want to maximise their profit which is shown in (6.8).

$$\mathbb{E}\{J_2\} = \sum_{\omega=1}^{N_\omega}\sum_{t=1}^{T}\pi_\omega\left(\sum_{m=1}^{N_M}P_{m,t,\omega}\Delta t\rho_t + \sum_{v=1}^{N_V}P_{v,t,\omega}\Delta t\tau_t\right) \tag{6.8}$$

where ρ_t and τ_t are the forecasted market price for electricity at time t. The overall expected total operating cost is the minimal difference between the operating cost and profit of renewable operators as shown in (6.9).

$$\mathbb{E}\{TC\} = \mathbb{E}\{J_1\} - \mathbb{E}\{J_2\} \tag{6.9}$$

6.2.1.2   Constraints

The system constraints is divided into five parts, the power balance constraint (6.10), the system ramping rates (6.11) to (6.14), the generator limits (6.15) to (6.18), spinning reserve constraints (6.19)

---

to (6.22) and the network transmission capacity constraints (6.23) to (6.24).

$$\sum_{g=1}^{N_G} P_{g,t,\omega} + \sum_{m=1}^{N_M} P_{m,t,\omega} + \sum_{v=1}^{N_V} P_{v,t,\omega} = \sum_{b=1}^{N_B} P_{b,t} \;\; \forall t, \omega \tag{6.10}$$

$$P_{g,t,\omega} - P_{g,t-1,\omega} \leq UR_g \Delta t \;\; \forall t, \omega \tag{6.11}$$

$$P_{g,t-1,\omega} - P_{g,t,\omega} \leq DR_g \Delta t \;\; \forall t, \omega \tag{6.12}$$

$$P_{r,t,\omega} - P_{r,t-1,\omega} \leq UR_g \Delta t \;\; \forall t, \omega \tag{6.13}$$

$$P_{r,t-1,\omega} - P_{r,t,\omega} \leq DR_g \Delta t \;\; \forall t, \omega \tag{6.14}$$

$$P_{g,t,\omega} \leq min(P_{g,max}, P_{g,t-1,\omega} + UR_g \Delta t) \;\; \forall t, \omega \tag{6.15}$$

$$P_{g,t,\omega} \geq max(P_{g,min}, P_{g,t-1,\omega} - DR_g \Delta t) \;\; \forall t, \omega \tag{6.16}$$

$$P_{m,t,\omega} \leq P_{m,t,gen} \;\; \forall t, \omega \tag{6.17}$$

$$P_{v,t,\omega} \leq P_{v,t,gen} \;\; \forall t, \omega \tag{6.18}$$

$$P_{g,t,\omega} + P_{r,t,\omega} \leq P_{g,max} \;\; \forall g, t, \omega \tag{6.19}$$

$$0 \leq P_{r,t,\omega} \leq SRR_{r,max} \;\; \forall t, \omega \tag{6.20}$$

$$\sum_{r=1}^{N_R} P_{r,t,\omega} \geq SSRR \;\; \forall t, \omega \tag{6.21}$$

$$\sum_{g=1}^{N_G} P_{g,t,\omega} + \sum_{r=1}^{N_R} P_{r,t,\omega} \geq \sum_{b=1}^{N_B} P_{b,t} \;\; \forall t, \omega \tag{6.22}$$

$$-P_{l,max} \leq P_{l,t,\omega} \leq P_{l,max}, \;\; \forall l, \forall t, \forall \omega \tag{6.23}$$

$$P_{l,t,\omega} = \sum_{g=1}^{N_G} G_{l,g} P_{g,t,\omega} + \sum_{m=1}^{N_M} F_{l,m} P_{m,t,\omega} +$$

$$\sum_{v=1}^{N_V} H_{l,v} P_{v,t,\omega} - \sum_{b=1}^{N_B} D_{l,D} P_{b,t} \tag{6.24}$$

The maximum spinning reserve requirement $SRR_{r,max}$ is equal to the maximum thermal generator capacity, and the system spinning reserve requirement (SSRR) is equal to 30% of the peak demand; where $G_{l,g}$, $F_{l,m}$, $H_{l,v}$, and $D_{l,D}$ denote the generator shift factor (GSF) coefficient between line l and thermal generator, wind farms, PV plant, and system demand at each bus. The transmission line power $P_{l,t,\omega}$ of line l at time interval t and scenario ω is calculated by nonlinear power flow for small size power systems, and DC power flow for a large system.

6.2.2 Incentive based demand response model

In this section, the addition of demand reduction strategy is added to the model (6.1) using an incentive to motivate residential customers participating in the demand response programme. A large-scale residential load management (RLM) program is implemented in South Africa by installing a DLC at a

local substation to switch on and off the electric water heaters. The motivation for this implementation comes from the fact that electric water heaters account for 30% to 50% of the electricity consumption in a household and the overall consumption of household is between 20% to 25% of the total electricity produced by the utility. The objective function in (6.3) is modified to include demand response as shown in (6.25).

$$\mathbb{E}\{J_3\} = \sum_{\omega=1}^{N_\omega}\sum_{t=1}^{T}\sum_{b=1}^{N_B} \pi_\omega \left(\left(\lambda_t^R - \xi_{b,t}^c\right)\left(P_{b,t,\omega}(1-u_{b,t,\omega}) + \tilde{P}_{b,t,\omega}u_{b,t,\omega}\right)\right)\Delta t \tag{6.25}$$
$$+ \sum_{\omega=1}^{N_\omega}\sum_{t=1}^{T}\sum_{b=1}^{N_B} \pi_\omega \Delta P_{b,t,\omega}u_{b,t,\omega}\xi_{b,t}^i\Delta t$$

Equation (6.25) is the total cost paid by the generation companies for demand reduction to participating residential customers, $\Delta P_{b,t}$ is the difference between the actual demand at bus b before and after the demand reduction see also (6.26); and $\xi_{b,t}$ is the incentive cost paid to residential customers during peak period T_p.

$$\Delta P_{b,t} = P_{b,t} - \tilde{P}_{b,t} \tag{6.26}$$

The switching status $u_{b,t,\omega}$ is a binary variable that is equal to 1 if the RLM is implemented at bus b in time t and scenario ω, and 0 indicating that no RLM is implemented.

The only change in the constraints is due to the change in demand which is replaced by in (6.27); the only the constraints affected by the demand reduction are (6.10), (6.21), and (6.22). The change on constraint (6.21) is because SSRR is equal to peak demand $P_{b,t}$.

$$P_{b,t} = \sum_{b=1}^{N_B}\left(P_{b,t}(1-u_{b,t,\omega}) + \tilde{P}_{b,t}u_{b,t,\omega}\right) \ \forall t, \omega \tag{6.27}$$

6.2.3   Risk constrained model

The model is further updated to include the value at risk in order to account for the potential profit loss. This means for a given probability $\mu \in (0,1)$, the value-at-risk (VaR) is equal to the largest value η ensuring that the probability of obtaining a profit less than η is lower than $(1-\mu)$. In other words, the VaR(μ,x) is $(1-\mu)$-quantile of the profit distribution [156]. Mathematically, the VaR(μ,x) is defined as shown in (6.28).

$$\text{VaR}(\mu,x) = \max\{\eta : Prob(\omega) \,|\, PF(x,\omega) < \eta \le 1-\mu\}, \forall \mu \tag{6.28}$$

The variable x represents all the decision variables and *Prob* is the probability. The updated objective function with VaR is shown in (6.29).

$$\text{Max } \mathbb{E}\{VaR(\mu,x)\} = \mathbb{E}\{(1-\beta)PF + \beta\eta\} \tag{6.29}$$

where η is a variable whose optimal value is equal to the VaR(μ,x) and β is the weighting parameter used to transform the two objective functions to a single objective function. In addition to the modified constraints the following additional related to the risk model are added.

$$\eta - PF \leq M\theta_\omega, \ \forall \omega \in N_\omega \tag{6.30}$$

$$\sum_{\omega=1}^{N_\omega} \pi_\omega \theta_\omega \leq 1 - \mu \tag{6.31}$$

where θ_ω is a binary variable which is equal to 1 if the profit in scenario ω is less than η and equal to 0 otherwise; and M is a large enough constant.

6.3   SOLUTION APPROACH

The proposed optimisation model is applied to IEEE 118-bus system. The test system consists of 54 thermal generators and 186 transmission lines. Two bulk RES generators are added to buses 20 and 33. The sizes of the PV and wind generators are 1000 MW and 3600 MW respectively. The details of the 118-bus system can be found in [83]. The transmission flow limit is simulated by using DC power flow. A sampling interval of one hour is considered for generation dispatch and the optimisation problem is solved over a 24-hour period. In cases where RES penetration level is unattained, a penalty of $100,000 per day is imposed on thermal generators by the system operator. In all case studies, a 10% RES obligation is used as a basis for comparison. In addition, the system spinning reserve requirement is based on 15% of the maximum thermal generator capacity and the maximum spinning reserve requirement of each generator is equal to the maximum generator capacity. The combined risk-constrained multi-objective stochastic economic dispatch with renewable obligation and demand response problem is a mixed integer quadratic programming problem (MIQP), which is simplified into a mixed integer linear programming (MILP) problem by replacing the quadratic cost functions with a piecewise linear function [157]. The reason for this replacement to minimise the computational time required to handle the quadratic constraint in the VaR constraint. The model can be solved by using commercial solvers such as CPLEX. MATPOWER has been used to for power system analysis in order to find the power transfer distribution factors used in the DC power flow.

The scenario generation methodology is applied to the data obtained from EirGrid [142] for one-year data in 2018. Time series forecasting is used for forecasting wind and PV power output. For simplicity,

wind and PV power output are assumed to follow a Weibull and normal distribution. The associated PV and wind power output are forecasted using moving average (MA) and autoregressive (AR) model. The prediction error of the output power at time t is obtained by minimising the mean square error of the AR or MA model from the historical data of RES output power. Furthermore, we assume that the system uncertainty are independent. Based on the distribution of uncertainty parameters, the Latin hypercube sampling technique is employed to generate 1000 scenarios with even probability where each scenario contains the information of the hourly load, the hourly wind and PV output power over the operating day. The fast-forward reduction algorithm is utilised to reduce the original 1000 scenarios to 10 scenarios [158]. In particular, we used MATLAB software to generate and reduce the scenarios [159] and [145]. Table. 6.1 shows the parameters used in the simulation studies.

Table 6.1. Constant parameters used in the simulations.

Description	Parameter 1	Parameter 2
M	1e6	-
μ	0.95	-
α (%)	10	-
τ ($/MWh)	1.70	2.0
ρ ($/MWh)	1.70	2.0
$MA\{2\}$	0.92	0.95
$AR\{2\}$	1.43	-0.49

In general, a large number of scenarios results in higher computational time while a small number of scenarios may reduce the accuracy of the results. All the test cases are implemented on a notebook with an Intel Core i5 at 2.70 GHz and 8 GB RAM. The optimisation problem is solved in approximately 360 seconds. The IEEE 118-bus system is used to demonstrate the effectiveness of the model considering the following cases;

1. Case 1: A deterministic model is used as a base case where the RO is set to 10% under DR implementation;

2. Case 2: A stochastic model is used with RO set to 10% without DR;

3. Case 3: A stochastic model in Case 2 with DR implementation; and

4. Case 4: Risk-constraint is implemented on the stochastic model with DR to measure the impact on the expected profit deviation.

In order to compare the proposed model, the expected profit, the actual RES penetration level and the demand reduction is used for comparison. The total installed capacity of RES is 4600 MW. All the transmission line thermal limits are maintained at 100%. The utility sells electricity to all customers based on the TOU tariff scheme, which is divided into three periods, i.e., peak, off-peak and standard. The electricity price are \$200/MWh, \$50/MWh and \$100/MWh. The customer willingness to buy electricity is \$120/MWh. In this study, peak periods are between 07:00 to 09:00 in the morning, 18:00 to 20:00 in the evening; the standard period is from 09:00 to 18:00 and from 20:00 to 21:00 and the remaining period is classified as off-peak. The total demand before and after the implementation of the RLM programme is shown in Figure 6.1.
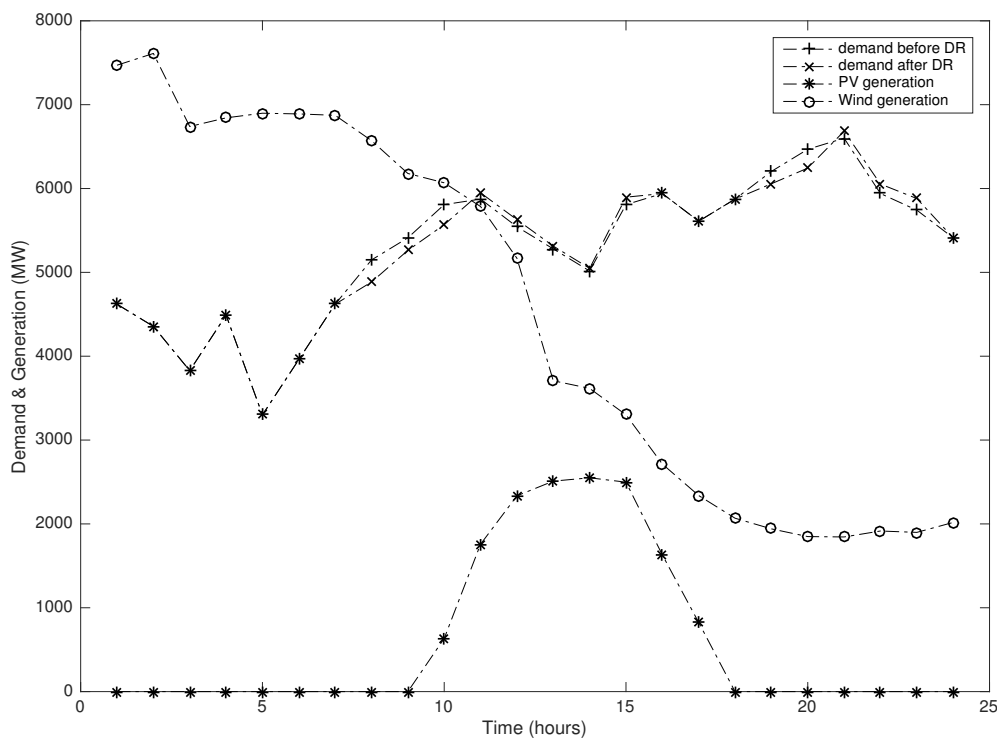
Figure 6.1. IEEE 118 demand before and after implementation of RLM.

The system baseline load is found in [83] and the real data from the RLM programme is used on load bus 2, 12, 18, 32 and 59 [111]. The total demand before and after the implementation of RLM is

126,854 and 125,830.20 MW. The framework for demand reduction is based on a load management programme which is developed by the system operator focusing specifically on residential customers. The programme considers participation of residential customers to reduce their demand by providing an incentive. The RLM participation can occur anytime of the day, however, an incentive is only paid during peak hours. As part of the RLM programme, a small control unit is installed in the customer's home. This unit will switch off the supply to the hot water heater during peak demand for a predetermined period. A group of hot water heaters are controlled and monitored centrally from each participating substation by means of a radio ripple-based communication.

6.4 NUMERICAL RESULTS

In order to evaluate the performance of the proposed method on a large-scale IEEE test system four cases are investigated and a comparison of them is evaluated.

6.4.1 Case 1: Deterministic base case

In this case the normal operation is investigated using a deterministic model. This means that the scenario index is set to one in the problem formulation to represent a deterministic model. The total renewable obligation is maintained as 10% and all the quadratic cost functions are changed into piecewise linear functions. A key performance indicator for this case study is the maximum profit achieved, the total RES penetration level and demand reduction attained. The total RES penetration achieved is 39.08% compared to the base requirement of 10%. The demand reduction of 5.412 MW is achieved which results in a total profit of $1,041,811.64.

Table 6.2. Total profit before and after RLM implementation with 10% RES penetration level, α=10% and λ_1=0.5

Description	DED without RLM	DED with RLM	Delta
Total cost ($)	1,060,336.99	1,041,811.64	18,525.35
Total P_D (MW)	126,854	126,848.588	5.412
Incentive ($)	–	216.48	216.48
SR (MW)	12,685.4	12,684.3	–
α_{act} (%)	38.40	39.08	0.68

The total profit achieved for the base scenario without RLM programme is higher than the case when RLM is implemented. This is an increase of $18,525.35, in terms of the profit which can be explained

by the decrease in demand. It is important to note that in both cases, the RES penetration level is realised and hence no penalty is imposed on the thermal generation companies. Moreover, for the required RES injection level of 10%, the spinning reserve required does not change at all. The overall incentive paid to participating customers is $216.48, and the actual achieved savings is the difference between the savings in operating cost and incentive paid to customers which is $18,308.87. It is important to note that a demand reduction of 5MW increases the RES penetration by 0.68% which shows the benefit of DRP.

6.4.2 Case 2: A stochastic model without demand response

In order to show the effectiveness of the DR model, first a stochastic model without DR is used as a baseline for comparison. The total profit and RES production are used for comparison purpose. The allocated spinning reserve are also included in the analysis. When a renewable obligation of 10% is used as a baseline, the stochastic model can inject an average 18.52% of renewable energy with a maximum injection of 26.70% and a worst injection of 10.49% which is still over the required RES obligation. The overall profit of $854,570.47 per day is achieved using the stochastic model. The average allocated spinning reserve allocation for the joint dispatch problem is 79146 MW while the minimum and maximum reserve allocation are 44265 MW and 118061 MW, respectively. The total demand for the 24-hour period is 126854 MWh and the thermal generators contribute an average of 81.47% with the minimum and maximum contribution of 73.30% and 89.50%, respectively. Table 6.3 summarises the stochastic model results in terms of achieved RES penetration and generation mix.

Table 6.3. Comparison between stochastic and deterministic model without DRP.

Description	Stochastic			Deterministic
	Best	Mean	Worst	
Thermal (MWh)	113539	103348.9	92990	78142.06
PV (MWh)	10308.96	7129.74	2751.00	17195.31
Wind (MWh)	31112.0	16375.41	3006.06	31516.62
SR (MW)	118061.03	79146.28	44265.00	12,685.4
RES (MWh)	33864	23505.15	13315.03	48711.94
RES (%)	26.69	18.53	10.49	38.40

The total renewable penetration for a deterministic case is very optimistic and gives higher RES penetration. However, it should be noted that since wind and PV have uncertainty due to weather dependent wind speed and solar irradiance. The deterministic case should only be considered with caution. Overall, the profit for a deterministic case is shown in Table 6.2 and it is higher than the stochastic case. Therefore, the stochastic case provides a more conservative estimation under different scenarios, i.e., best, medium and worst case whereas the deterministic model only provides a single scenario without any variance.

6.4.3 Case 3: Stochastic model with demand response

In this case a stochastic model with DR is investigated under RO. The total demand before and after RLM is the same as before. The stochastic model under DR is investigated to find the maximum profit that can be realised for the generation companies and the maximum demand reduction achievable. When the stochastic model is used, the average renewable penetration level is 17.83% and the minimum and maximum are 26.67% and 10.18%, respectively. In all scenarios, the RES penetration is over 10% target. The average demand reduction for the 10 scenarios is 90.92 MW and all the participating substation are active during peak and valley period. Notice that during peak hours, the flexible demand from the electric water heaters is reduced. A maximum demand reduction of 398.33 MW is achieved in one of the scenarios and a minimum demand reduction of -87.59 MW is also achieved. The negative demand means that there is an increase in demand by 87.59 MW over the entire dispatch period. Therefore, in this scenario there is no demand reduction. Table 6.4 shows a comparison of demand reduction for stochastic and deterministic case.

Table 6.4. Comparison between stochastic and deterministic model without DRP.

Description	Stochastic $\beta=0$			Deterministic
	Best	Mean	Worst	
Thermal (MWh)	113878.5	104162.7	92725.71	78142.06
PV (MWh)	10494.82	7304.92	3013.00	8081.63
Wind (MWh)	30371.06	15295.42	2424.25	41493.82
SR (MW)	117621.5	77914.16	43841.44	12,685.4
RES (MWh)	33730.06	22600.34	12919.08	49572.43
RES (%)	26.67	17.83	10.18	39.08
DR (MW)	398.33	90.93	-87.59	5.41

Figure 6.2 shows the demand reduction for 10 scenarios with the two lower and upper limits. Note that the lower limits are related to the total demand reduction and the top limit is the actual demand without any demand reduction.
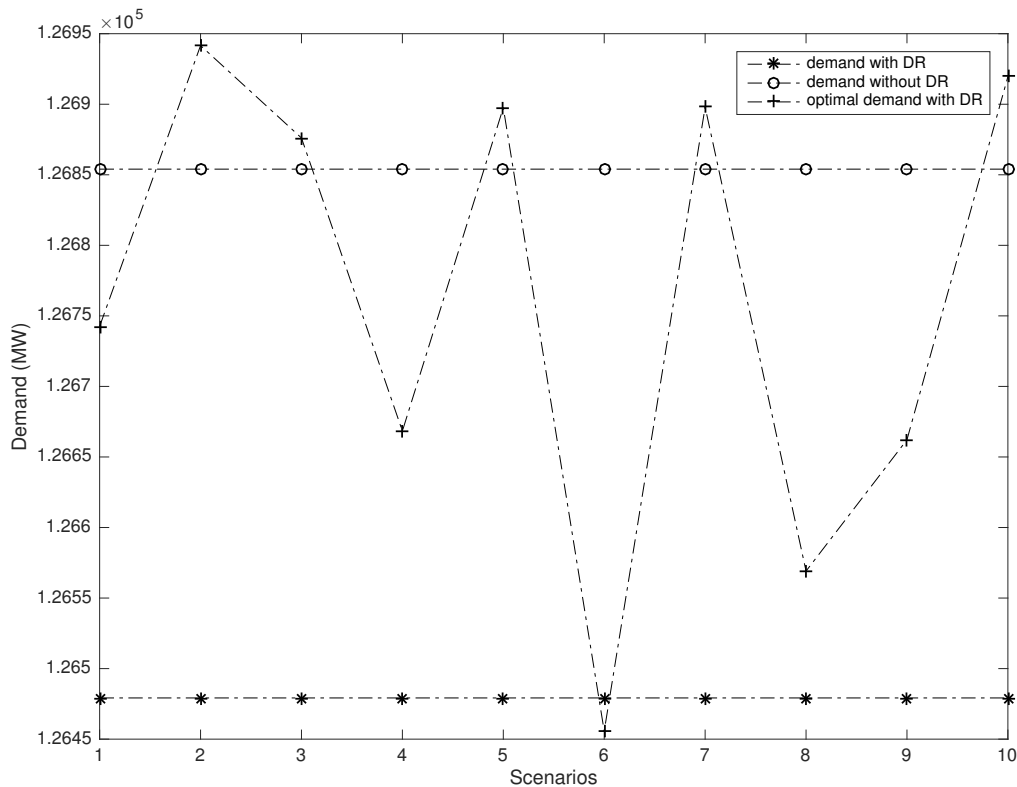
Figure 6.2. Demand response participation under different stochastic scenarios with RES obligation set to 10%.

The average incentive paid to customers is $3,636.80 and the overall profit achieved is $988,642.98. The average substation participation level is 43 with the minimum and maximum participation of 15 and 59 times per day on the RLM substations.

6.4.4   Case 4: Stochastic model with demand response and Value-at-Risk

In order to characterise the risk associated with maximising the profit of generation companies under demand response and renewable obligation a VaR is used as a risk measure to profit loss. This risk measure allows a comparison between a risk averse strategy and risk-based strategy for the generation companies. A risk neutral strategy is already considered in case study 3 with $\beta = 0$, in this case the risk factor in (6.29) is set to $\beta = 1$ to analyse the extent of incorporating risk to the model. The probability used in the analysis is $\mu = 0.95$ and the average RES penetration level is increased slightly

from 17.83% to 17.85% with the minimum and maximum penetration level of 10.18% and 26.86%, respectively. The average demand reduction is 87.92 MW and the minimum and maximum demand reduction are -87.60 MW and 357.86 MW. The average profit achieved considering the risk on profit is \$987,494.29 and VaR of \$940,850.23. This result indicates that the highest VaR is not achieved by the means of maximising demand reduction. In fact, for the maximum demand reduction result in a VaR of \$780,521.50 and the expected profit of \$988,642.98. Table 6.5 shows the summary of the expected profit, RES penetration and demand reduction compared to the average values of stochastic case without VaR.

Table 6.5. Comparison between stochastic and deterministic model without DRP.

| Description	Stochastic $\beta = 1$			Case 3
	Best	Mean	Worst	
Thermal (MWh)	114018.3	104140.10	92507.16	104162.7
PV (MWh)	10494.83	7264.85	3013.00	7304.92
Wind (MWh)	30629.98	15361.17	2424.26	15295.42
SR (MWh)	117621.5	77914.16	43841.44	77914.16
RES (MW)	33988.98	22626.02	12919.08	22600.34
RES (%)	26.87	17.85	10.18	17.83
DR (MW)	357.86	87.92	-87.60	90.93

The impact of the risk factor on the average demand reduction is shown in Table 6.5. The risk factor reduces the average demand while also increasing the RES penetration. It is important to notice that the average spinning reserve allocation does not change regardless of the risk factor, while the average thermal generation is reduced slightly which corresponds to the slight increase in RES penetration.

6.4.5   Case 5: Comparison of the different cases

In order to evaluate the effectiveness of the proposed model. The previous case studies are compared to show the benefits of the proposed model. In the first case, the classical deterministic model is used for two cases that consider the impact of demand response. It can be seen from Table 6.2 that including demand response increases the RES penetration slightly while the profit is reduced. Further to the deterministic model, in Case 2, a stochastic model without DR is investigated and compared to the classical deterministic model. From Table 6.3 the stochastic model shows better qualities in terms of

the prediction of RES penetration level and provides a mean and standard deviation. This shows the benefit of using stochastic model to handle the uncertainty related to RES generation. The overall RES penetration is decreased for the stochastic model compared to the deterministic model but provides a measurable confidence interval. This means that the best-case scenario that can ever exist is related to RES penetration of 38.40% compared to the probable best scenario of 26.69%. In Case 3, the impact of DR is also included in the model to measure the increase of RES penetration due to demand response. As clearly shown in Table 6.4, there is an increase in the average demand of 90.93 MW when compared to the deterministic case. Moreover, the average spinning reserves allocation are reduced for the stochastic case which also translates into an increase in the profit. The average RES penetration is, however, reduced when compared to the deterministic case. When Table 6.3 and 6.4 stochastic results are compared, there is a slight decrease in the average RES penetration level of 0.7%. However, the profit for the DR scenario is increased by $132,923.82 for a small reduction in RES penetration.

A further comparison between the stochastic DR case with VaR reveals that incorporating the risk to the model improves the profitability of the generation companies and increases the RES penetration. Although there is a slight decrease in demand reduction, the overall benefit in profitability complements this decrease. Figure 6.3 shows the renewable penetration under different case studies.
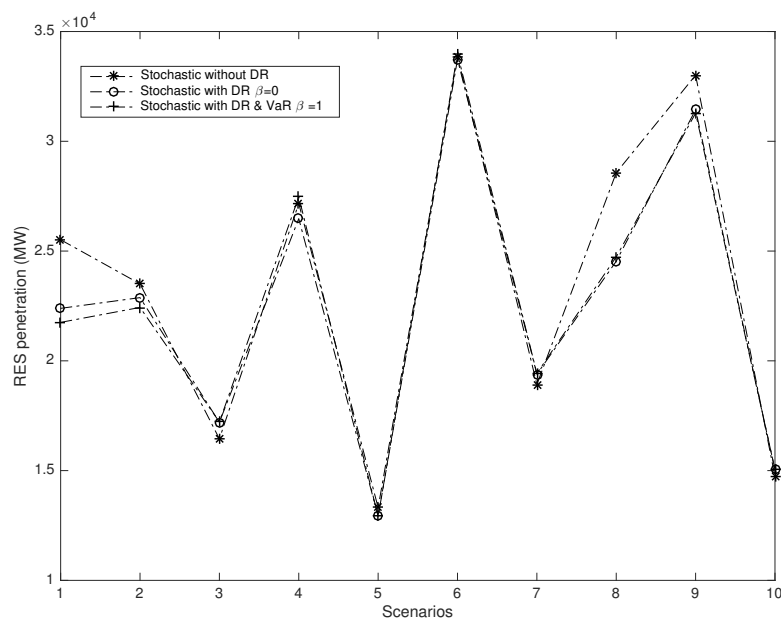
Figure 6.3. Demand response participation under different stochastic scenarios with RES obligation set to 10%.

6.5   CONCLUSION

In this chapter, a stochastic risk-based demand response under renewable obligation is proposed as a tool to increase RES penetration while achieving demand reduction. The proposed model takes advantage of the residential load management programme to present an optimal joint strategy for increasing RES penetration, allocating spinning reserves and reducing demand to deal with RES fluctuations. To this end, the proposed risk-based DR model is used to evaluate the optimal solution considering the risk of profit loss for generation companies. The proposed model illustrates the importance of including financial risk in finding the best compromise between increasing demand reduction while increasing RES penetration from an economical point of view. It also shows that the highest average demand reduction does not necessarily imply the optimal RES penetration and an increase in the profitability of generation companies. Finally, the proposed model shows that both RES generation companies and thermal unit companies can benefit from DRP.

CHAPTER 7   CONCLUSION

In this chapter a detailed conclusion of all the previous chapters is summarised and the chapter ends with a recommendation for future study.

7.1   CONCLUSION

This work proposes a comprehensive optimal framework for renewable obligation and demand response for residential customers using economic dispatch approach. In Chapters 3 and 3.6 the RO and DR models are presented in a deterministic form to show the effectiveness of the proposed framework. The last two chapters 4.6 and 5.6 consider a more complex multi-stage stochastic demand response model under renewable obligation framework. This approach shows improved results compared to the deterministic case and the contributions are highlighted below.

1. Using a deterministic renewable obligation model, a target of 10% was used to evaluate the energy mix and from the results higher RES penetration was achieved in the range of 45%.

2. An extension to the deterministic model was introduced in Chapter 4.6 which shows the impact of RES penetration under multi-stage stochastic programming. The results of the multi-stage stochastic programming show a more conservative RES penetration compared to the deterministic case. A maximum RES penetration of 26% was achieved for the large system compared to 36% of the deterministic case. However, the total operating cost is significantly reduced for the stochastic case.

3. A deterministic demand response model was presented in Chapter 4, the results shows that more RES can be increased using demand response tool. An overall increase of 15.8% was achieved with an operating cost reduction of 3.49% for the deterministic case.

4. A stochastic programming approach was used in Chapter 6 to investigate the maximum RES penetration that can be achieved while increasing the profit for thermal generating companies. The total RES penetration achieved was 17.83% without financial risk, and a RES penetration

of 17.85% is achieved when considering financial risk. The overall model shows that included financial risk to the analysis can assist the thermal generation companies to anticipate loss of profit while increasing RES penetration. More importantly, the demand reduction reduced by 3MW from a base case without financial risk to a case with financial risk. The impact of financial risk to the stochastic model can assist system operators by providing better bidding curves for the generation companies while incorporating demand response under renewable obligation policy framework.

The current research shows positive results for a joint demand response and renewable obligation policy strategy is applied to residential customers. There is savings in the total operating cost and an increase in the profitability for the generation companies. This can be achieved under any of the deterministic and stochastic programming frameworks.

7.2 RECOMMENDATION AND FUTURE WORK

There are several future research extensions from the current work which are briefly enumerated below:

1. The incorporation of the renewable energy certificate market that can be included in the current model.

2. The inclusion of the supply and demand bid curves to select the optimal energy price in the secondary market.

3. The inclusion of elasticity to the demand response model to allow maximum demand response for the flexible residential load.

4. The incorporation of a bi-level and robust model to find the worst-case demand reduction and renewable penetration level.

All these points are left open to be investigated further in research papers.

REFERENCES

[1] D. W. Ross and S. Kom, "Dynamic economic dispatch of generation," *IEEE Trans. Power Apparatus and Systems*, vol. 99, pp. 2060 – 2068, 1980.

[2] T. Bechert and H. Kwatny, "On the optimal dynamic dispatch of real power," *IEEE Trans. Power Apparatus and Systems*, vol. PAS-91, pp. 889 – 898, 1972.

[3] T. Bechert and N. Chen, "Area automatic generation control by multi-pass dynamic programming," *IEEE Trans. Power Apparatus and Systems*, vol. PAS-96, pp. 1460 – 1469, 1977.

[4] C. Lupangu and R. C. Bansal, "A review of technical issues on the development of photovoltaic systems," *Renewable and Sustainable Energy Reviews*, vol. 73, pp. 950–965, 2017.

[5] K. Nghitevelekwa and R. C. Bansal, "A review of generation dispatch with large-scale photovoltaic PV systems," *Renewable and Sustainable Energy Reviews*, vol. 81, pp. 615–624, 2018.

[6] R. C. Bansal, Ed., *Handbook of Distributed Generation: Electric Power Technologies, Economics and Environmental Impacts*.   Springer, 2017.

[7] M. Senatla and R. C. Bansal, "A review of planning methodologies used for determination of optimal generation capacity mix: the cases of high shares of PV and wind," *IET Renewable Power Generation*, vol. 12, pp. 1222–1233, 2018.

[8] S. S. Reddy, P. R. Bijwe, and A. R. Abhyankar, "Real-time economic dispatch considering renewable power generation variability and uncertainty over scheduling period," *IEEE Systems*

Journal, vol. 4, pp. 1440–1451, 2015.

[9] J. Hetzer, D. C. Yu, and K. Bhattari, "An economic dispatch model incorporating wind power," *IEEE Transactions on Energy Conversion*, vol. 23, pp. 603–611, 2008.

[10] B. Borowy and Z. Salameh, "Optimum photovoltaic array size for a hybrid wind/PV system," *IEEE Trans. Energy Conversion*, vol. 9, pp. 482 – 488, 1994.

[11] S. J. Plathottam and H. Salehfar, "Unbiased economic dispatch in control areas with conventional and renewable generation sources," *Electric Power Systems Research*, vol. 119, pp. 313–321, 2015.

[12] IRENA, "Renewable power generation costs in 2017," International Renewable Energy Agency, Abu Dhabi, United Arab Emirates, 2018. Accessed: 10 July 2020. [Online]. Available: http://www.irena.org/publications.

[13] A. Bracale, G. Carpinelli, and P. D. Falco, "A probabilistic competitive ensemble method for short-term photovoltaic power forecasting," *IEEE Trans. Sustainable Energy*, vol. 8, pp. 551–559, 2017.

[14] A. H. Shahirinia, E. S. Soofi, and D. C. Yu, "Probability distributions of outputs of stochastic economic dispatch," *Int. Electrical Power and Energy Systems*, vol. 81, pp. 308–316, 2016.

[15] M. Wang and H. Gooi, "Spinning reserve estimation in microgrids," *IEEE Trans. Power Systems*, vol. 26, pp. 1164–1174, 2011.

[16] H. Kanchev, F. Colas, V. Lazarov, and B. Francois, "Emission reduction and economical optimization of an urban microgrid operation including dispatched PV-based active generators," *IEEE Trans. Sustainable Energy*, vol. 5, pp. 1397–1405, 2014.

[17] X. Liu and W. Xu, "Minimum emission dispatch constrained by stochastic wind power availability and cost," *IEEE Trans. Power Systems*, vol. 25, pp. 1705–1713, 2010.

REFERENCES

[18] P. Meibom, R. Barth, B. Hasche, H. Brand, C. Weber, and M. O'Malley, "Stochastic optimization model to study the operational impacts of high wind penetration in Ireland," *IEEE Trans. Power Systems*, vol. 26, pp. 1367–1379, 2011.

[19] Y. Ma, Y. Hao, S. Zhao, and H. Bi, "Security constrained economic dispatch of wind-integrated power system considering optimal system state selection," *IET Generation, Transmission and Distribution*, vol. 11, pp. 27–36, 2017.

[20] V. K. Jadoun, N. Gupta, K. R. Niazi, A. Swarnkar, and R. C. Bansal, "Multi-area environmental economic dispatch with reserve constraints using enhanced particle swarm optimization," *Electric Power Components and Systems*, vol. 43, pp. 1669–1681, 2015.

[21] D. C. Secui, "The chaotic global best artificial bee colony algorithm for the multi-area economic/emission dispatch," *Energy*, vol. 93, pp. 2518–2545, 2015.

[22] J. S. Alsumait, "Solving dynamic economic dispatch problems using pattern search based methods with particular focus on the West Doha power station in Kuwait," Ph.D. dissertation, University of Southampton, 2010.

[23] R. Liang and J. Liao, "A fuzzy optimization approach for generation scheduling with wind and solar energy systems," *IEEE Trans. Power Systems*, vol. 22, pp. 1665–1674, 2007.

[24] F. Bouffard and F. Galiana, "Stochastic security for operations planning with significant wind power generation," *IEEE Trans. Power Systems*, vol. 23, pp. 306–316, 2008.

[25] V. R. Pandi, B. K. Panigrahi, R. C. Bansal, and S. Das, "Economic load dispatch using hybrid swarm intelligence based harmony search algorithm," *Electric Power Components and Systems*, vol. 39, pp. 751–767, 2011.

[26] P. Chakraborty, G. G. Roy, B. K. Panigrahi, R. C. Bansal, and A. Mohapatra, "Dynamic economic dispatch using harmony search algorithm with modified differential mutation operator," *Electrical Engineering (Springer)*, vol. 94, pp. 1–9, 2012.

REFERENCES

[27] IRENA and CEM, "Renewable energy auctions: a guide to design," International Renewable Energy Agency, Abu Dhabi, United Arab Emirates, 2015. Accessed: 10 July 2020. [Online]. Available: http://www.irena.org/publications.

[28] C. Böhringer, A. Cuntz, D. Harhoff, and E. Asane-Otoo, "The impact of the German feed-in tariff scheme on innovation: Evidence based on patent filings in renewable energy technologies," *Energy Economics*, vol. 67, pp. 545–553, 2017.

[29] N. J. Martin and J. L. Rice, "Examining the use of concept analysis and mapping software for renewable energy feed-in tariff design," *Renewable Energy*, vol. 113, pp. 211–220, 2017.

[30] M. McPherson, M. Mehos, and P. Denholm, "Leveraging concentrating solar power plant dispatchability: A review of the impacts of global market structures and policy," *Energy Policy*, vol. 139, p. 111335, 2020.

[31] T. hyeong Kwon, "Policy mix of renewable portfolio standards, feed-in tariffs, and auctions in South Korea: Are three better than one?" *Utilities Policy*, vol. 64, p. 101056, 2020.

[32] UN, "The Paris agreement on climate change," United Nations, Paris, France, 2015, Accessed: 10 July 2020. [Online]. Available: http://unfccc.int/process-and-meetings/the-paris-agreement/the-paris-agreement.

[33] S. Talari, M. Shafie-khah, G. J. Osório, J. Aghaei, and J. P. Catalão, "Stochastic modelling of renewable energy sources from operators' point-of-view: A survey," *Renewable and Sustainable Energy Reviews*, vol. 81, pp. 1953–1965, 2018.

[34] W. Su, J. Wang, and J. Roh, "Stochastic energy scheduling in microgrids with intermittent renewable energy resources," *IEEE Trans. Smart Grid*, vol. 5, pp. 1876–1883, 2014.

[35] Y. He, Y. Yan, and Q. Xu, "Wind and solar power probability density prediction via fuzzy information granulation and support vector quantile regression," *Int. Journal of Electrical Power and Energy Systems*, vol. 113, pp. 515–527, 2019.

[36] A. Akpınar, M. İ. Kömürcü, M. Kankal, İ. H. Özölçer, and K. Kaygusuz, "Energy situation and renewables in turkey and environmental effects of energy use," *Renewable and Sustainable Energy Reviews*, vol. 12, pp. 2013–2039, 2008.

[37] W. Ding and F. Meng, "Point and interval forecasting for wind speed based on linear component extraction," *Applied Soft Computing*, vol. 93, p. 106350, 2020.

[38] J. Hu, J. Tang, and Y. Lin, "A novel wind power probabilistic forecasting approach based on joint quantile regression and multi-objective optimization," *Renewable Energy*, vol. 149, pp. 141–164, 2020.

[39] Y. He and H. Li, "Probability density forecasting of wind power using quantile regression neural network and kernel density estimation," *Energy Conversion and Management*, vol. 164, pp. 374–384, 2018.

[40] M. R. Patel, *Wind and Solar Power Systems Design, Analysis and Operation*, 2nd ed. Taylor & Fracis, 2006.

[41] J. F. Manwell, J. G. McGowan, and A. L. Rogers, *Wind Energy Explained: Theory, Design and Application*, 2nd ed. Wiley, 2009.

[42] M. Zhang, X. Ai, J. Fang, W. Yao, W. Zuo, Z. Chen, and J. Wen, "A systematic approach for the join dispatch of energy and reserve incorporating demand response," *Applied Energy*, vol. 230, pp. 1297–1291, 2018.

[43] M. H. Ouahabi, H. Elkhachine, F. Benabdelouahab, and A. Khamlichi, "Comparative study of five different methods of adjustment by the weibull model to determine the most accurate method of analyzing annual variations of wind energy in Tetouan - Morocco," *Procedia Manufacturing*, vol. 46, pp. 698–707, 2020.

[44] C. Ozay and M. S. Celiktas, "Statistical analysis of wind speed using two-parameter weibull distribution in Alaçatı region," *Energy Conversion and Management*, vol. 121, pp. 49–54, 2016.

REFERENCES

[45] R. Sharifi, S. Fathi, and V. Vahidinasab, "A review on demand-side tools in electricity market," *Renewable and Sustainable Energy Reviews*, vol. 72, pp. 565–572, 2017.

[46] M. H. Imani, M. J. Ghadi, S. Ghavidel, and L. Li, "Demand response modeling in microgrid operation: a review and application for incentive-based and time-based programs," *Renewable and Sustainable Energy Reviews*, vol. 94, pp. 487–499, 2018.

[47] A. R. Jordehi, "Optimisation of demand response in electric power systems, a review," *Renewable and Sustainable Energy Reviews*, vol. 103, pp. 308–319, 2019.

[48] F. Shariatzadeh, P. Mandal, and A. K. Srivastava, "Demand response for sustainable energy systems: A review, application and implementation strategy," *Renewable and Sustainable Energy Reviews*, vol. 45, pp. 343–350, 2015.

[49] Q. Cui, X. Wang, X. Wang, and Y. Zhang, "Residential appliances direct load control in real-time using cooperative game," *IEEE Trans. Power Systems*, vol. 31, pp. 226–233, 2016.

[50] A. Malik, N. Haghdadi, I. MacGill, and J. Ravishankar, "Appliance level data analysis of summer demand reduction potential from residential air conditioner control," *Applied Energy*, vol. 235, pp. 776–785, 2019.

[51] M. Afzalan and F. Jazizadeh, "Residential loads flexibility potential for demand response using energy consumption patterns and user segments," *Applied Energy*, vol. 254, pp. 1–17, 2019.

[52] N. I. Nwulu and X. Xia, "Implementing a model predictive control strategy on the dynamic economic emission dispatch problem with game theory based demand response programs," *Energy*, vol. 91, pp. 404–419, 2015.

[53] Q. Hu, "Incentive based residential demand aggregation," Ph.D. dissertation, University of Tennessee, Knoxville, 2015.

[54] H. Aalami, M. P. Moghaddam, and G. Yousefi, "Modeling and prioritizing demand response programs in power markets," *Electric Power Systems Research*, vol. 80, pp. 426–435, 2010.

REFERENCES

[55] EU, "Renewable energy directive 2009/28/EC," European Union Council, Brussels, Belgium, 2009, Accessed: 10 July 2020. [Online]. Available: http://www.dccae.gov.ie/en-ie/energy/topics/Renewable-Energy/irelands-national-renewable-energy-action-plan-(nreap)/Pages/Action-Plan.aspx.

[56] DMRE, "Integrated resource plan 2019," Department of Mineral Resource and Energy, Pretoria, South Africa, 2019, Accessed: 10 July 2020. [Online]. Available: http://www.energy.gov.za/IRP/2019/IRP-2019.

[57] G. Shrimali and E. Baker, "Optimal feed-in tariff schedules," *IEEE Trans. Eng. Manag*, vol. 59, pp. 310–323, 2012.

[58] G. Wang, V. Kekatos, A. J. Conejo, and G. B. Giannakis, "Ergodic energy management leveraging resource variability in distribution grids," *IEEE Trans. Power Systems*, vol. 31, pp. 4765–4775, 2016.

[59] Y. Zhou, L. Wang, and J. D. McCalley, "Designing effective and efficient incentive policies for renewable energy in generation expansion planning," *Applied Energy*, vol. 88, pp. 2201–2223, 2011.

[60] F. Careri, C. Genesi, P. Marannino, M. Monagna, S. Rossi, and L. Siviero, "Generation expansion planning in the age of green economy," *IEEE Trans. Power Systems*, vol. 26, pp. 2214–2223, 2011.

[61] J. P. Chaves-Avila, F. Benez-Chicharro, and A. Ramos, "Impact of support schemes and market rules on renewable electricity generation and system operation: the Spanish case," *IET Renewable Power Generation*, vol. 11, pp. 238–244, 2016.

[62] K. Geetha, V. S. Deve, and K. Keerthivasan, "Design of economic dispatch model for Gencos with thermal and wind powered generators," *Int. Journal Electrical Power and Energy Systems*, vol. 68, pp. 222 – 232, 2015.

[63] L. Deng, B. F. Hobbs, and P. Renson, "What is the cost of negative bidding by wind? A unit

commitment analysis of cost and emissions," *IEEE Trans. Power Systems*, vol. 30, pp. 1805 – 1814, 2015.

[64] M. Hedayati-Mehdiabadi, P. Balasubramanian, K. W. Hedman, and J. Zhang, "Market implications of wind reserve margin," *IEEE Trans. Power Systems*, vol. 33, pp. 5161–5170, 2018.

[65] G. Liu and K. Tomsovic, "Quantifying spinning reserve in systems with significant wind power generation," *IEEE Trans. Power Systems*, vol. 27, pp. 2385–2393, 2012.

[66] L. Yao, X. Want, C. Duan, J. Gua, X. Wu, and Y. Zhang, "Data-driven distributionally robust reserve and energy scheduling over Wassertain balls," *IET Generation, Transmission and Distribution*, vol. 12, pp. 178–189, 2018.

[67] T. Adefarati and R. C. Bansal, "Integration of renewable distributed generators into the distribution system: A review," *IET Renewable Power Generation*, vol. 10, pp. 878–884, 2016.

[68] V. H. Hinojosa and F. G. Longatt, "Preventive security-constrained DCOPF formulation using power transmission distribution factors and line outage distribution factors," *Energies*, vol. 11, pp. 1497 – 1510, 2018.

[69] Z. Song, L. Goel, and P. Weng, "Optimal spinning reserve allocation in deregulated power systems," *IET Trans. Generation, Transmission and Distribution*, vol. 152, pp. 483 – 488, 2005.

[70] T. Qui, B. Xu, Y. Wang, Y. Dvorkin, and D. S. Kirschen, "Stochastic multistage coplanning of transmission expansion and energy storage," *IEEE. Trans. Power Systems*, vol. 32, pp. 643 – 651, 2016.

[71] H. Daneshi and A. K. Srivastava, "Security-constrained unit commitment with wind generation and compressed air energy storage," *IET Trans. Generation, Transmission and Distribution*, vol. 6, pp. 167 – 175, 2012.

[72] Y. Fu, M. Liu, and L. Li, "Multiobjective stochastic economic dispatch with variable wind generation using scenario-based decomposition and asynchronous block iteration," *IEEE Trans. Sustainable Energy*, vol. 7, pp. 139–149, 2016.

[73] S. S. Reddy, B. K. Panigrahi, R. Kundu, R. Mukherjee, and S. Debchoudhury, "Energy and spinning reserve scheduling for a wind-thermal power system using CMA-ES with mean learning technique," *International Journal of Electrical Power and Energy Systems*, vol. 53, pp. 113–122, 2013.

[74] DBEI, "Renewable obligation for 2019/20," Department for Business, Energy, & Industrial Strategy, London, UK, 2019, Accessed: 10 July 2020. [Online]. Available: http://www.gov.uk/government/publications/renewables-obligation-level-calculations-2019-to-2020.

[75] L. Mokgonyana, J. Zhang, H. Li, and Y. Hu, "Optimal location and capacity planning for distributed generation with independent power production and self-generation," *Applied Energy*, vol. 188, pp. 140–150, 2017.

[76] OFGEM, "Guidance for generators that receive or would like to receive support under the Renewable Obligation (RO) scheme," Independent National Regulatory Authority, London, UK, 2019, Accessed: 10 July 2020. [Online]. Available: http://www.ofgem.gov.uk/ro.

[77] X. Li, L. Fang, Z. Lu, J. Zhang, and H. Zhao, "A line flow Granular Computing approach for Economic dispatch with line constraints," *IEEE Trans. Power Systems*, vol. 32, pp. 4832–4842, 2017.

[78] B. Stott, J. Jardim, and O. Alsac, "DC power flow revisited," *IEEE Trans. Power Systems*, vol. 24, pp. 1290 –1300, 2009.

[79] C. Roman and W. Rosehart, "Evenly distributed pareto points in multi-objective optimal power flow," *IEEE Trans. Power Systems*, vol. 26, pp. 1011–1012, 2006.

[80] J. Arora, Ed., *Introduction to optimum design*, 4th ed. Elsevier Academic Press, 2017.

REFERENCES

[81] WASA, "CSIR online," Wind Atlas for South African Projects, Accessed: 10 July 2020. [Online]. Available: http://wasa.csir.co.za/web/welcome.aspx.

[82] SODA, "Solar energy services for professionals," Solar Radiation Data, Accessed: 10 July 2020. [Online]. Available: http://www.soda-pro.com/home.

[83] ECE, "Index of data," Illinois Institute of Technology, Accessed: 10 July 2020. [Online]. Available: http://motor.ece.iit.edu/data/118bus_ro.xls.

[84] R. D. Zimmerman and C. E. M. Sanchez, "Free open-source tools for electric power system simulation and optimization," Matpower, Accessed: 10 July 2020. [Online]. Available: http://matpower.org.

[85] G. Liu, "Generation scheduling for power systems with demand response and high penetration of wind energy," Ph.D. dissertation, University of Tennessee, Knoxville, 2014.

[86] T. G. Hlalele, R. M. Naidoo, J. Zhang, and R. C. Bansal, "Dynamic economic dispatch with maximal renewable penetration under renewable obligation," *IEEE Access*, vol. 8, pp. 38 794–38 808, 2020.

[87] S. Zhou, Z. Shu, Y. Gao, H. B. Gooi, S. Chen, and K. Tan, "Demand response program in Singapores wholesale electricity," *Electric Power Systems Research*, vol. 142, pp. 279–289, 2017.

[88] B. Lokeshgupta and S. Sivasubramani, "Multi-objective dynamic economic and emission dispatch with demand side management," *Int. Electric Power and Energy Systems*, vol. 97, pp. 334–343, 2018.

[89] M. M. Eissa, "First time real time incentive demand response program in smart grid with i-energy management system with different resources," *Applied Energy*, vol. 212, pp. 607–621, 2018.

[90] J. D. Khazzoom, "Economic implications of mandated efficiency in standards for household appliances," *Energy*, vol. 1, pp. 21–40, 1980.

[91] S. Borenstein, "A microeconomic framework for evaluating energy efficiency rebound and some implications," *Energy*, vol. 36, pp. 1–21, 2015.

[92] A. Asadinejad and K. Tomsovic, "Optimal use of incentive and price based demand response to reduce costs and price volatility," *Electric Power Systems Research*, vol. 144, pp. 215–223, 2017.

[93] M. M. R. Sahebi and S. H. Hosseini, "Stochastic security constrained unit commitment incorporating demand side reserve," *Int. Journal of Electrical Power and Energy systems*, vol. 56, pp. 175–184, 2014.

[94] M. A. Mirzaei, A. S. Yazdankhan, and B. Mohammadi-Ivatloo, "Stochastic security-constrained operation of wind and hydrogen energy storage systems integrated with price-based demand response," *Hydrogen Energy*, vol. 44, pp. 14 217–14 227, 2019.

[95] A. Dolatabadi and B. Mohammadi-Ivatloo, "The role of demand response in single and multi-objective wind-thermal generation scheduling: A stochastic programming," *Energy*, vol. 64, pp. 854–867, 2014.

[96] R. Azizipanah-Abarghooee, F. Golestaneh, H. B. Gooi, J. Lin, F. Bavafa, and V. Terzija, "Corrective economic dispatch and operational cycles for probabilistic unit commitment with demand response and high wind power," *Applied Energy*, vol. 182, pp. 634–651, 2016.

[97] H. Abdi, E. Dehvani, and F. Mohammadi, "Dynamic economic dispatch problem integrated with demand response considering non-linear responsive load models," *IEEE Trans. Smart Grid*, vol. 7, pp. 2586–2595, 2015.

[98] R. Lu and S. H. Hong, "Incentive-based demand response for smart grid with reinforcement learning and deep neural network," *Applied Energy*, vol. 236, pp. 937–949, 2019.

[99] N. I. Nwulu and X. Xia, "Multi-objective dynamic economic emission dispatch of electric power generation integrated with game theory based demand response programs," *Energy Conversion and Management*, vol. 89, pp. 963–974, 2015.

[100] Y. Wang, Y. Huang, Y. Wang, M. Zeng, F. Li, Y. Wang, and Y. Zhang, "Energy management of smart micro-grid with response loads and distributed generation considering demand response," *Journal of Cleaner Production*, vol. 197, pp. 1069–1083, 2018.

[101] S. Nan, M. Zhou, and G. Li, "Optimal residential community demand response scheduling in smart grid," *Applied Energy*, vol. 201, pp. 1280–1289, 2018.

[102] C. G. Monyei and A. O. Adequmi, "Demand side management potentials for mitigating energy poverty in South Africa," *Energy Policy*, vol. 111, pp. 298–311, 2011.

[103] IDM, "Integrated demand management programme," Eskom, Accessed: 10 July 2020. [Online]. Available: http://www.eskom.co.za/sites/idm/Pages/Home.aspx.

[104] S. M. Basnet, H. Aburub, and W. Jewell, "Residential demand response program: Predictive analytics, virtual storage model and its optimization," *Journal of Energy Storage*, vol. 23, pp. 183–194, 2019.

[105] P. Kohlhepp, H. Harb, H. Wolisz, S. Waczowicz, D. Müller, and V. Hagenmeyer, "Large-scale grid integration of residential thermal energy storages as demand-side flexibility resource: A review of international field studies," *Renewable and Sustainable Energy Reviews*, vol. 101, pp. 527–547, 2019.

[106] T. Terlouw, T. AlSkaif, C. Bauer, and W. van Sark, "Multi-objective optimization of energy arbitrage in community energy storage systems using different battery technologies," *Applied Energy*, vol. 239, pp. 356–372, 2019.

[107] N. O'Connell, P. Pinson, H. Madsen, and M. O'Malley, "Benefits and challenges of electrical demand response: A critical review," *Renewable and Sustainable Energy Reviews*, vol. 39, pp. 686–699, 2014.

REFERENCES

[108] F. Harkouss, F. Fardoun, and P. H. Biwole, "Multi-objective optimization methodology for net zero energy buildings," *Journal of Building Engineering*, vol. 16, pp. 57–71, 2018.

[109] E. kianmehr, S. Nikkhah, and A. Rabiee, "Multi-objective stochastic model for joint optimal allocation of DG units and network reconfiguration from DG owner's and DisCo's perspectives," *Renewable Energy*, vol. 132, pp. 471–485, 2019.

[110] M. Nasr, S. Nikkhah, G. B. Gharehpetian, E. Nasr-Azadani, and S. H. Hosseinian, "A multi-objective voltage stability constrained energy management system for isolated microgrids," *Int. Journal of Electrical Power and Energy Systems*, vol. 117, p. 105646, 2020.

[111] P. A. de Villiers and C. A. van der Merwe, "Residential load management research," North-West University, Tech. Rep., 2008.

[112] F. Hu, K. J. Hughes, D. B. Ingham, L. Ma, and M. Pourkashanian, "Dynamic economic and emission dispatch model considering wind power under energy market reform A case study," *Int. Journal on Electrical Power and Energy Systems*, vol. 110, pp. 184–196, 2019.

[113] V. K. Jadoun, V. C. Pandey, N. Gupta, K. R. Naizi, and A. Swarnkar, "Integration of renewable energy sources in dynamic economic load dispatch problem using an improved fireworks algorithm," *IET Renewable Power Generation*, vol. 12, pp. 1004–1011, 2018.

[114] J. Yu, X. Shen, and H. Sun, "Economic dispatch for regional integrated energy system with district heating network under stochastic demand," *IEEE Access*, vol. 7, pp. 46 659–46 667, 2019.

[115] V. Bassi, E. Pereira-Bonvallet, M. Abdullah, and R. Palma-Behnke, "Cycling impact assessment of renewable energy generation in the costs of conventional generators," *Energies*, vol. 11, p. 1640, 2018.

[116] M. Hermans, K. Bruninx, and E. Delarue, "Impact of CCGT start-up flexibility and cycling costs toward renewables integration," *IEEE Trans. Sustainable Energy*, vol. 9, pp. 1468–1476, 2018.

REFERENCES

[117] Z. Cao, Y. Han, J. Wang, and Q. Zhao, "Two-stage energy generation schedule market rolling optimisation of highly wind power penetrated microgrids," *Int. Journal of Electrical Power and Energy Systems*, vol. 112, pp. 12–27, 2019.

[118] M. M. Moarefdoost, A. J. Lamadrid, and L. F. Zuluaga, "A robust model for ramp-constrained economic dispatch problem with uncertain renewable energy," *Energy Economics*, vol. 56, pp. 310–325, 2016.

[119] H. Zhang, D. Yue, and X. Xie, "Robust optimization for dynamic economic dispatch under wind uncertainty with different levels of uncertainty budget," *IEEE Access*, vol. 4, pp. 7633–7644, 2016.

[120] A. Lorca and X. A. Sun, "Adaptive robust optimization with dynamic uncertainty sets for mult-period economic dispatch under significant wind," *IEEE Trans. Power Systems*, vol. 30, pp. 1702–1713, 2015.

[121] Y. Xu, M. Yin, Z. Y. Dong, R. Zhang, D. J. Hill, and Y. Zhang, "Robust dispatch of high wind power-penetrated power systems against transient instability," *IEEE Trans. Power Systems*, vol. 33, pp. 174–186, 2018.

[122] L. Wang, B. Zhang, Q. Li, W. Song, and G. Li, "Robust distributed optimization for energy dispatch of multi-stakeholder multiple microgrids under uncertainty," *Applied Energy*, vol. 255, p. 113845, 2019.

[123] Z. Lin, H. Chen, Q. Wu, W. Li, M. Li, and T. Ji, "Mean-tracking model based stochastic economic dispatch for power systems with high penetration of wind power," *Energy*, vol. 193, p. 116826, 2020.

[124] Y. Liu and N. K. C. Nair, "A two-stage stochastic dynamic economic dispatch model considering wind uncertainty," *IEEE Trans. Sustainable Energy*, vol. 7, pp. 819–829, 2016.

[125] W. Lei, M. Shahidehpour, and L. Tao, "Stochastic security-constrained unit-commitment," *IEEE Trans. Power Systems*, vol. 22, pp. 800–811, 2007.

[126] A. Papavasiliou, Y. Mou, L. Cambier, and D. Scieur, "Application of stochastic dual dynamic programming to the real-time dispatch of storage under renewable supply uncertainty," *IEEE Trans. Sustainable Energy*, vol. 9, pp. 547–558, 2018.

[127] H. Khaloie, A. Abdollahi, M. Shafie-khah, A. Anvari-Moghaddam, S. Nojavan, P. Siano, and J. P. Catalão, "Coordinated wind-thermal-energy storage offering strategy in energy and spinning reserve markets using a multi-stage model," *Applied Energy*, vol. 259, p. 114168, 2020.

[128] M. Xie, J. Xiong, S. Ke, and M. Liu, "Two-stage compensation algorithm for dynamic economic dispatching considering copula correlation of multiwind farms generation," *IEEE Trans. Sustainable Energy*, vol. 8, pp. 763–771, 2017.

[129] Q. Tan, Y. Ding, Q. Ye, S. Mei, Y. Zhang, and Y. Wei, "Optimization and evaluation of a dispatch model for an integrated wind-photovoltaic-thermal power system based on dynamic carbon emissions trading," *Applied Energy*, vol. 253, p. 113598, 2019.

[130] A. Soroudi, A. Rabbie, and A. Keane, "Stochastic real-time scheduling of wind-thermal generation units in an electricity utility," *IEEE Systems Journal*, vol. 11, pp. 1622–1631, 2017.

[131] N. Li and K. W. Hedman, "Economic assessment of energy storage in systems with high levels of renewable sources," *IEEE Trans. Sustainable Energy*, vol. 6, pp. 1103–1111, 2015.

[132] S. Wang, B. Tarroja, L. S. Schell, B. Shaffer, and S. Samuelsen, "Prioritizing among the end uses of excess renewable energy for cost-effective greenhouse gas emission reductions," *Applied Energy*, vol. 235, pp. 284–298, 2019.

[133] IRENA, "Renewable energy target setting," International Renewable Energy Agency, Abu Dhabi, United Arab Emirates, 2015. Accessed: 10 July 2020. [Online]. Available: http://www.irena.org/publications.

[134] M. Basu, "Multi-region dynamic economic dispatch of solar–wind–hydro–thermal power system incorporating pumped hydro energy storage," *Engineering Applications of Artificial Intelligence*, vol. 86, pp. 182–196, 2019.

[135] A. A. Eladl and A. A. ElDesouky, "Optimal economic dispatch for multi heat-electric energy source power system," *Int. Journal of Electrical Power and Energy Systems*, vol. 110, pp. 21–35, 2019.

[136] T. Adefarati and R. C. Bansal, "Reliability, economic and environmental analysis of a microgrid system in the presence of renewable energy sources," *Applied Energy*, vol. 236, pp. 1089–1114, 2019.

[137] A. Kumar, N. K. Meena, A. R. Singh, Y. Deng, X. He, R. C. Bansal, and P. Kumar, "Strategic integration of battery energy storage systems with the provision of distributed ancillary services in active distribution systems," *Applied Energy*, vol. 253, pp. 118–129, 2019.

[138] M. N. Kabir, Y. Mishra, and R. C. Bansal, "Probabilistic load flow for distribution systems with uncertain PV generation," *Applied Energy*, vol. 163, pp. 343–351, 2016.

[139] K. Lee and M. Al-Sharkawi, Eds., *Modern Heuristic Optimization Techniques: Theory and Applications to Power Systems*.   John Wiley & Sons, 2018, vol. 39.

[140] L. Ju, Q. Tan, R. Zhao, S. Gu, and W. Wang, "Multi-objective electrothermal coupling scheduling model for a hybrid energy system comprising wind power plant, conventional gas turbine, and regenerative electric boiler, considering uncertainty and demand response," *Journal of Clearner Production*, vol. 237, pp. 1–16, 2019.

[141] J. M. Marales, A. Conejo, H. Madsen, P. Pinson, and M. Zugno, Eds., *Integrating renewables in electricity markets*.   Springer, 2014.

[142] ELIA, "Data download," Elia grid company, Accessed: 10 July 2020. [Online]. Available: http://www.elia.be/en/grid-data/data-download.

[143] M. Mazidi, A. Zakariazadeh, S. Jadid, and P. Siano, "Integrated scheduling of renewable generation and demand response programs in microgrids," *Energy Conversion and Management*, vol. 86, pp. 1118–1127, 2014.

[144] Latin hypercube sampling. (2019). Mathworks. Accessed: 10 July 2020. [Online]. Available: http://www.mathworks.com/matlabcentral/fileexchange/56384-lhsgeneral-pd-correlation-n.

[145] Scenario reduction algorithm. (2019). Mathworks. Accessed: 10 July 2020. [Online]. Available: http://www.mathworks.com/matlabcentral/fileexchange?q=Scenred.

[146] J. Dupacova, N. Growe-kuska, and W. Romisch, "Scenario reduction in stochastic programming: An approach using probability metrics," *Math. Prog Series B*, vol. 95, pp. 493–511, 2003.

[147] Q. Zhai, X. Guan, J. Cheng, and H. Wu, "Fast identification of inactive security constraints in SCUC problems," *IEEE Trans. Power Systems*, vol. 25, pp. 1946–1954, 2010.

[148] IBM. Manual: IBM ILOG CPLEX optimization studio getting started with CPLEX v12.0. (2012). Accessed: 10 July 2020. [Online]. Available: http://www.ibm.com/support/knowledgecenter/SSSA5P_12.8.0/ilog.odms.studio.help/pdf/gscplex.

[149] Eskom, "Annual financial statements 31 March 2018," Eskom, South Africa, 2018. Accessed: 10 July 2020. [Online]. Available: http://www.eskom.co.za/IR2018/Documents/Eskom2018AFS.pdf.

[150] H. Aalami, M. P. Moghaddam, and G. Yousefi, "Demand response modeling considering interruptible/curtailable loads and capacity market programs," *Applied Energy*, vol. 87, pp. 243–250, 2010.

[151] A. Papavasiliou and S. S. Oren, "Large-scale integration of deferrable demand and renewable energy sources," *IEEE Trans. Power Systems*, vol. 29, pp. 489–499, 2014.

[152] X. Zhang, M. Shahidehpour, A. Alabdulwahab, and A. Abusorrah, "Hourly electricity demand response in the stochastic day-ahead scheduling of coordinated electricity and natural gas networks," *IEEE Trans. Power Systems*, vol. 31, pp. 592–601, 2016.

[153] S. Ghavidel, M. J. Ghadi, A. Azizivahed, J. Aghaei, L. Li, and J. Zhang, "Risk-constrained bidding strategy for a joint operation of wind power and CAES aggregators," *IEEE Trans.*

Sustainable Energy, vol. 11, pp. 457–466, 2020.

[154] S. Ghavidel, A. Rajabi, M. J. Ghadi, A. Azizivahed, L. Li, and J. Zhang, "Risk-constrained demand response and wind energy systems integration to handle stochastic nature and wind power outage," *IET Energy Systems Integration*, vol. 1, pp. 114–120, 2019.

[155] T. G. Hlalele, R. M. Naidoo, R. C. Bansal, and J. Zhang, "Multi-objective stochastic economic dispatch with maximal renewable penetration under renewable obligation," *Applied Energy*, vol. 270, pp. 1–16, 2020.

[156] A. Conejo, M. Carrion, and J. Marales, Eds., *Decision making under uncertainty in electricity markets*. Springer, 2010.

[157] L. He, Z. Lu, L. Geng, J. Zhang, X. Li, and X. Guo, "Environmental economic dispatch of integrated regional energy system considering integrated demand response," *Int. Journal of Electrical Power and Energy Systems*, vol. 116, p. 105525, 2020.

[158] N. Growe-kuska, H. Heitsch, and W. Romisch, "Scenario reduction and scenario tree construction for power management problems," in *Proc. Power Tech Conf., IEEE Bologna*, vol. 3, 2003, pp. 1–6.

[159] Time series analysis and forecast. (2019). Mathworks. Accessed: 10 July 2020. [Online]. Available: http://www.mathworks.com/matlabcentral/fileexchange/54276-time-series-analysis-and-forecast.

ADDENDUM A   DERIVATIONS

A.1   QUADRATIC COST FUNCTION LINEARIZATION

The fuel cost function is represented by a quadratic function which is non-convex that can be converted into a set of incremental piecewise linear functions [157]. The economic dispatch formulation uses this quadratic cost function for all the thermal units in all the standard IEEE test systems as given in chapters 3 to 6. The function is commonly divided into the production range between minimum output and the capacity of the unit. Figure A.1, shows a quadratic function that is approximated by K straight lines.
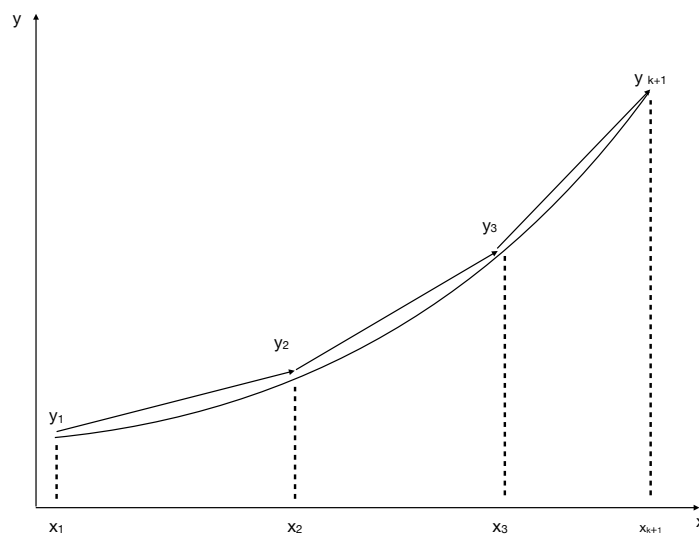
Figure A.1. Piecewise linearization of a quadratic cost function.

The linear function is composed of two points on both ends, the linear values of y and x are calculated

as shown in (A.1) and (A.2) respectively. The continuous variable is represented by θ as shown in (A.3) and (A.4).

$$y = y_1 + \sum_{k \in \Omega_K} (y_{k+1} - y_k) \theta_k \tag{A.1}$$

$$x = x_1 + \sum_{k \in \Omega_K} (x_{k+1} - x_k) \theta_k \tag{A.2}$$

$$0 \leq \theta_k \leq 1, \; k \in \Omega_K \tag{A.3}$$

$$\theta_{k+1} \leq l_k \leq, \; 1 \leq k \leq K \tag{A.4}$$